



Dottorato di Ricerca in Scienze della Terra e Del Mare
Dipartimento di Scienze della Terra e del Mare
Settore Scientifico Disciplinare BIO/07

New Insights into the Functioning of Mediterranean Rocky Reef ecosystem When Algal Forests Are Lost

La Dottoressa

Chiara Bonaviri

Il Tutor

Prof.ssa Salvatrice Vizzini

Il Co-tutor

Prof.ssa Paola Gianguzza

Il coordinatore

Prof. Alessandro Aiuppa

Sommario

General Abstract	4
1. General introduction	6
2. Coralline barrens and benthic megafauna: an intimate connection	12
2.1 Introduction	13
2.2 Material and methods	15
2.2.1 Study area	15
2.2.2 Descriptive approach, data collection and processing	16
2.2.3 Isotopic approach, data collection and processing	17
Results 2.3	22
2.4 Discussion	31
3. Benthic megafauna contributes to the functioning of Mediterranean rocky reefs in mature urchin barren grounds.	37
3.1 Introduction	38
3.2.1 ECOPATH model approach	42
3.2.2 Defining of functional groups and data source	43
3.3 Results	53
3.3.1 Characteristics of Ecosystem energy flow	53
3.3.2 Differential Biomass and Production Distribution in Forest and Barren States	55
3.3.3 Network flow indicators	61
3.4 Discussion	63
4. Unravelling hidden predator-prey interactions among sea urchin juveniles and micropredators by prey DNA amplification.....	67
4.1 Introduction	68
4.2 Materials and methods	71
4.2.1 Sample collection	71
4.2.2 Taxonomic identification	72
4.2.2 DNA extraction	81
4.2.3 Primer design	82
4.2.4 Amplification	83
4.2.5 COI-1 barcoding	84
4.3 Results	85
4.3.1 Invertebrate assemblages	85

4.3.2 DNA quality and barcoding	86
4.3.4 Barcoding of urchin juveniles	89
4.3.5 Primer efficiency	90
4.3.6 Detection of urchin DNA in invertebrate samples	97
4.4 Discussion.....	122
5. Conclusion	129
Bibliography	131

General Abstract

In the Mediterranean, overfishing of large predatory fish, particularly *Diplodus* spp., can cause severe sea urchin outbreaks, leading to significant shifts in benthic communities. Variations in sea urchin grazing intensity may trigger transitions between complex algal-dominated states ("Forest") and simpler, sea urchin-dominated states ("Barren"). Barren states, which are characterized by low diversity and productivity, can persist for long periods, even within marine protected areas (MPAs). The recovery of key sea urchin predators in MPAs is slow due to initial overexploitation, resulting in persistent sea urchin population explosions.

Forest states, with their rich biodiversity, transfer substantial quantities of carbon, nitrogen, and phosphorus to coastal food webs, whereas barren systems have lower diversity and productivity. However, recent studies suggest that barren systems can provide microhabitats for various cryptic and invertebrate species, which may contribute to maintaining the barren state. The shift between forest and barren states affects the entire food web, altering growth, feeding dynamics, and energy flow.

This thesis aims to elucidate the functioning of forest and barren states in Mediterranean rocky reefs through a multidisciplinary approach, including descriptive, isotopic, mass balance, and molecular analyses.

1. **Descriptive and Isotopic Approach:** The study tested the hypothesis that coralline barrens enhance benthic megafauna abundance and diversity. Isotopic analyses revealed a comparable trophic structure between the two states, with higher isotopic uniqueness in barrens, primarily influenced by sea urchins and carnivorous starfish. Results indicated that coralline barrens support a diverse benthic megafauna, challenging the notion of barrens as low-diversity habitats.
2. **Mass Balance Approach:** Food-web models of algae forests and urchin barrens, representing pristine and collapsed states of rocky reefs, were developed. Both states showed dominance of low trophic level consumers and significant energy flow through detritus. Despite differences in primary production and energy utilization, both states exhibited similar complexity and stability. This highlights the importance of understanding ecosystem dynamics for effective management and conservation.
3. **Molecular Approach:** Investigating the persistence of barren states despite predator recovery, this study explored the role of micropredation in controlling sea urchin populations. Specific primers for detecting mtDNA of sea urchins *Paracentrotus lividus* and *Arbacia lixula* were designed. Testing invertebrates collected during urchin settling events identified potential micropredators, suggesting that micropredation may help maintain the forest state by controlling sea urchin populations.

The findings provide insights into the structure and functioning of rocky reef ecosystems in different stable states, underscoring the need for comprehensive management strategies to preserve these critical habitats.

1. General introduction

Human activities exert high pressure on the environment often leading to substantial environmental impacts, from local to global spatial scales and during a wide array of time windows (Green, 1979). Human impacts alter the biotic structure and composition of biological communities, thus affecting ecosystems functioning (Hooper et al., 2005). Habitat loss is one of the major impacts in marine coastal areas (Valiela, 2006), which is expected to have detrimental consequences on the properties of ecosystems, as well as their capacity to provide goods and services (Kremen, 2005). Coastal ecosystems are among the most biologically diverse and productive on Earth, providing a multitude of valuable ecological, economic, and cultural services (Barbier et al., 2011). However, coastal ecosystems are facing unprecedented threats from human activities, resulting in widespread habitat modification and loss (Valiela, 2006; Airoidi & Beck, 2007). Habitat loss is considered one of the major impacts on coastal marine ecosystems, mostly affecting algae forests, seagrass meadows, salt marshes, and coral reefs, and it has become a pressing concern globally due to its far-reaching consequences for biodiversity, ecosystem function, and the well-being of coastal communities (Seitz et al., 2014). The causes of coastal habitat loss are multifaceted and often interconnected, stemming from both direct and indirect anthropogenic pressures. Direct drivers include urbanization, coastal development, and aquaculture expansion, which lead to the physical destruction and fragmentation of coastal ecosystems. Indirect drivers, such as climate change, pollution, overfishing, and invasive species, exacerbate habitat loss by altering environmental conditions, degrading water quality, and disrupting ecological processes (Valiela 2006; Duarte & BBVA Foundation - Cap Salines Lighthouse Coastal Research Station Colloquium, 2007: Madrid, 2009). For instance, overfishing is causing the decrease of abundance and size of apex predators with consequence on ecosystems dynamics (Jackson et al., 2001). Additionally, the increase of the mean global sea surface temperature and the higher frequency of climate anomalies have already provoked changes on local abundance, geographic distribution, and mortality rates of species (Parmesan et al., 2003). Loss and spatial re-distribution of species can, either alone or

synergistically with other factors, modify the identity and strength of species interactions causing sudden modifications of food webs topology and triggering catastrophic shifts of ecosystems (Folke et al., 2004; Jackson et al., 2001).

Ecosystem shifts often result in profound alterations to their structure, in some cases leading to the formation of so-called alternative meta-stable states.

Each state exhibits distinct species composition, relative abundances, and diversity, which serve as key variables defining the system across specific spatial and temporal scales (Suding et al., 2004). The transition from a community state to the alternative one is abrupt and provoked by ecological processes stemming from a strong disturbance, such as substantial organic enrichment or loss of keystone predators. In response, the system undergoes quick and sharp variations in species composition and abundances, facilitating the maintenance of the newly established conditions induced by the disturbance (Petraitis & Dudgeon, 2004). Moreover, subsequent alterations post-disturbance activates feedback mechanisms involving biotic and abiotic factors. These mechanisms confer resilience and meta-stability to the system, enabling it to withstand changes in disturbance regimes or even the reinstatement of the abiotic conditions present prior to the disturbance event (Suding et al., 2004).

One notable example of alternative stable states in marine coastal systems is evident in tropical rocky reefs, where two stable states exist: one dominated by corals and the other by macroalgae. Over recent decades, many Caribbean coral reefs have shifted from coral-dominated to algae-dominated states (Knowlton, 2004). This transition is influenced by two key factors: physical disturbances like storms initially favored macroalgae over corals, while the subsequent loss of grazers, notably the *Diadema antillarum* sea urchin species due to a massive infection in the early 1980s, further facilitated the transition. Despite the sea urchin population showing signs of recovery in recent years, there appears to be a critical minimum density below which population growth becomes negative, attributed to the "Allee effect". Additionally, positive feedback, such as the inhibition of sea urchin settlement by macroalgae, likely play a role in stabilizing the macroalgae communities (Knowlton, 2004).

In marine ecosystems at temperate latitudes, a reduction in predation on or harvesting of sea urchins can lead to an increase in their abundance. This, in turn, provokes one of the most dramatic changes in coastal ecosystems: the transition from lush algal forests to communities dominated by encrusting algal assemblages, a condition known as the “barren state.” (Fig.1) (Filbee-Dexter & Scheibling, 2014; Gagnon et al., 2004; Knowlton, 2004; Konar & Estes, 2003; Ling et al., 2015.; Shears & Babcock, 2003; Steneck et al., 2002).

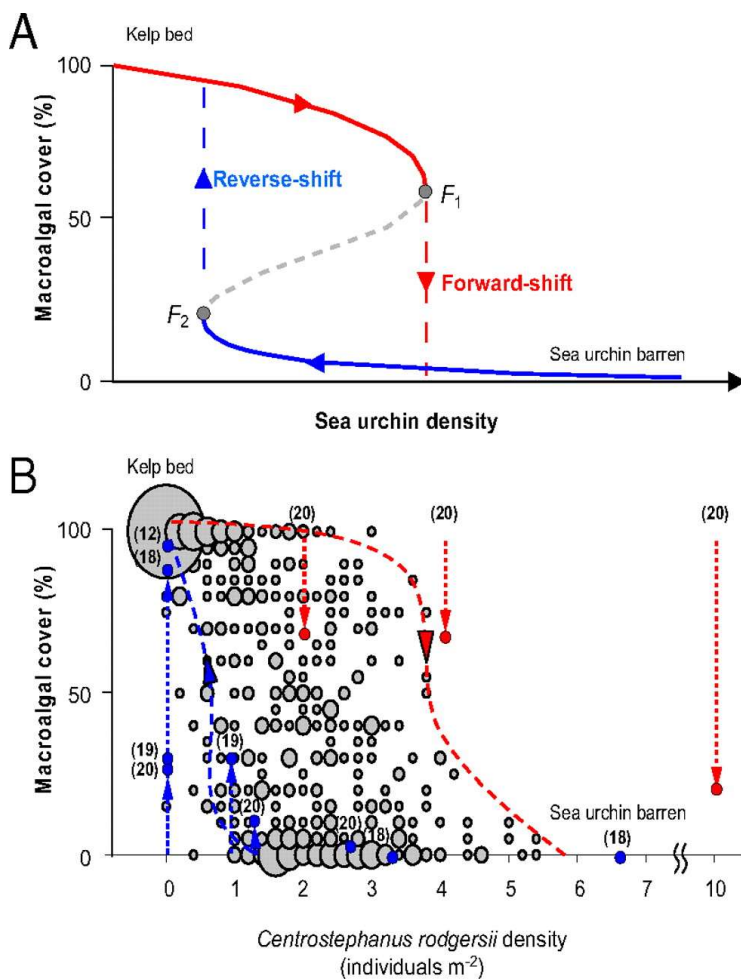


Fig.1.1 Catastrophic shift between algae forest and sea urchin barren (from Ling et al 2009). According to this model, if the ecosystem is in the forest state near the upper branch but nearing the threshold values F_2 , even a small increase in sea urchin densities can rapidly push it past the threshold and trigger a catastrophic shift to the alternative and stable barren state. This transition exhibits hysteresis, making it resistant to restoration efforts.

This transition converts once productive kelp habitats into desolate barrens, significantly impacting marine biodiversity and ecosystem services (Filbee-Dexter & Scheibling, 2014). Such shifts have been observed in various locations, including the NE Pacific, the Norwegian coast, the NW Atlantic, and Tasmania, from the 1960s through the 2000s (Ling et al., 2015). Despite understanding the general causes behind sea urchin population fluctuations, the detailed processes of kelp bed degradation and potential recovery are not clearly defined. Notably, after depleting the macroalgal biomass, sea urchins do not die off but survive on less nutritious diets, leading to long-lasting barren states, lasting over 80 years in Japan, with individual urchins living up to 50 years in these environments. Once the barren state is established, positive feedback mechanisms play a major role in maintaining this condition, highlighting the severity of the regime shift. Importantly, stressors caused by human activities hamper the resilience of desirable macroalgal beds while simultaneously strengthening that of urchin barrens (Ling et al., 2015). Thus, the formation of urchin barrens is a significant, long-term ecological issue affecting rocky reefs worldwide.

In the Mediterranean Sea, many studies described the key role of the sea urchin *Paracentrotus lividus* in driving infralittoral system dynamics (Sala et al., 1998 and references therein). At high density (7-20 ind/m²), *P. lividus* has a bulldozing effect on macroalgae assemblages such as erect algae forest formed by fuclean algae (*Cystoseira sensu lato*, including the genera *Cystoseira*, *Ericaria* and *Gongolaria*; Novoa, 2020), leading to the formation of barren areas. Once a barren area is formed, the co-occurring sea urchin *Arbacia lixula* contributes to the maintenance of the barren (Agnetta et al., 2013, 2015; Bonaviri et al., 2011). Overfishing of large predatory fish, especially *Diplodus spp.*, can lead to severe sea urchin outbreaks and promote the shifts towards the barren state. Barren states are geographically widespread and can persist for long periods, even within marine protected areas (MPAs) (Bonaviri et al., 2009; Galasso et al., 2015). Theoretically, banning of extractive human activities usually leads to the recovery of key predators of sea urchins (such as fishes, lobsters, and sea stars),

which control sea urchin populations and allow for the restoration of macroalgal-dominated states (Guidetti, 2006). However, large barren areas are found in the oldest Mediterranean MPAs, where the recovery of top predators is slow due to initial overexploitation, resulting in sea urchin population outbreaks driven by the combined effect of the lack of natural predators and the prohibition of human harvesting (Galasso et al., 2015).

Macroalgal forests and associated organisms are known to be highly productive compared to structurally simpler barren states. Algae forests transfer vast quantities of carbon, nitrogen, and phosphorus to coastal food webs either through direct transfer of animal biomass (e.g., predation, movements of individuals) or out-welling of dissolved and particulate organic matter. Conversely, barren systems are assumed to be characterized by low diversity and productivity. There is indirect evidence that deforestation can negatively affect the productivity of individual species or groups of species, with effects likely to propagate along food chains (Bianchelli et al., 2016; Pinna et al., 2020; Steneck et al., 2002). Recent studies in the North Pacific have indicated that although barren systems exhibit low structural complexity, they can provide a high number of microhabitats for a wide variety of cryptic and invertebrate species, which in turn can contribute to maintaining the community associated with the barren state (Chenelot et al., 2011). The shift to a new organizational state with different species compositions and trophic interactions may generate feedback loops that maintain the community in the new state and cause cascading effects up the food web (Salomon et al., 2008). As a matter of fact, the two alternative states (macroalgal forest and barren grounds) occur under the same range of environmental (chemical and physical) and biological conditions, but function differently (Salomon et al., 2008). It has been hypothesized that the loss of forests and the consequent fall in biodiversity correspond to a simplification of the entire food web (Mcclanahan & Sala, 1997). Such a shift towards a simpler community state is expected to affect growth, feeding dynamics, relative abundance of consumer functional groups, and overall energy flow. Furthermore, in barren states, the primary production source could shift from a primarily benthic algal pathway to phytoplankton and

phytodetrital pathways. Barren-dominated areas are widespread in the Mediterranean, but information on associated biodiversity and functioning remains scarce.

The aim of this thesis is to clarify aspects of the functioning of forest and barren states in the Mediterranean rocky reefs by using a multidisciplinary approach (descriptive, isotopic, mass balance, and molecular).

The thesis comprises three research chapters. In the first chapter, a descriptive and isotopic approach is employed to examine the hypothesis that the presence of coralline barren enhances the abundance and diversity of benthic megafauna, utilizing a barren *versus* forest patch system. The second chapter utilizes data on benthic biomass, productivity, and diet composition of meiofauna, macrofauna, and megafauna to develop food web mass balance models for both forest and barren habitats, aiming to assess crucial aspects of the functioning of Mediterranean barrens and forests. In the third chapter, the potential impact of predation of micropredators on sea urchin recruits is evaluated using a molecular approach.

2. Coralline barrens and benthic megafauna: an intimate connection

Abstract

Despite significant advances being made in the understanding of the transition from algal forests to coralline barrens, it is recognized that knowledge concerning the ecosystems of coralline barrens, in terms of community composition and functioning, remains limited, with important gaps to be filled yet. In the study conducted using a barren *vs.* forest patch system, the hypothesis that the presence of coralline barren enhances the abundance and diversity of benthic megafauna was tested. Additionally, trophic functional diversity was analyzed through isotopic analyses of $\delta^{13}\text{C}$ and $\delta^{15}\text{N}$. It was found that the distribution of benthic megafauna biomass differed markedly between coralline barrens and algal forests, with a higher abundance and diversity being observed in the barren state. The isotopic diversity metrics of the benthic megafauna assemblage indicated a comparable trophic structure between the two states, although a higher isotopic uniqueness in coralline barrens was determined, primarily influenced by sea urchins, especially *A. lixula*, and carnivorous starfish. It was shown that in a patchy coralline barren *vs.* algal forest system, a more diversified benthic megafauna assemblage in the barren resulted in limited trophodynamic changes, possibly determined by the behavior of certain trophic groups such as filter feeders, deposit feeders, and omnivores. Finally, the results evidenced a close association between coralline barrens and benthic megafauna, contradicting the commonly held view of coralline barrens as depauperate habitats with low diversity and productivity.

2.1 Introduction

Canopy-forming brown algae serve as habitat formers, offering valuable ecosystem services with some of the highest levels of primary production for underwater communities (Steneck et al. 2002). They attract and sustain diverse faunal communities, offering food and shelter for numerous species and improving nutrient cycling (Steneck et al., 2002) . It is widely accepted that coralline barrens are systems characterized by low primary productivity and complexity with prominent consequences in terms of ecosystem functioning, goods and services delivered to humans (Orfanidis et al., 2021). This paradigm naturally evokes a perception of coralline barrens as "lifeless" in people collective consciousness, where sea urchins lead to a depletion of coastal fauna that relies on the Fucales forests habitat for shelter, and nourishment (Bianchelli et al., 2016; Cheminée et al., 2017; Pinna et al., 2020; Tamburello et al., 2022). The decline of macroalgal forest is documented in the Mediterranean Sea (Fabrizzi et al., 2020; Tamburello et al., 2022) and there is growing interest in identifying processes that can enhance or prevent their restoration. In this context, knowledge of species composition which characterize the barren state can shed light on new potential interactions among species that in turn may generate self-perpetuating mechanisms (i.e., hysteresis) that maintain the barren state even if the initial conditions are restored (Baskett & Salomon, 2010; Bernal-Ibáñez et al., n.d.; Gizzi et al., 2021; Scheffer & Carpenter, 2003). Notwithstanding considerable progress in understanding shifts between alternative stable states, biodiversity and trophic structure of the coralline barrens is still scant and important gaps remain to be filled. For instance, despite their low primary productivity, the smooth crustose surface of encrusting coralline algae sustains an unexpectedly diverse and abundant cryptic macro fauna (Chenelot et al., 2011b). In turn, this might lead to unexpected impacts on the neglected benthic megafauna (*sensu* Moleón et al., 2020), including but not limited to starfish, sea urchins, sponges, holothurians, bryozoans, polychaetes, echiurans, sea anemones, and large mollusks. Using a mosaic landscape, with interspersed patches of both coralline barren and *Cystoseira* s.l. forests, the hypothesis that the presence of coralline barrens increases the abundance and diversity of benthic megafauna was tested. Furthermore, due to the different structures of the two algal assemblages (macroalgae *vs.* encrusting

coralline algae), a study utilizing stable isotopes of carbon and nitrogen was conducted to investigate the trophic structure and functioning of benthic megafaunal assemblages in barren and *Cystoseira* s.l. forest states. Through this approach, a possible new trophic paradigm was constructed, illustrating how a community with apparently low biodiversity substantially contributes to the ecosystem trophodynamics by virtue of the role played by neglected compartments such as the benthic megafauna. In this process, a potentially new trophic perspective was developed, demonstrating how a community with low biodiversity can rejuvenate through the contributions of overlooked elements like the benthic megafauna. This information is deemed crucial for the assessment of possible strategies aimed to the conservation and restoration of rocky shores globally, highlighting indirect multilayer effects, feedback mechanisms, and emergent properties across taxonomic and functional groups.

2.2 Material and methods

2.2.1 Study area

The data were collected during summer 2010, in the upper infralittoral of the volcanic “Ustica Island” Marine Protected Area (MPA), located in the north coast of Sicily (Western Mediterranean, 38°42’20” N-10°43’43” E). The MPA of Ustica Island, created in 1986, encompasses a total area of 16,000 ha and contains three zones with different degrees of protection. The no take zone (zone A) extends for 65 ha along the western part of the island, whereas the general reserve (zone B) and the take zone (zone C) equally share the remaining area. Unlike other Mediterranean MPAs, the Ustica infralittoral zone developed in wide barren areas after protection enforcement (Galasso et al., 2015) and until 2009 sea urchins, *P. lividus* and *A. lixula*, and encrusting corallines such as *Lithophyllum* spp., *Pseudolithophyllum expansum* (Philippi), *Lithothamnium* spp., *Mesophyllum coralloides* (J.Ellis) dominated the substrates of the no-take zone. In recent years, the recovery of mesopredators such *Martasterias glacialis* (L.) reduced sea urchin abundance likely promoting (Galasso et al., 2015; Gianguzza et al., 2016) the resurgence of *Cystoseira* (*sensu lato*) patches. This configuration provided a binary landscape dominated either encrusting coralline algae and erected macro algae assemblage, forming a mosaic of interspersed patches of tens of meters in diameter (Gianguzza et al., 2010). We selected four random patches, two characterized by barren and two by *Cystoseira* s.l. forest, each 200 m apart, from a set of patches with similar orientation, water motion, and topography (Agnetta et al., 2013) (Fig. 2.1).

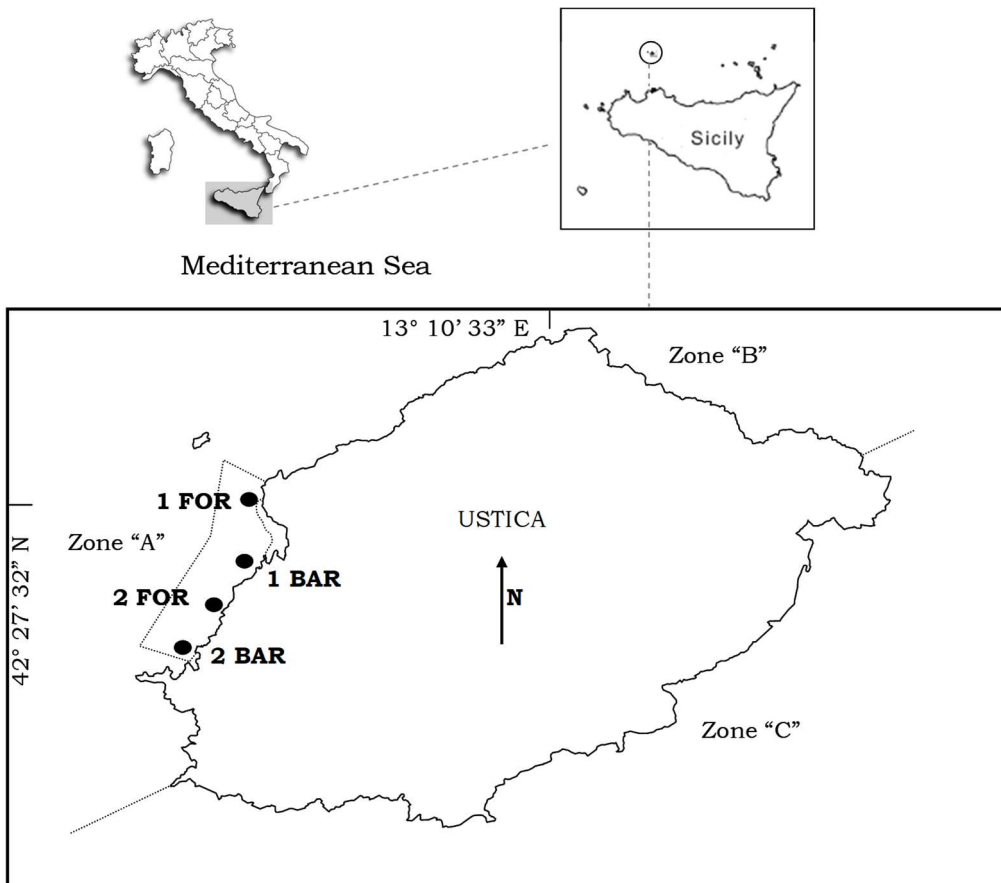


Fig.2.1 Map of Ustica Island and sampling patches (1, 2) of each rocky sublittoral community state (forest, FOR; barren, BAR).

2.2.2 Descriptive approach, data collection and processing

The abundance and biodiversity of benthic megafauna (invertebrates > 20 mm total length *sensu* Moleón et al. (2020) were assessed in barren grounds and macroalgal forest patches to test the specific hypothesis that both variables are higher in barren grounds than in macroalgal forest. Counts of benthic megafauna (number of individuals) were collected in the morning from 09:00 to 12:00 h by Underwater Visual Census (UVC) along six strip transects of 50 x 5 m (250 m²) parallel to the coast, at a depth of 5 m by two scuba divers. Due to cryptic behavior of some species (e.g., starfish and brittle stars), crevices and holes were carefully inspected (about 20 minutes per transect) while diving. Colonial taxa (e.g. Bryozoa, Porifera and Anthozoa) were sampled as number of colonies per transect (Wulff, n.d.).

Benthic megafauna was sampled with an experimental design that included two factors: community State (St), fixed with 2 levels (macroalgal Forest and Barren ground) and Patch (Pa), random and nested

within State with 2 levels (1 and 2). There were 6 replicates for each combination of factors. Benthic megafauna abundances were compared between State levels by permutational MANOVA (Anderson, 2001). Raw data were log transformed and the analysis was run based on a matrix of Bray Curtis similarities among samples. For each taxon ANOVAs were also performed on Euclidean distance resemblance matrix.

Common diversity indices such as total abundance of individuals (N), total number of species (S), Margalef's species richness (d), Pielou's evenness (J'), Shannon-Weaver's diversity (H' on log-e) and Simpson's index (1- λ) were calculated for each of the 24 samples, then single ANOVAs were performed for the above experimental design on every diversity index here considered using Euclidean distances to compile the resemblance matrix. Analyses were run on Primerv6 & Permanova+ softwares.

2.2.3 Isotopic approach, data collection and processing

In recent years, the analysis of stable isotopes has been frequently utilized to investigate ecosystem functioning by tracing the origins and pathways of organic matter in both terrestrial and aquatic environments (Vizzini, 2009). Isotopic ecological studies have been conducted in various aquatic settings, including rivers (Jepsen & Winemiller, 2002), lakes (O'Reilly et al., 2002), estuaries (Garcia et al., 2007), lagoons (Vizzini et al., 2003; Vizzini & Mazzola, 2008) and coastal marine areas (Hobson et al., 2002; Kang et al., 2008). Isotopes are different forms (derived from the Greek word meaning "same place") of an element that share identical chemical properties (same atomic number) but possess different weights and physical characteristics (due to their different numbers of neutrons). For instance, natural hydrogen exists in three isotopes: protium (^1H), which contains 1 proton and 1 neutron; deuterium (^2H), which contains 1 proton and 2 neutrons; and tritium (^3H), which contains 1 proton and 3 neutrons. Some isotopes are stable (non-radioactive) and require energy to alter their nuclear configuration, while others are unstable (radioactive) and spontaneously decay into stable configurations. Natural abundance of isotopes

changes in response to physical and biological processes. Because isotopes diverge between light and heavy forms, rates of reaction and incorporation into biological structures may vary.

The underlying theory behind isotopic analysis revolves around the concept that organisms accumulate specific concentrations of chemical elements from their environment. In predator-prey interactions, for example, there is an observed enrichment of "heavy" stable isotopes in the tissues of consumers. Within a trophic network, consumers tend to enrich in heavy stable isotopes relative to their prey. The stable isotopes most employed in trophic web studies are those of carbon and nitrogen. Isotopic compositions are expressed as δ -values, calculated as differences in parts per thousand compared to certain standard values, as depicted by equation (1):

$$\delta^{15}\text{N} \text{ or } \delta^{13}\text{C} = [(R_{\text{campione}} - R_{\text{standard}}) / R_{\text{standard}}] \times 1000$$

where R is either the ratio $^{15}\text{N}/^{14}\text{N}$ or $^{13}\text{C}/^{12}\text{C}$

Fractionation is the term given to the changes in isotope ratio that result from these reactions. For instance, various plant types (trees, grasses) might assimilate atmospheric carbon into their organic structures via diverse photosynthetic pathways, leading to distinct isotopic carbon ratios (Post, 2002). The carbon isotope experiences minor variations (1‰) between prey and predator, offering insights into the origin of food resources and the primary producers forming the foundation of trophic networks (Peterson & Fry, 1987a). $\delta^{13}\text{C}$ significantly differs among primary producers and undergoes minor fluctuations across trophic levels. In contrast, $\delta^{15}\text{N}$ displays a substantial increase from one trophic level to the next one, aiding in determining a consumer position within trophic networks. Discrepancies between two levels typically range from 3 to 5‰ (Peterson & Fry, 1987b), with the commonly acknowledged increment being 3.4‰. The carbon reference value is derived from the PDB (Chicago PDB Marine Carbonate Standard), specifically Pee Dee Belemnite, obtained from a Cretaceous marine

fossil, *Belemnitella americana*, discovered in the 'Pee Dee' formation in South Carolina. Conversely, the standard reference value for nitrogen is atmospheric nitrogen (N_2).

Stable isotope analyses offer a comprehensive and time-integrated measurement of the relationship between consumers and their resources, and they have been increasingly used to quantify the trophic implications of a wide range of ecological processes (Layman et al., 2012; Peterson & Fry, 1987b), like e.g. trophic subsidies (Salomon et al., 2008). Isotopic analyses are also robust tools for quantifying organismal interactions and energy fluxes across terrestrial, marine, or freshwater ecosystems (Peterson & Fry, 1987b). Various analytical approaches have been developed to interpret stable isotope data (as reviewed in Layman et al., 2012), including mixing models to assess the relative contribution of different prey to a consumer diet (Hopkins & Ferguson, 2012; Parnell et al., 2010; Phillips & Gregg, 2003), and metrics to quantify the isotopic structure of organismal groups (Layman et al., 2012).

In the present thesis, the most important components of benthic megafauna in either alternative state of the rocky sublittoral community, namely barren grounds and macroalgal forsts, were investigated through a Stable Isotope (SI) approach. $\delta^{13}C$ and $\delta^{15}N$ data were used to test for differences in isotopic functional diversity. Individuals of benthic megafauna were hand-collected by SCUBA divers from the central area of each of the 4 patches. To avoid variations in $\delta^{13}C$ and (mostly) $\delta^{15}N$ as a function of individual size, individuals of the same size were used for isotopic analysis. Given that starfishes have a remarkable capacity for arm regeneration (Di Trapani et al., 2020; Lawrence & Larrain, 1994), we collected a piece of an arm of starfishes as a sample. To analyze sea urchins, the lantern muscle of *P. lividus* and *A. lixula* was extracted as a sample. The foot muscle of gastropods, muscles of holothurians and whole body for all other species were used as samples. The first centimeter of sediment was scraped to investigate the isotopic composition of the SOM (Agetta et al., 2013).

All samples were replicated, sealed separately in plastic bags and preserved at $-20\text{ }^{\circ}C$. Defrosted samples were dried at $60^{\circ}C$ (48 h) and ground to a fine powder (Caut et al., 2009). Samples were treated separately for $\delta^{15}N$ and $\delta^{13}C$. Prior to $\delta^{13}C$ analyses, samples were acidified with drop-by-drop

2 normal HCl to remove carbonates. C and N stable isotopes were analysed by a continuous-flow isotope-ratio mass spectrometer (Thermo Delta Plus XP) coupled to an elemental analyser CHN (Thermo EA 11112). Experimental precision, based on the standard deviation of replicates of the internal standard, was 0.2‰. Isotope ratios were expressed relative to PeeDee Belemnite (PDB) standard for carbon; and to N₂ in air for nitrogen. Ratios were calculated by the equation provided by Peterson and Fry (1987b). Bi-plots were drawn in order to visualize the isotopic structure of benthic megafauna relative to barren grounds (BAR) and macroalgal forests (FOR). To consider the potential effect of lipid content we explored the data after applying the mathematical lipid normalization according to the equation proposed by Post (2002). Normalization resulted in a $\delta^{13}\text{C}$ of 1.3 ± 0.5 (standard deviation, SD) for most organisms, therefore it was chosen to analyze the original isotopic values instead.

Moreover, the difference between the trophic structure of barren and forest patches was tested using the isotopic diversity metrics developed by (Cucherousset & Villéger, 2015). Accordingly, we calculated the following functional indexes: i) the isotopic divergence (IDiv), that is a weighted distance between all organisms and the convex hull's centre of gravity. IDiv is minimal (i.e. tends to 0) when most of the points (weighted by species biomass) are close to the centre of gravity. On the opposite, IDiv tends to 1 when organisms with the most extreme stable isotope values dominate the food web. ii) the isotopic dispersion (IDis), a weighted-deviation to the average position of points in the stable isotope space divided by the maximal distance to the centre of gravity. IDis equals 0 when all species have the same isotopic values and it increases to 1 when most of the weighted points (organisms) show contrasted stable isotope values. iii) the isotopic evenness (IEve), quantifies the regularity in the distribution of organisms and of their weight along the shortest tree that links all the points. IEve tends to 1 when points are evenly distributed in the stable isotope space; iv) the isotopic uniqueness (IUni), measures how much pairs of neighbor species are isotopically different. This index equals 0 when each

organism has at least one organism with the same position in the stable isotope space and tends to 1 when most of the organisms are isolated in the stable isotope space.

Finally, the total area (TA) estimated by the convex hull for barren and forest benthic megafauna were compared by overlap indices such as similarity and nestedness (Cucherousset & Villéger, 2015), after evaluating the potential effect of the non-normal distribution of data (Fig. 2.1). All isotopic indices and overlap were calculated in the R environment (R Core Team 2023 v. 4.3.1) following the script provided by Cucherousset and Villéger (2015).

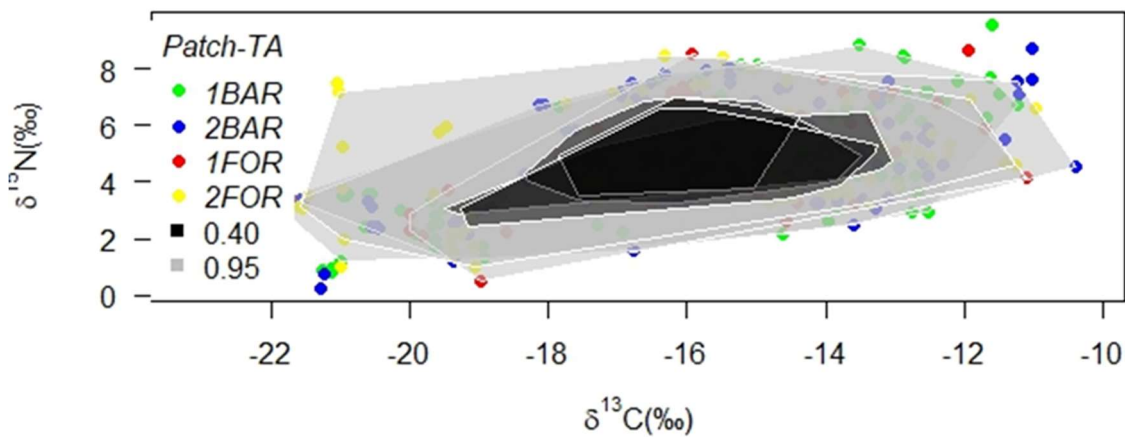


Fig. 2.1- Figure depicting TA alpha areas (selection 0.40 and 0.95 of TA) for each barren and forest patch calculated as suggested by (Fey et al., 2021). Overlaps (consider non normal distribution of data) show not significant difference between states and are very similar to TA analysis (Cucherousset & Villedger 2015), further details in the main text.

Results 2.3

Abundance of megafauna was significantly higher in barren patches than in forest ones (pseudo $F_{1,2} = 9.28$; Monte Carlo simulation $P = 0.002$). A total of 14,845 specimens belonging to 20 species and six taxonomic groups (Annelida, Bryozoa, Cnidaria, Echinodermata, Mollusca, Porifera) were surveyed in barren patches and a total of 3961 specimens belonging to 17 species of the above-mentioned taxonomic groups were recorded in forest. Cumulative abundance of *A. lixula* and *P. lividus* echinoids resulted the main component of the megafauna (61.46% and 26.77% of the total number of benthic megafauna respectively), followed by cnidarians: *Anemonia viridis* (Forsskål, 1775) and *Aiptasia mutabilis* (Gravenhorst, 1831) 2.75% and 1.9% respectively. Univariate analysis showed that the starfish *Marthasterias glacialis* (L.), sea urchins *P. lividus* and *A. lixula*, holothurians *Holoturia tubulosa* (Gmelin, 1788) and *H. polii* (Delle Chiaje, 1824), serpulids *Protula* spp. and Arcidae were significantly more abundant in barren than in forest patches. Moreover, *Coscinasterias tenuispina* (Lamarck, 1816), *Stramonita haemastoma* (Linnaeus, 1767), *Conus* spp. and *Patella caerulea* (Linnaeus, 1758) were species exclusively found in barren whereas *Myriapora truncata* (Pallas, 1766) was met only in forest patches (Tab. 2.3.1).

	Barren	Forest	ANOVA (state)	
Annelida				
<i>Protula</i> spp.	21.50±3.86	1.08±0.79	P=0.03*	F _{1,2} =27.86
Bryozoa				
<i>Myriapora truncata</i>	0	2.33±0.85		
Schizoporellidae	5.07±1.15	3.75±0.99	P=0.49	F _{1,2} =0.66
Cnidaria				
<i>Aiptasia mutabilis</i> .	23.75±5.21	26.58±5.74	P=0.79	F _{1,2} =0.09
<i>Anemonia viridis</i>	34.04±17.21	28.58±19.63	P=0.61	F _{1,2} =0.34
Echinodermata				
<i>Arbacia lixula</i>	760.42±101.27	98.33±38.38	P=0.043*	F _{1,2} =20.33
<i>Coscinasterias tenuispina</i>	0.33±0.18	0		
<i>Holothuria</i> spp.	7.25±1.75	0.42±0.22	P=0.003**	F _{1,2} =349.63
<i>Marthasterias glacialis</i>	2.33±0.78	0.17±0.11	P=0.026*	F _{1,2} =35.05
<i>Ophidiaster ophidianus</i>	2.92±0.77	1.25±0.54	P=0.335	F _{1,2} =1.55
Ophiuroidea	3±1.03	0.50±0.25	P=0.154	F _{1,2} =5.17
<i>Paracentrotus lividus</i>	331.25±56.84	154.17±46.94	P=0.038*	F _{1,2} =23.73
Mollusca				
Arcidae	21±4.66	1.92±0.95	P=0.029*	F _{1,2} =31.31
Buccinidae	2.5±0.97	0.08±0.08	P=0.14	F _{1,2} =5.28
<i>Conus</i> spp.	1.75±0.86	0		
<i>Hexaplex trunculus</i>	5.83±1.43	2.75±1.03	P=0.217	F _{1,2} =3.04
<i>Patella caerulea</i>	4±1.61	0		
<i>Stramonita haemastoma</i>	0.42±0.14	0		
Porifera				
Irciniidae	0.5±0.28	1.17±0.44	P=0.19	F _{1,2} =3.75
Others Porifera	0.42±0.18	0.17±0.11	P=0.46	F _{1,2} =0.79
<i>Spirastrella cunctatrix</i>	7.08±1.78	2.83±0.69	P=0.34	F _{1,2} =0.66

Tab 2.3.1- Benthic mega-invertebrates. Mean density (ind./250m² ± S.E.) values on barren grounds vs. macroalgal forest states (patches pooled) and analysis of variance between states (* = P<0.05, ** = P<0.01).

The species richness of benthic mega-invertebrates (S) significantly varies between barren and forest patches, with barren patches containing an average of 8.58 ± 0.1920 species (mean \pm standard error), compared to 5.58 ± 0.35 species in forest patches (as shown in ANOVAs, Table 2). However, other diversity indices measured did not show statistically significant differences (according to ANOVAs, Table 2.3.2).

	N	S	d	J'	H'	1- λ
Barren	1237.08 \pm 86.05	8.58 \pm 0.19	1.07 \pm 0.03	0.45 \pm 0.03	0.98 \pm 0.06	0.50 \pm 0.04
Forest	330.08 \pm 78.81	5.58 \pm 0.35	0.87 \pm 0.09	0.67 \pm 0.04	1.14 \pm 0.09	0.59 \pm 0.04
ANOVA	F _{1,2} =0.009	F _{1,2} =0.019		n.s.	n.s.	n.s.

Table 2.3.2 – Diversity indices calculated for the two alternative states (barren grounds vs. macroalgal forest) and analysis of variance for each index. S=species richness, N=number of individuals, d=Margalef index, J' =Pielou index, H'= Shannon-Weaver index, 1-Lambda= Simpson index. Average \pm E.S.

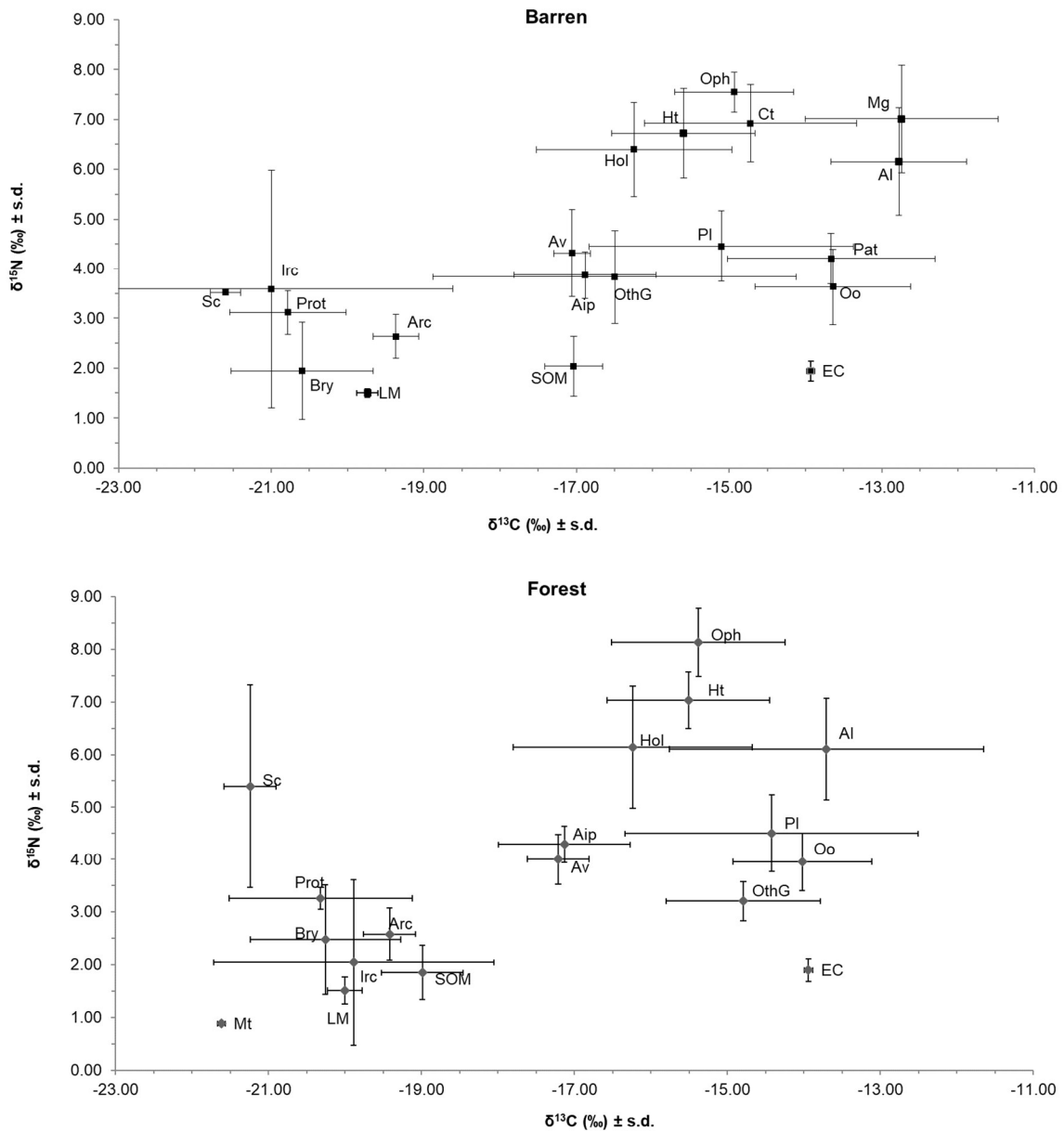


Fig. 2.3.2- Stable Isotopes diagram of megafauna and Suspended Organic Matter (SOM) in barren ground and macroalgal forest alternative states (Aip = *Aiptasia* spp.; Al = *Arbacia lixula*; Arc = Bivalves [Arcidae]; Av = *Anemonia viridis*; Bry = Bryozoans [Schizoporellidae]; Ct = *Coscinasterias tenuispina*; Hol = *Holothuria* spp.; Ht = *Hexaplex trunculus*; Irc = Irciniidae; Mg = *Marthasterias glacialis*; Mt = *Myriapora truncata*; Oo = *Ophidiaster ophidianus*; Oph = *Ophioderma* spp.; OthG = Other gastropods; Pat = *Patella* spp.; PI = *Paracentrotus lividus*; Prot = *Protula* spp.; Sc = *Spirastrella cuncatrix*; SOM = Sedimentary Organic Matter, *LM = *Cystoseira* spp. *sensu lato*, *EC = encrusting coralline), *data from Agnetta et al. (2013).

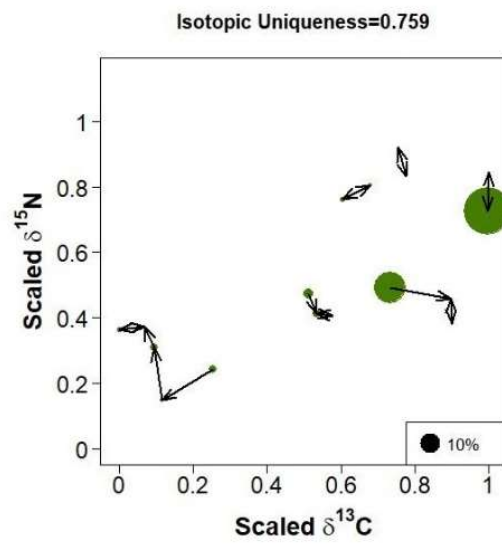
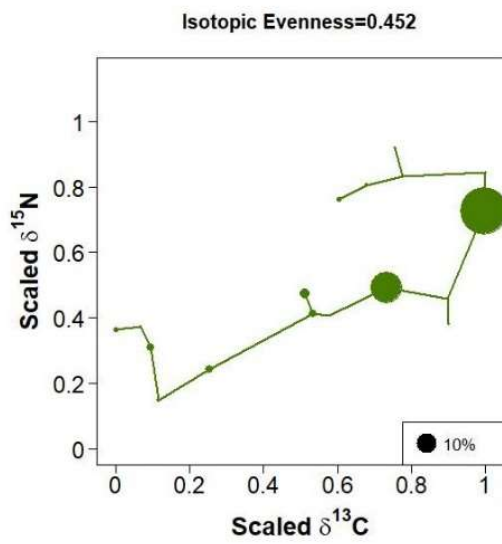
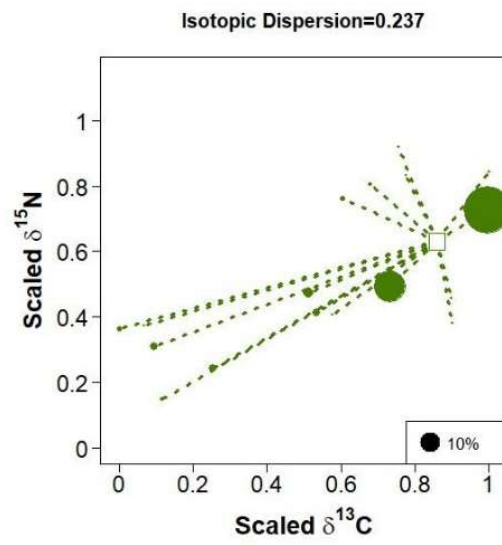
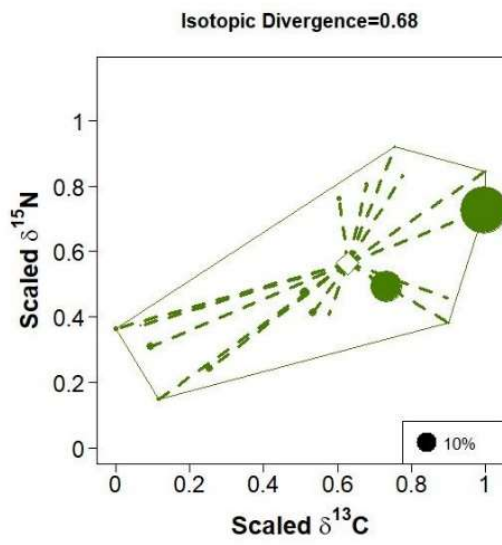
Species/taxon	BAR										FOR									
	Patch 1					Patch 2					Patch 1					Patch 2				
	$\delta^{13}\text{C}$		$\delta^{15}\text{N}$			$\delta^{13}\text{C}$		$\delta^{15}\text{N}$			$\delta^{13}\text{C}$		$\delta^{15}\text{N}$			$\delta^{13}\text{C}$		$\delta^{15}\text{N}$		
n	mean	s.d.	mean	s.d.	n	mean	s.d.	mean	s.d.	n	mean	s.d.	mean	s.d.	n	mean	s.d.	mean	s.d.	
Echinodermata																				
Asteroidea																				
<i>Marthasterias glacialis</i>	11	-12.99	1.11	7.03	1.02	8	-12.40	1.44	6.99	1.22										
<i>Coscinasterias tenuispina</i>	5	-13.66	1.32	6.43	0.90	8	-15.38	1.02	7.23	0.52										
<i>Ophidiaster ophidianus</i>	10	-13.72	1.24	3.43	0.81	10	-13.56	0.80	3.84	0.07	5	-14.78	0.79	3.79	0.49	10	-13.64	0.72	4.04	0.58
Ophiuroidea																				
<i>Ophioderma</i> spp.	2	-15.30	0.09	7.79	0.46	2	-14.56	1.14	7.31	0.21	2	-14.85	1.54	7.85	0.97	2	-15.91	0.61	8.41	0.06
Echinoidea																				
<i>Paracentrotus lividus</i>	10	-14.84	1.62	4.62	0.55	10	-15.37	1.88	4.29	0.84	10	-15.06	1.83	4.70	0.40	10	-13.78	1.87	4.30	0.94
<i>Arbacia lixula</i>	10	-12.59	0.87	6.75	1.08	10	-12.96	0.92	5.56	0.73	10	-14.20	2.20	6.28	1.08	10	-13.21	1.88	5.93	0.86
Holothuroidea																				
<i>Holothuria</i> spp.	10	-15.50	1.36	5.86	0.88	10	-16.84	0.95	6.89	0.72	5	-16.11	0.15	7.09	0.13	8	-16.31	2.04	5.55	1.12
Mollusca																				
<i>Hexaplex trunculus</i>																				
<i>Patella</i> spp.	10	-15.19	0.91	6.89	1.08	10	-16.00	0.81	6.55	0.69	6	-14.90	1.17	7.00	0.45	10	-15.87	0.86	7.05	0.60
Arcidae	9	-13.31	0.89	4.46	0.35	9	-14.02	1.69	3.96	0.55										
Other gastropods	10	-19.52	0.23	2.57	0.48	6	-19.11	0.21	2.74	0.37	6	-19.55	0.43	2.68	0.38	6	-19.28	0.16	2.47	0.60
	5	-17.46	2.14	3.49	0.98	4	-15.30	2.34	4.26	0.81	3	-15.16	1.17	3.01	0.36	2	-14.24	0.55	3.50	0.12
Cnidaria																				
<i>Anemonia viridis</i>																				
<i>Aiptasia</i> spp.	4	-17.32	0.08	5.20	0.70	6	-16.88	0.06	3.73	0.24	6	-17.27	0.25	3.78	0.24	6	-17.15	0.53	4.23	0.56
	10	-16.84	1.09	3.96	0.48	10	-16.93	0.80	3.78	0.45	5	-17.32	1.24	4.45	0.45	6	-16.97	0.43	4.16	0.19
Anellida																				
<i>Protula</i> spp.																				
	11	-20.76	0.79	3.22	0.44	10	-20.81	0.78	3.00	0.43	4	-20.93	1.29	3.18	0.09	3	-19.50	0.28	3.37	0.30
Bryozoa																				
Schizoporellidae																				
<i>Myriapora truncata</i>	6	-20.82	0.78	1.28	0.82	4	-20.26	1.16	1.24	1.07	1	-19.23		2.92		4	-20.51	0.92	2.36	1.17
											2	-21.53	0.02	0.86	0.02	2	-21.65	0.00	0.90	0.01
Porifera																				
<i>Spirastrella cunctatrix</i>																				
	1	-21.74		3.50		1	-21.46		3.53		1	-21.72		3.48		4	-21.12	0.24	5.87	1.86
Irciniidae	2	-18.94	0.01	1.52	0.27	2	-23.06	0.01	5.66	0.09	2	-21.07	2.97	2.53	2.85	3	-19.10	0.06	1.72	0.70
SOM	3	-17.30	0.11	2.46	0.36	3	-16.80	0.07	1.65	0.08	3	-18.61	0.07	2.21	0.06	3	-19.31	0.11	1.86	0.65

Table 2.3.3 – $\delta^{13}\text{C}$ and $\delta^{15}\text{N}$ mean values (‰) \pm 1 standard deviation (S.D.) of benthic mega-invertebrates at patch 1 and patch 2 of barren grounds (BAR) and macroalgal forest (FOR) state. SOM: sedimentary organic matter.

IDiv and IDis isotopic diversity metrics, showed similar values comparing BAR and FOR state (Fig. 2.3.3). Sea urchins, especially *A. lixula*, and carnivorous starfish cause complementary indices such as IEv and IUni to be in the opposite direction. IEv was lower at BAR than at FOR, that is, isotopic values of points were less evenly distributed in BAR. IUni was higher (i.e. points more unique) at BAR state. Although abundant echinoderms determine several trophic differences, overall benthic fauna in barren grounds and macroalgal forest yielded high overlap indices in terms of similarity and nestedness (Fig. 3.3.4).

IDiv and IDis isotopic diversity metrics, showed similar values comparing barren grounds and macroalgal forest alternative states (Fig. 2.3.3). Sea urchins, especially *A. lixula*, and carnivorous starfish cause complementary indices such as IEv and IUni to be in the opposite direction.

Barren ground



Macroalgal forest

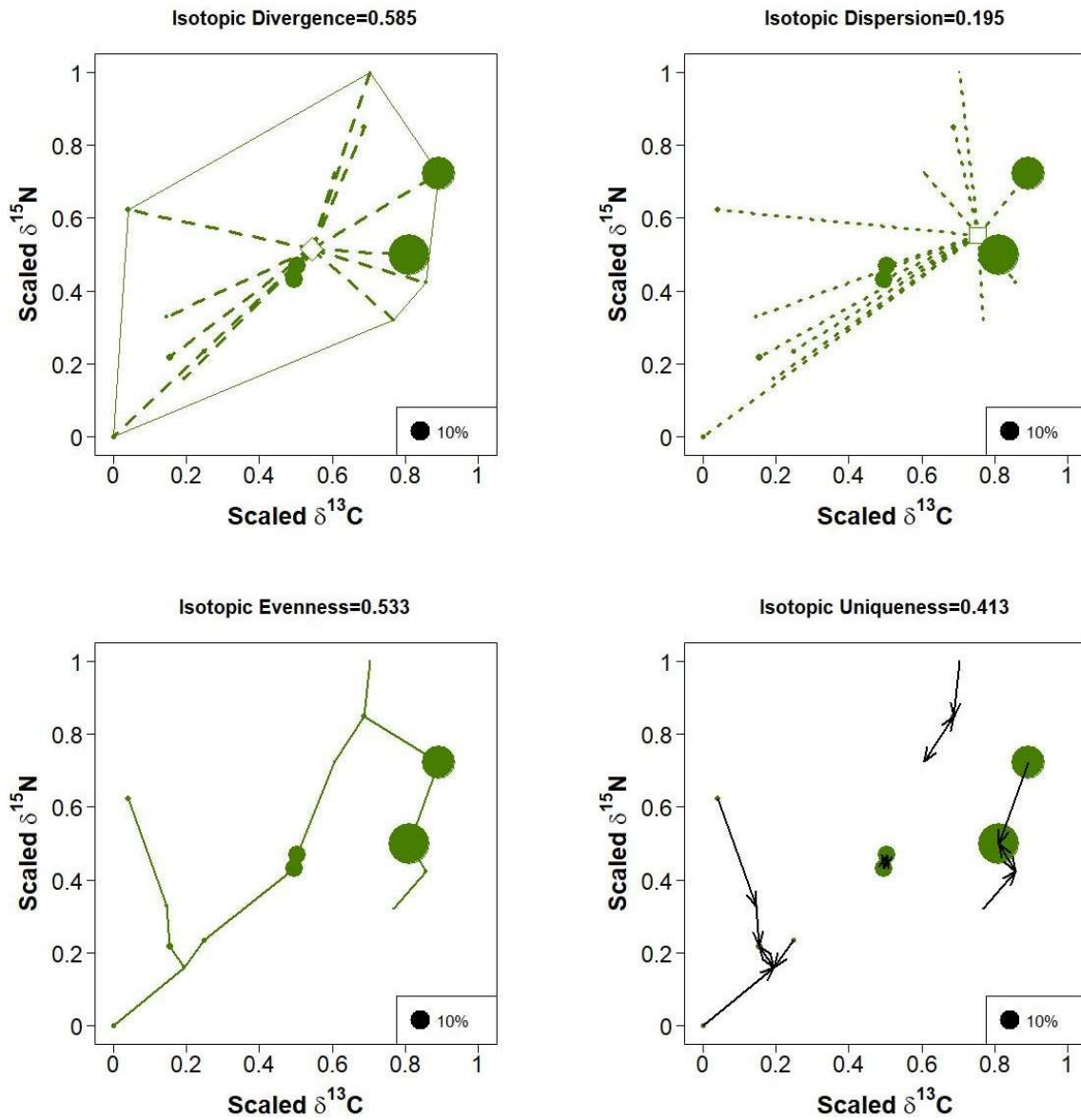


Fig. 2.3.3- Plots illustrating the four isotopic diversity metrics calculated from stable isotope values of benthic megafauna from barren grounds (BAR) and macroalgal forest (FOR) alternative states.

IEv was lower for the barren ground megafauna than for the macroalgal forest one, that is, isotopic values of points were less evenly distributed for the megafauna in barren grounds. IUni was higher (i.e., points more unique) for the megafauna at barren grounds. Although abundant echinoderms determine

several trophic differences, overall benthic megafauna in both barren grounds and macroalgal forest yielded high overlap indices in terms of similarity and nestedness (Fig. 2.3.4).

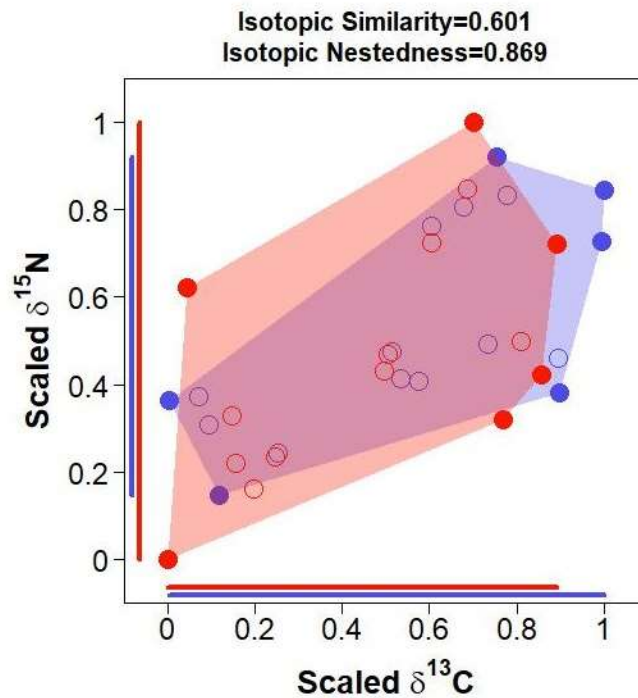


Fig. 2.3.4- Isotopic overlap metrics between organisms of benthic megafauna sampled in barren (blue points and area) and forest (purple points and area) in a two-dimensional isotopic space. Isotopic overlap metrics are measured using the isotopic richness of the two groups (i.e. convex hull volume represented by the red and blue areas, respectively) and the volume of isotopic space they shared (i.e. volume of their intersection, delimited by the purple line). Isotopic similarity is the ratio between the volume shared (purple area) and the volume of the union of the two convex hulls (delimited by full points). Isotopic nestedness is the ratio between the volume shared and the volume of the smallest convex hull (here in blue). Isotopic overlap on each stable isotope axis is illustrated by the overlap of the colored segments symbolizing the range of values for each group.

2.4 Discussion

Research on encrusting coralline algae (*i.e.*, all forms that grow roughly radially on hard substrates and exhibit a thickness lesser than 1 cm) has recently expanded among marine ecologists and geologists (McCoy & Kamenos, 2015). In most shallow temperate waters, coralline algae provide important ecosystem services: induce settlement and recruitment of numerous invertebrates and provide habitats for a variety of grazing and burrowing infauna (Adey & Halfar, n.d.; Chenelot et al., 2011a). Recent studies consistently indicate that a loss of biodiversity is a major and recurrent consequence of catastrophic regime shifts from macroalgal forest to barren ground states (Fabbrizzi et al., 2020; Tamburello et al., 2022). According to the 'mass ratio hypothesis' (Grime, 1998), dominant species like *Cystoseira* s.l. are characterized by their few numbers, tall stature, and expansive morphology, making them crucial for ecosystem functioning due to the substantial biomass they generate. In contrast, subordinate species such as encrusting coralline algae are more numerous but contribute a smaller proportion to the total community biomass, thus being considered less significant in ecosystem functioning.

Interestingly, the data presented here do not support this notion for benthic megafauna, as their abundance and biodiversity were notably higher and strongly associated with the presence of encrusting corallines in barren areas. Patches of both barren ground and macroalgal forest exhibited striking differences in terms of benthic megafauna species richness. This discrepancy arises from the substantial number of individuals found in barren ground patches, which far surpasses the species count, and the unique distribution of individuals among species (evenness), rendering this state more diverse than the macroalgal forest one. However, while diversity indices were not all statistically significant, the disparity remains evident. Just as macroalgal forested areas influence the status of macro- and meio-fauna (Bianchelli & Danovaro, 2020; Costa et al., 2018) and impact their interactions with fish, barren ground areas could similarly play a pivotal role in attracting benthic megafauna species (Rassweiler et al., 2010; Tuya et al., 2006). Previous research has indicated that encrusting coralline communities

display a phenomenon known as consumer-mediated coexistence. Grazers can disrupt competition hierarchies by favoring species resistant to grazing over fast-growing species (Dethier & Steneck, 2001; Steneck *et al.*, 2002b). According to McCoy & Kamenos (2015), encrusting corallines in barren areas can have both positive and negative interactions with grazers. They benefit from high levels of herbivory on upright species (Steneck, 1983, 1986), and the presence of grazers may even enhance local productivity of coralline crusts (Wai & Williams, 2005). Steneck (1983) suggested that, in addition to sea urchins, limpets and chitons are capable of grazing on coralline algae, displaying several convergent adaptations for grazing on hard substrates. The observation that limpets, known grazers of microalgal films, appear to be deterred by the presence of upright macroalgae in forested areas and selectively inhabit barren patches confirms Steneck (1983) hypothesis. Conversely, the presence of an infaunal community weakens the algal thallus structurally (Steneck and Paine, 1986; Adey *et al.*, 2013) and may exacerbate the potential effects of heavy grazing and excavating, particularly by species such as *A. lixula* and *P. lividus*, on the structural integrity of thick coralline algal crusts. Interestingly, Hind *et al.* (2019) demonstrated that although encrusting coralline algae are more abundant, they are significantly less diverse in urchin barrens than in macroalgal forests, the former being dominated by a few herbivore-tolerant coralline algae species.

In a scenario where consumer interactions shape coexistence, two feedback mechanisms may underpin the stability of barren zones dominated by coralline algae, shedding light on the role of benthic megafauna in enhancing diversity. Those mechanisms are driven by the factors that enable sea urchins to sustain high populations. Indeed, the continued presence of sea urchins in barren grounds is mediated by chemical signals released by encrusting coralline algae. Those chemicals encourage the settlement and metamorphosis of sea urchin larvae (Pearce & Scheibling, 1990). Such a process restricts the proliferation of *Cystoseira s.l.* and other non-coralline macroalgae, preventing them from overshadowing the coralline algal species. As a result, sea urchin grazing promotes the recruitment of new individuals into the community, enhancing local diversity, particularly among certain benthic

megafauna like sea urchins and predatory starfish (Hernández et al., 2010; Baskett & Salomon 2010; Zhang et al. 2011). Thus, in barren zones, the improved recruitment can be seen as a species-specific process that encourages a variety of cooperative interactions among benthic megafauna, thereby enhancing the suitability of the barren grounds as habitat for species such as sea urchins and carnivorous starfish. Intensive grazing by sea urchins can lead to significant ecosystem shifts on rocky shores, posing challenges for sessile epiphytic species reliant on non-coralline algae while promoting the increase of benthic megafauna, especially echinoderms. Research at Ustica Island highlights a facilitative interaction between the coexisting sea urchin species, *P. lividus* and *A. lixula*, promoting the development of coralline dominated barren grounds. This, in turn, raises sea urchin density and biomass, along with their availability as prey for mesopredators (Agnetta et al., 2013, 2015; Bonaviri et al., 2009, 2011; Gianguzza et al., 2010, 2016). This is notably evident for the two large carnivorous starfish, *M. glacialis* and *C. tenuispina*, which are conspicuously found on barren grounds. The strong trophic relationship between starfish and sea urchins is reflected by the isotopic signatures reported here and demonstrated for *M. glacialis* (Galasso et al., 2015; Gianguzza et al., 2016). The observed pattern is driven by the opportunistic feeding behavior of these starfish, which selects the prey based on its availability in the field.

Contrastingly, the minimal presence of *Cystoseira* s.l. and the absence of its associated macrofauna in the barren grounds may have facilitated the development of specific detritus pathways, favouring filter feeding invertebrates, such as Arcidae, *A. mutabilis*, *A. viridis*, and *Protula* spp. Furthermore, the notable abundance of deposit-feeders such as holothurians in barren grounds further emphasizes the positive correlation between the substantial availability of nutrient-rich detritus large benthic invertebrate species. Previous studies have already documented a strong positive correlation between holothurians and sea urchins (Rassweiler et al., 2010; Tuya et al., 2006). Specifically, Tuya et al. (2006) suggested that holothurians may benefit from a significant amount of fresh particulate organic matter (POM), primarily derived from sea urchin fecal pellets. In our investigation, the isotopic signature of

holothurians only partially matched that of the suspended organic matter (SOM) from barren ground patches, indicating that the SOM we collected did not entirely correspond to the signature of sea urchin fecal pellets, or holothurians supplemented their diet with other food sources, particularly for nitrogen. One plausible explanation is that sea urchin fecal pellets are not uniformly distributed throughout the studied habitat but rather exhibit a spatially patchy distribution, warranting separate collection as a distinct food source. In the absence of erect macroalgae, sea urchins may alter their behaviour from passively feeding on drift-algae to actively roaming and scraping encrusting coralline and sessile invertebrates (Harrold and Reed, 1985). Recent studies highlighted that encrusting coralline algae in barren grounds (BAR) can support a rich cryptic invertebrate community, partially composed by sipunculids (Chenelot et al., 2011a). Results of a previous work showed that sipunculids were the main food assimilated by *A. lixula* providing $71\% \pm 7\%$ (55%–88%) of the carbon and nitrogen while other guilds (suspension feeders, corticated foliose, calcareous algae, crustaceans omnivores, meso-herbivores, and particulate feeders, represented $\approx 5\%$ each (Agnetta et al., 2013). This reinforces the hypothesis that infaunal borers could support the trophic web structure of the benthic megafauna in barren ground patches. Further investigation is needed to evaluate the suggested trophic interactions. This study is limited because it was not year-round representative, but rather limited to the summer season; and also because the cryptic invertebrate community living under the thick encrusting coralline stratum was not sampled and included in the SI.

Despite the depauperate appearance of barren grounds, considered a system with lower biodiversity and production than the macroalgal forest state, this study showed significantly higher species richness and abundance of benthic megafauna assemblages in barren ground patches than in macroalgal forest ones. Our finding fit well with a recent study conducted in the rocky reefs of New South Wales (Kingsford & Byrne, 2023). These are characterized by a mosaic of habitats, including kelp forest and urchin-grazed barren grounds. These habitats support diverse of assemblages of dependent species. Decades of research have demonstrated that kelps form extensive forests with distinctive fish and

invertebrate faunas and the 'barrens' boulder habitat provides shelter and other resources for commercial fishes, charismatic fishes and invertebrates; thus, the barrens are not deserts (Kingsford and Byrne 2023). Since taxonomic and functional diversity of coralline crust assemblage is affected by the shift from macroalgal forest to barren ground state (Hind et al., 2019), it is necessary to understand how this diversity change drives the ecological processes in which the associated fauna is involved.

Stable isotope analysis indicated limited differences between macroalgal forest and barren ground states with respect to isotopic diversity in these subtidal rocky bottoms. This possibly reflects that several sessile species acquired a mix of detritus coming from contiguous patches of either macroalgal forest and barren grounds. Instead, mobile organisms consume food across different patches (Agnetta et al., 2013; Di Trapani et al., 2020). Alternatively, it can be hypothesized that the organisms collected in macroalgal forests fed also in barren grounds. The strength of trophic links is mediated by the biomass of predators and prey. Since distribution of benthic megafauna was positively skewed in favor of barren grounds and several organisms appeared only in barren patches (e.g. carnivorous starfish), this last hypothesis appears more plausible and can also explain the isotopic uniqueness of macrofauna in barren grounds, which mirrors its functional diversity. As subordinate species, encrusting coralline algae cannot colonize patches dominated by erect macroalgae. However, coralline algae high efficiency in resource use ("filter effects", Grime, 1998) adds to their capacity to withstand sea urchin grazing in order to thrive in patches that the dominant erect macroalgae are not able to colonize. This mechanism leads to spatial niche differentiation between barren grounds and macroalgal forest alternative states, ultimately displaying resource complementarity instead of resource competition.

Species diversity has two primary components: species richness (the number of species in a community) and species composition (the identity of the species present in a community) (Cleland, 2011). Although most research on the relationship between ecosystem diversity and stability has focused on species richness, the variation in species composition provides the mechanistic basis to explain the relationship between species richness and ecosystem functioning. Megafauna abundance and its diversity may

indeed influence the amount and diversity of resources consumed by this group within the barren ground patches (Tavares et al., 2019). In particular, benthic megafauna is composed mostly by mobile omnivores like sea urchin and starfish. These can shift and broaden their diet with prey of different trophic levels, thereby increasing affecting the trophic diversity of this group (Agnetta et al., 2013). The trophic diversity of the benthic megafuna found in the barren system has likely an effect on the efficiency by which these consumers convert resources into biomass (Hays et al., 2016), giving to this group a fundamental role in the transfer of energy. Our results evidence an intimate connection between coralline barrens and benthic megafuna, opposing the common view of coralline barrens as lifeless habitats, with low diversity and productivity. The overlooked benthic megafauna, which provide key ecosystem functions such as nutrient cycling, organic matter transport and sediment mixing, may substantially contribute to the secondary production in coralline barrens counterbalancing the lower biomass and biodiversity of meio- and macro-fauna with respect to those in macroalgal forests.

3. Benthic megafauna contributes to the functioning of Mediterranean rocky reefs in mature urchin barren grounds.

Abstract

Two temperate rocky reef food-web models representing the trophic diversity of the Mediterranean rocky reef community were built considering the two stable states: macroalgae forest and barren grounds. These are characterized by opposite amounts of erect macroalgae biomass and represent alternative meta-stable states of temperate rocky reefs. The food webs described herein include 46 functional nodes or groups (comprising auto- and heterotrophs), elucidating how the loss of macroalgae biomass from rocky reefs modifies the trophic roles and feeding behaviour of the different components of the rocky reef community and how these changes modify its functioning. Results reveal that both alternative states exhibit a dominance of consumers with low trophic levels (TLs), with most of the energy flow occurring within the first three trophic levels. Detritus plays a significant role in energy recycling, with a substantial proportion of energy flowing into and from detritus in both alternative states. Transfer efficiency from detritus is higher than from primary producers, emphasizing the importance of recycling in supporting ecosystem stability. Functional group analysis indicates different biomass and production distributions between forest and barren states, with corresponding rearrangements in the intensity of biomass flow as well as the roles of the distinct functional groups. Megafauna covers different functional roles in barrens and support a stable food web, counterbalancing the significant reduction in biomass and biodiversity of meio- and macro- fauna observed in this system. Network flow analysis reveals similar complexity and meta-stability between the two systems, despite differences in primary production and energy utilization. Overall, the study provides insights into the structure and functioning of rocky reef communities under alternative meta-stable states. It also emphasizes the importance of understanding ecosystem dynamics to identify disturbance thresholds leading to abrupt changes in rocky reef communities. Such information is critical for the effective management and conservation of subtidal rocky reefs.

3.1 Introduction

Macroalgae forests, found in shallow marine rocky reefs, are among the most productive and biodiverse ecosystems. They serve as a crucial link between coastal and pelagic systems, sustaining complex food webs (Krumhansl & Scheibling, 2012; Steneck et al., 2002; Teagle et al., 2017; Vergés & Campbell, 2020). Canopy forming macroalgal species provide substratum and shelter for mobile organisms, which consume their thallus or their associated assemblages (Norderhaug et al., 2005), act as nursery grounds for pelagic and benthic organisms (Graham, 2004; Steneck et al., 2002), and produce macroalgal detritus which fuels secondary production via the detritivore pathway (Duggins et al. 1989; Yorke et al., 2019). These processes concentrate living biomass, amplify secondary production, and connect shallow and deep ecosystems in coastal areas (Filbee-Dexter & Scheibling, 2016; Steneck et al., 2002; Taylor et al., 1998).

The functional roles of canopy-forming algae encompass various species with different growth forms and life strategies. From fast-growing giant kelp dominating temperate and arctic rocky coastlines to smaller, long-lived Fucales (genera *Cystoseira*, *Ericaria*, and *Gongolaria*, hereafter *Cystoseira* s.l.) dominating the Mediterranean shallow subtidal rocky reefs (Steneck et al., 2002; Vergés & Campbell, 2020). Despite variations in dominant species, algal forests, face global threats from cumulative local and global anthropogenic stressors. Factors such as overfishing of predators leading to grazer population outbreaks, habitat destruction, water pollution, increases in seawater temperatures and heat waves, as well as consequent changes in species physiology and distribution have resulted in the loss of macroalgal forests across large areas worldwide (Steneck et al., 2002; Bonaviri et al., 2017; Wernberg et al., 2018) Consequently, barren ground systems dominated by encrusting organisms and sea urchins develop and persist for years (Ling et al., 2015). Barren grounds exhibit low structural complexity, diversity, and productivity, with their formation considered to have detrimental effects on ecosystem functioning and unexpected cascading effects on coastal rocky reefs (Bianchelli & Danovaro, 2020; Filbee-Dexter & Scheibling, 2014b).

Interestingly, urchin barren formation triggers different processes contributing to their persistence. Urchins act as ecosystem engineers; in barren ground areas, they adopt an untrammled feeding behavior (Andrew & Underwood, 1993; Dill et al., 2003). By grazing on algae, they prevent algal overgrowth, thus preserving the current ecological balance. This grazing pressure leads to the replacement of erect, palatable algae species with encrusting, grazing-resistant species (Bulleri et al., 2002). Additionally, omnivorous scraper sea urchin species join the cutter-grazer ones, contributing to the stability of the system (Agnetta et al., 2013). Macrofauna assemblages associated with encrusting algae emerge (Chenelot et al., 2011a; Ojeda & Dearborn, 1989; Włodarska-Kowalczyk et al., 2009) and benthic megafauna abundance, including sea urchins, increases (Fanelli & Piraino, 1998; Galasso et al., 2015; Tuya et al., 2006, this thesis). Indeed, despite the low structural complexity of barren grounds, they host a substantial amount of living biomass, likely sustained over years. This living component of the barrens may have unforeseen effects on trophic structure, energy flow, matter recycling, stability, productivity, and ecosystem connectivity in rocky reef systems.

Encrusting coralline algae, abundant in barren systems, possess high organic contents akin to turf-forming algae and should be regarded as an important food resource (Maneveldt et al., 2016). The sea urchin may directly consume encrusting algae and indirectly boost their productivity by facilitating their rapid colonization on bare surface (Agnetta et al., 2013; Wai & Williams, 2005). Moreover, sea urchins, usually abundant in barren areas, can play a positive trophic role by capturing algae litter before it is exported, thereby making it available to a suite of benthic detritivores (Yorke et al., 2019b). Sea urchins efficiently convert a significant portion of their consumed food into detrital fecal matter (Mamelona & Pelletier, 2005), which is considered a source of fresh particulate organic matter (POM) for deposit feeders like holothurians and Sipuncula worms, more abundant in barren grounds compared with macroalgal forest (Chenelot et al., 2011; Tuya et al., 2006).

Additionally, the smooth crustose surface of encrusting coralline algae sustains an unexpectedly diverse and abundant cryptic macrofauna, which may constitute food for large invertebrates and fish (Agnetta et al., 2013; Chenelot et al., 2011; Ojeda & Dearborn, 1989).

In the Mediterranean Sea, macroalgae forests host an abundant and diversified fauna, with a high number of trophic guilds (Antoniadou & Chintiroglou, 2006; Pinna et al., 2020) and serve as feeding and nursery grounds for coastal fish (Chenelot et al., 2011). Habitat destruction due to the fishing of the date mussel *Lithophaga lithophaga*, outbreaks of the sea urchin *P. lividus* due to overfishing of its predators (the seabreams *Diplodus vulgaris* and *D. sargus*), and the expansion of thermophilic herbivorous fish (*Siganus luridus*, *S. rivualtus*) trigger the formation of large barren grounds in different areas of the Mediterranean Sea (Agnetta et al., 2015; Bonaviri et al., 2009; Fanelli et al., 1994; Sala et al., 2011). Once formed, barren maintenance may be reinforced by the grazing of the thermophilic omnivorous scraper urchin *A. lixula* and other grazers such as limpets and Polyplacophora (Piazzi et al., 2016) .

Urchin population persistence is favored by the reduction of micropredators of urchin recruits associated with erect algae (Bonaviri et al., 2012a) and sustained by food and shelter resources present in the barren (Agnetta et al., 2013). Intriguingly, although most macro-zoobenthos experience severe reductions in Mediterranean barrens, certain groups such as Sipuncula and Porifera are abundant (Pinna et al., 2020). Conversely, Sipuncula and Porifera found in barrens might constitute part of the diet of larger animals such as urchins and starfish (Agnetta et al., 2013; Di Trapani et al., 2020). In the second chapter of the present thesis, it has been reported a rich benthic megafauna assemblage formed by starfish, urchins, sponges, holothurians, bryozoans, polychaetes, echiurans, anemones, and mollusks in Mediterranean barren grounds. Notably, while barren ground systems are well-documented alternatives to macroalgal forests in temperate rocky reefs, a comprehensive understanding of the structure and functioning of the food web in barren grounds is lacking, particularly concerning the role of organisms inhabiting barrens in the energy transfer in rocky reefs.

Food web models are useful tools for depicting the properties of marine ecosystems and for studying the effects of community changes on their functioning (Coll & Libralato, 2012). In this context, the mass-balance food-web model ECOPATH has been widely used in marine ecosystems to analyze trophic interactions and energy transfer among different functional groups. It helps identify those functional groups that have a significant effect on the ecosystem and characterizes overall activity, size, maturity, energy export, metabolism, efficiency of energy utilization, and complexity of the ecosystem, as well as the effects of disturbances (Agnetta et al., 2019, 2022; Keramidas et al., 2023).

In order to compare the overall functioning of the two meta-stable alternative states of sublittoral rocky reefs systems in the Mediterranean Sea, two ECOPATH food-web models were constructed for barrens and forests, respectively, using data from large, mature and shallow rocky systems dominated by either macroalgae forests or barren grounds off the Adriatic coast.

3.2 Material and methods

3.2.1 ECOPATH model approach

Here, two food-web models for the Mediterranean rocky reef were built, considering two different stable states of the reef: macroalgal forest and barren ground, dominated respectively by erect- and encrusting algae. ECOPATH, the static component of the EwE software (www.ecopath.org; Christensen, Walters, Pauly, & Forrest, 2008), was used for that purpose. ECOPATH describes yearly biomass and flows among interconnected functional groups (hereafter FGs) based on a quantitative mass-balance approach (Christensen & Walters, 2004). In particular, Ecopath balances energy flows and biomass among FGs, which represent species or groups of species with similar ecological and trophic roles. Additionally, it facilitates the consideration of the impact of fishing activities on each functional group. The energy equilibrium within and between groups is maintained through two linear equations: one equating the production of each functional group (P_i) to predator consumption (M_{2i}), export from the system (e.g., fisheries yield, Y_i), other forms of mortality ($M_{0i=1}$ -Ecotrophic efficiency, EE), and biomass accumulation (BA_i); and another equating food consumption (Q_i) to the sum of production (P_i), respiration (R_i), and the unassimilated food (UN_i) of each FG. Input parameters for each FG include biomass (B_i), production rate (P/B_i) (equivalent to total mortality rate), consumption rate (Q/B_i), dietary information (represented by the diet matrix DC_{ij} , indicating the fraction of prey i in the diet of predator j), and the unassimilated food ratio (UN_i) for each group. The model typically estimates growth efficiency (P/Q), respiration rate (R/B), and the proportion of production either consumed within the system by predators or exported (known as Ecotrophic Efficiency, EE) for each group. This enables an assessment of whether the food web model is balanced, as indicated by $P/Q < 0.5$ for all groups, R/B consistent with the metabolism of the group, and $EE < 1$ for all groups; with higher values typically observed for top predators and smaller organisms (Christensen et al., 2004).

In order to better define the functional role of the different FGs we considered four different food-web indicators: (1) System Throughput (ST), the contribution of each FG to the sum of all flow in the

ecosystem (Total System Throughput); (2) Relative Ascendency, the contribution of each FG to the Ascendency, which measures the degree of organization of the ecosystem and its ability to cope with perturbations (Ulanowicz, 1997) ; (3) Keystoneness, which individuates keystone FGs, i.e.: those FGs which, despite their low biomass, can potentially induce large change in biomass to other FGs; (4) Overall Relative Effect, a measure of the impact that a small change in the biomass of a FG has on the biomass of all other FGs in the food web. Keystoneness and overall relative effect are obtained from the mixed trophic impact, according Libralato et al., (2006).

Ecological indicators of the entire food webs are calculated based on network analysis (Ulanowicz, 1986). We considered Total System Throughput (TST) as a measure of size of the system (Finn, 1976) and its metabolism (Ortiz-Zayas et al., 2005). TST consists of total consumption (TC), total exports (TEX), total respiration (TR), and total flows into detritus (TDET). To characterize the overall activity of the ecosystem, we considered total primary production (TPP) and total biomass (TB) (Ortiz-Zayas et al., 2005). Net system production (NSP), the difference value between TPP and TR, represents the sum of the productivity of all producers. TPP/TR describes system maturity (Odum, 1969; Christensen, 1995). Connectance index (CI) and System Omnivory Index (SOI) reflect the complexity of the internal connections within the system (Christensen & Walters, 2004; Libralato, 2013).

3.2.2 Defining of functional groups and data source.

The model comprises FGs and single species. FGs represent the studied rocky reef and were chosen based on previous studies and literature for both Forest and Barren areas of the studied regions (Bianchelli et al., 2016; Pinna et al., 2020). Species were aggregated into FGs based on similarities in ecological roles, diet, habitat use, and size. In particular, the models include 12 fish groups, 11 groups of benthic megafauna, 15 groups of benthic macrofauna, 1 group of meiofauna. Additionally, 2 plankton groups, 2 detritus groups, and 5 benthic primary producer groups were considered. Single species components such as the sea urchins *P. lividus*, *A. lixula*, the bearded fireworm *Hermodice carunculata*

and the octopus *Octopus vulgaris* were included based on their abundance and ecological role (Tab. 3.2.1)

N.	Group name	Short description	Taxon
1	PesUAd	Fish preying upon adult sea urchin	<i>Diplodus sargus, Diplodus vulgaris</i>
2	PesUJu	Fish preying upon juvenile sea urchin	<i>Coris julis, Thalassoma pavo</i>
3	PesPePL	Pelagic planktivore fish	<i>Atherina boyeri</i>
4	PesNO	Benthopelagic omnivore fishes	<i>Liza aurata, Mugil cephalus</i>
5	PesNPL	Benthopelagic planktivore fish	<i>Boops boops</i>
6	PesNP	Benthopelagic piscivore fishes	<i>Dentex dentex, Epinephelus costae, Epinephelus marginatus</i>
7	PesNE	Benthopelagic herbivore fishes	<i>Sparisoma cretense</i>
8	PesNC	Benthopelagic carnivore fishes	<i>Apogon imberbis, Chromis chromis, Dicentrarchus labrax, Diplodus annularis, Diplodus puntazzo, Labrus merula, Oblada melanura, Seriola dumerilii, Serranus cabrilla, Serranus scriba, Sparus aurata, Spondylisoma cantharus, Symphodus cinereus, Symphodus doderleini, Symphodus mediterraneus, Symphodus melanocercus, Symphodus ocellatus, Symphodus roissali, Symphodus rostratus, Symphodus tinca</i>
9	PesCrO	Cryptic omnivore fishes	<i>Gobius bucchichi, P. sanguinolentus, Parablennius rouxi, Parablennius zvonimiri</i>
10	PesBP	Benthic piscivore fishes	<i>Muraena helena</i>
11	PesBE	Benthic herbivore fishes	<i>Sarpa salpa</i>
12	PesBC	Benthic carnivore fishes	<i>Mullus surmuletus, Scorpaena porcus/maderensis</i>
13	Octvu	Octopus	<i>Octopus vulgaris</i>
14	Arlix	Sea urchin	<i>Arbacia lixula</i>
15	Paliv	Sea urchin	<i>Paracentrotus lividus</i>
16	Hermo	Fireworm	<i>Hermodice carunculata</i>
17	Ophiu	Brittle star	<i>Ophiura spp.</i>
18	MTunF	Tunicates	<i>Halocynthia papillosa, Microcosmus spp.</i>
19	MSclF	Stony corals	<i>Balanophylla spp.</i>
20	MPorF	Sponges	<i>Protula spp., Chondrilla nucula, Chondrosia reniformis, Cliona spp., Encrusting red sponge, Ircinia spp., Keratosa, Petrosia spp.</i>
21	MPolF	Polychaetes, filter feeders (>2cm)	<i>Protula spp., Sabella spallanzani, Terebellidae</i>
22	MOloD	Sea cucumber	<i>Holothuria forskali, Holothuria tubulosa, Holothuria polii</i>
23	MMolS	Whelk	<i>Hexaplex trunculus</i>
24	MMolF	Bivalves	<i>Arcidae, Gastrochaena spp., Ostrea edulis</i>
25	MBriF	Bryozoans	<i>Schizoporellidae</i>
26	MAstO	Omnivore sea stars	<i>Echinaster sepositus, Hacelia attenuata, Ophidiaster ophidianus</i>
27	MAstC	Carnivorous sea stars	<i>Marthasterias glacialis</i>
28	meiof	Meiofauna	
29	mSipD	Sipuncula	
30	mPolFf	Filter feeder polychaetes	
31	mPolE	Herbivore polychaetes	
32	mPolD	Detritivore polychaetes	
33	mPolC	Carnivore polychaetes	
34	mMollo	Omnivore gasteropods	

35	mMollF	Filter feeder molluscs	
36	mMollE	Herbivore molluscs	
37	mMollC	Carnivore molluscs	
38	mDecO	Omnivore decapods	
39	mAmpO	Omnivore amphipods	
40	mAmpF	Filter feeder amphipods	
41	mAmpD	Detritivore amphipods	
42	mAmpC	Carnivore amphipods	
43	ZooPL	Zooplankton	
44	PhytoPL	Phytoplankton	
45	Encr	Encrusting coralline algae	
46	Turf	Turf algae	
47	EA	Corticated algae	
48	Cys	Leathery macrophyte	
49	Mphyto	Microphytobenthos	

Tab 2.3.1- Description of the functional groups

Biomass estimation of the benthic organisms in barren grounds and macroalgal forest alternative states is based on both literature and data collected during two sampling campaigns conducted in June 2014 and 2015. Data were collected at two sites, Croatia and Montenegro (approximately 100 km apart), where two areas (approximately 100 m apart) at a depth of 6 m were randomly chosen in both barren grounds and macroalgal forest states of the sublittoral rocky ecosystem (Fig. 3.2.1).

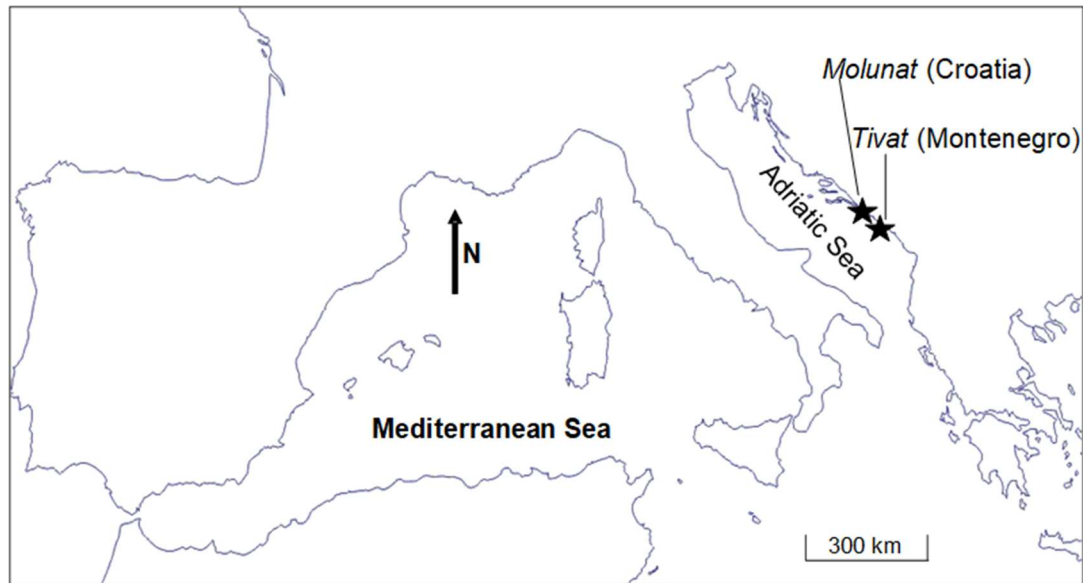


Fig. 3.2.1 Map of the study sites.

During the sampling campaigns, the collection of benthic organisms (following the methodology described in Piazzzi et al., 2018; Pinna et al., 2020) and the visual censuses of megafauna (methodology described in the first chapter of this thesis) and fish (following the methodology described in Harmelin-Vivien and Harmelin, 1975) were conducted. Mean macroalgal biomass was measured as dry biomass, microphytobenthos biomass was estimated by subtraction of the wet weight of macroalgae from the total algal wet weight, biomass of macrofauna was either measured as dry weight (in the case of molluscs and polychaetes) or estimated from measurements of abundance (for crustaceans). Biomass of megafauna and fish was calculated on the basis of their relative abundance and published length-weight relationships. Biomass of lower TLs (zooplankton, phytoplankton) and detritus groups were estimated from the output of Adriatic Sea Ecopath models (Piroddi et al., 2015). Biomass was expressed as dry weight, and conversion factors were applied whereas appropriate (Reed et al., 2016; Ricciardi & Bourget, 1998). Species-specific parameters and dietary data were compiled mainly from publicly available published and unpublished information, as detailed in Table 3.2.2

N.	Functional group	Small description	Diet	P/B	Q/B
1	PesUAd	Fish predating on adult sea urchin	Osman et al. 2009; Guidetti 2006	Mertz and Myers 1998, www.fishbase.org	www.fishbase.org
2	PesUJu	Fish predating on juvenile sea urchin	Kabasakal 2001; Sinopoli et al. 2017	www.fishbase.org	www.fishbase.org
3	PesPePL	Fish predating on pelagic planktivorous fish	Trabelsi 1994	www.fishbase.org	www.fishbase.org
4	PesNO	Benthopelagic omnivorous fish	Cardona 2001	www.fishbase.org	www.fishbase.org
5	PesNPL	Benthopelagic planktivorous fish	Milisenza et al. 2014; Derbal 2008	Brando et al. 2014	www.fishbase.org
6	PesNP	Benthopelagic piscivorous fish	El-Fergani 2014; Renones et al. 2002; Lopez & Orvay 2005	Mertz and Myers 1998, www.fishbase.org	www.fishbase.org
7	PesNE	Benthopelagic herbivorous fish	Azzurro et al. 2007	www.fishbase.org	www.fishbase.org
8	PesNC	Benthopelagic carnivorous fish	Arculeo et al. 1993; Bell & Harmelin 1993; Bradai et al. 1998; Bussotti et al. 2018; Ouannes-Ghorbel & Bouain 2006; Ouannes-Ghorbel et al. 2005; Matić-Skoko et al. 2004; Slama et al. 2007; Pallaoro 2004; Pipitone & Andaloro 1995; Rogdakis et al. 2010; Stergiou & Karpouzi 2002;	www.fishbase.org	www.fishbase.org
9	PesCrO	Cryptic omnivore fish	Stergiou & Karpouzi 2002	www.fishbase.org	www.fishbase.org
10	PesBP	Benthic piscivorous fish	Matić-Skoko et al. 2010	www.fishbase.org	www.fishbase.org
11	PesBE	Benthic herbivorous fish	Dobroslavić et al. 2013	www.fishbase.org	www.fishbase.org
12	PesBC	Benthic carnivorous fish	Labropoulou & Eleftheriou 1997; Pallaoro & Jardas 1991	Mertz and Myers 1998, www.fishbase.org	www.fishbase.org
13	Octvu	<i>Octopus vulgaris</i>	Guerra 1978	Empirical equation (Bray 2001)	Boyle 1990, Wells and Clarke 1996
14	Arlix	<i>Arbacia lixula</i>	Agnetta et al. 2013; Frantzis et al. 1988	Albouy et al. 2010	Empirical equation (Brey 2010)
15	Paliv	<i>Paracentrotus lividus</i>	Agnetta et al. 2013; Frantzis et al. 1989		Empirical equation (Brey 2010)

16	Hermo	<i>Hermodice carunculata</i>	Simonini et al. 2018; Righi et al. 2020	Romano et al. 2016	Empirical equation (Brey 2010)
17	Ophiu	<i>Ophiura</i> spp.	Carlier et al. 2007	Romano et al. 2016	Empirical equation (Brey 2010)
18	MTunF	Tunicates	Filter feeders	Romano et al. 2016	Empirical equation (Brey 2010)
19	MScIF	Stony corals	Filter feeders	Romano et al. 2016	Empirical equation (Brey 2010)
20	MPorF	Sponges	Filter feeders	Romano et al. 2016	Empirical equation (Brey 2010)
21	MPolF	Filter feeder polychaetes	Filter feeders	Romano et al. 2016	Empirical equation (Brey 2010)
22	MOloD	Sea cucumber	Deposit feeders	Romano et al. 2016	Empirical equation (Brey 2010)
23	MMolS	<i>Hexaplex trunculus</i>	Sawyer et al. 2008	Romano et al. 2016	Empirical equation (Brey 2010)
24	MMolF	Bivalves	Filter feeders	Romano et al. 2016	Empirical equation (Brey 2010)
25	MBriF	Bryozoans	Filter feeders	Romano et al. 2016	Empirical equation (Brey 2010)
26	MAstO	Omnivore sea stars	Di Trapani et al. 2020	Romano et al. 2016	Empirical equation (Brey 2010)
27	MAstC	Carnivore sea star	Gianguzza et al. 2016	Romano et al. 2016	Empirical equation (Brey 2010)
28	meiof	Meiofauna	General knowledge	Romano et al. 2016	Empirical equation (Brey 2010)
29	mSipD	Sipuncula	Jumars et al. 2015	Romano et al. 2016	Empirical equation (Brey 2010)
30	mPolFf	Filter feeder polychaetes	Jumars et al. 2015	Romano et al. 2016	Empirical equation (Brey 2010)
31	mPolE	Herbivore polychaetes	Jumars et al. 2015	Romano et al. 2016	Empirical equation (Brey 2010)
32	mPolD	Detritivore polychaetes	Jumars et al. 2015	Romano et al. 2016	Empirical equation (Brey 2010)
33	mPolC	Carnivore polychaetes	Jumars et al. 2015	Romano et al. 2016	Empirical equation (Brey 2010)
34	mMollo	Omnivore gasteropods	General knowledge	Romano et al. 2016	Empirical equation (Brey 2010)

35	mMollF	Filter feeder molluscs	General knowledge	Romano et al. 2016	Empirical equation (Brey 2010)
36	mMollE	Herbivore molluscs	General knowledge	Romano et al. 2016	Empirical equation (Brey 2010)
37	mMollC	Carnivore molluscs	General knowledge	Romano et al. 2016	Empirical equation (Brey 2010)
38	mDecO	Omnivore decapods	General knowledge	Romano et al. 2016	Empirical equation (Brey 2010)
39	mAmpO	Omnivore amphipods	Guerra Garcia et al. 2014	Romano et al. 2016	Empirical equation (Brey 2010)
40	mAmpF	Filter feeder amphipods	Guerra Garcia et al. 2014	Romano et al. 2016	Empirical equation (Brey 2010)
41	mAmpD	Detritivore amphipods	Guerra Garcia et al. 2014	Romano et al. 2016	Empirical equation (Brey 2010)
42	mAmpC	Carnivore amphipods	Guerra Garcia et al. 2014	Romano et al. 2016	Empirical equation (Brey 2010)
43	ZooPL			OPATM-BFM	OPATM-BFM
44	PhytoPL			OPATM-BFM	OPATM-BFM
45	Encr	Encrusting coralline algae		Duarte and Cebrián 1996	
46	Turf	Turf algae		Duarte and Cebrián 1996	
47	EA	Corticated algae		Duarte and Cebrián 1996	
48	Cys	Leathery macrophyte		Duarte and Cebrián 1996	

Tab 2.3.2- Functional groups and source for parameters and dietary data.

Input parameters (i.e., production per unit of biomass, P/B; and consumption per unit biomass, Q/B, were estimated from empirical parameters) and data on the diet of each FG were obtained as the weighted average of the values available for the species in that group (Table 3.2.3), with the proportion of local species biomass within the group used as the weighting factor.

Number Group name	Forest	Barren	Forest	Barren	Forest	Barren	Forest	Barren	Forest	Barren
	TL		B		P/B	Q/B	EE		P/C	
1.PesUAd	2.7	2.7	0.5	0.5	1.7	5.4	0.0000	0.0000	0.3148	0.3148
2.PesUJu	2.4	2.5	0.1	0.2	1.7	5.4	0.0000	0.0000	0.3148	0.3148
3.PesPePL	2.7	2.7	0.0	0.0	0.9	10.3	0.9439	0.3490	0.0913	0.0913
4.PesNO	2.9	2.9	0.0	0.1	1.1	10.8	0.7366	0.7920	0.0991	0.0991
5.PesNPL	3.0	3.0	0.0	0.0	1.4	5.0	0.9494	0.6074	0.2700	0.2700
6.PesNPL	2.9	2.9	0.1	0.0	0.6	2.6	0.5213	0.4288	0.2190	0.2192
7.PesNPL	2.0	2.0	0.1	0.0	0.8	12.0	0.3204	0.2440	0.0648	0.0648
8.PesNC	2.5	2.6	0.7	0.4	1.6	5.3	0.4961	0.8247	0.2996	0.3047
9.PesCrO	2.3	2.3	0.0	0.0	0.7	5.7	0.5199	0.9333	0.1272	0.1272
10.PesBP	3.3	3.3	0.0	0.0	0.7	3.2	0.6363	0.8070	0.2200	0.2188
11.PesBE	2.0	2.0	0.1	0.0	0.8	3.9	0.1019	0.9202	0.2000	0.2000
12.PesBC	2.9	3.0	0.0	0.1	1.0	4.3	0.8534	0.2156	0.2188	0.2194
13.Octvu	2.1	2.9	0.3	0.1	1.8	12.0	0.0726	0.1895	0.1477	0.1477
14.Arlix	2.2	2.0	2.4	30.6	0.5	2.9	0.1335	0.0124	0.1742	0.1742
15.Paliv	2.0	2.0	9.8	54.2	0.4	1.5	0.0615	0.0120	0.2397	0.2403
16.Hermo	2.3	2.2	0.0	0.1	6.2	31.1	0.0000	0.0000	0.2000	0.2000
17.Ophiu	2.6	2.5	0.1	0.0	2.7	12.2	0.4791	0.9360	0.2182	0.2181
18.MTunF	2.0	2.0	1.2	1.4	0.4	3.6	0.0397	0.2724	0.1052	0.1050
19.MScIF	2.0	2.0	0.0	0.1	1.4	6.0	0.0106	0.0724	0.2383	0.2383
20.MPorF	2.0	2.0	37.3	32.4	0.0	0.8	0.8838	0.7328	0.0225	0.0250
21.MPolF	2.0	2.0	0.0	0.0	6.2	15.5	0.8205	0.1874	0.4016	0.4015
22.MOloD	2.0	2.0	0.2	0.4	0.4	3.3	0.0346	0.2352	0.1310	0.1317
23.MMolS	2.2	2.2	0.0	0.4	4.0	22.2	0.0036	0.0471	0.1800	0.1800
24.MMolF	2.0	2.0	0.0	1.0	6.3	29.9	0.6388	0.2688	0.2100	0.2100
25.MBriF	2.0	2.0	0.0	0.1	0.2	0.8	0.7256	0.8559	0.2500	0.2500
26.MAstO	2.2	2.3	0.6	0.5	0.5	3.2	0.0311	0.2182	0.1512	0.1512
27.MAstC	3.1	3.1	0.0	0.1	0.3	1.3	0.0000	0.0000	0.1970	0.1970
28.meiof	2.0	2.0	0.2	0.0	9.0	36.0	0.5908	0.6571	0.2500	0.2500
29.mSipD	2.0	2.0	3.3	2.6	8.0	32.0	0.2400	0.2482	0.2500	0.2501
30.mPolFf	2.0	2.0	0.7	0.1	6.2	15.5	0.0684	0.4781	0.4016	0.4015
31.mPolE	2.0	2.0	0.6	0.0	6.2	15.5	0.0269	0.7771	0.4016	0.4015
32.mPolD	2.0	2.0	1.1	0.1	6.2	15.5	0.0340	0.8818	0.4016	0.4015
33.mPolC	2.1	2.1	2.6	0.4	6.2	15.5	0.0578	0.6549	0.4016	0.4015
34.mMollO	2.0	2.0	0.0	0.0	6.8	29.5	0.0984	0.9755	0.2298	0.2297
35.mMollF	2.0	2.0	0.1	0.1	6.3	29.9	0.8246	0.8836	0.2100	0.2100
36.mMollE	2.0	2.0	0.0	0.0	0.3	11.7	0.1998	0.8526	0.0291	0.0291
37.mMollC	2.5	2.5	0.0	0.0	6.8	37.2	0.7123	0.9097	0.1824	0.1823
38.mDecO	2.1	2.1	0.1	0.0	2.1	11.2	0.2128	0.7510	0.1851	0.1848
39.mAmpO	2.0	2.2	0.5	0.0	6.0	27.8	0.0353	0.9402	0.2156	0.2157
40.mAmpF	2.0	2.0	0.0	0.0	6.0	27.8	0.6690	0.6987	0.2156	0.2157
41.mAmpD	2.0	2.1	0.7	0.0	6.0	27.8	0.0238	0.8728	0.2156	0.2157

Table 3.2.3- Final parameters for ECOPATH models representing the *Cystoseira* macroalgal forest and barren ground alternative states of the Mediterranean rocky subtidal ecosystem. TL stands for Trophic Level, B stands for Biomass [as tons per km⁻², dry weight], P/B for turnover rate [as year⁻¹], Q/B for consumption rate [as year⁻¹], EE for Ecotrophic Efficiency [dimensionless], and P/C

The initial Ecopath model, constructed based on the input parameters outlined in (Table 3.2.3), underwent an evaluation through a pre-balancing analysis (PREBAL), (Heymans et al., 2016). This assessment aimed to determine the coherence of the data with fundamental ecological principles. Several diagnostics were employed in this study to examine: biomass variation across taxa/trophic levels (with biomass ideally spanning 5–7 orders of magnitude and exhibiting a slope of 5–10% decline on a logarithmic scale), vital rates across taxa/trophic levels (expected to generally decline with increasing trophic level), the growth efficiency rate P/Q (ideally <0.5), the Respiration/Assimilation rate (expected to be <1), and the Ecotrophic Efficiency (EE) (expected to be <1).

3.3 Results

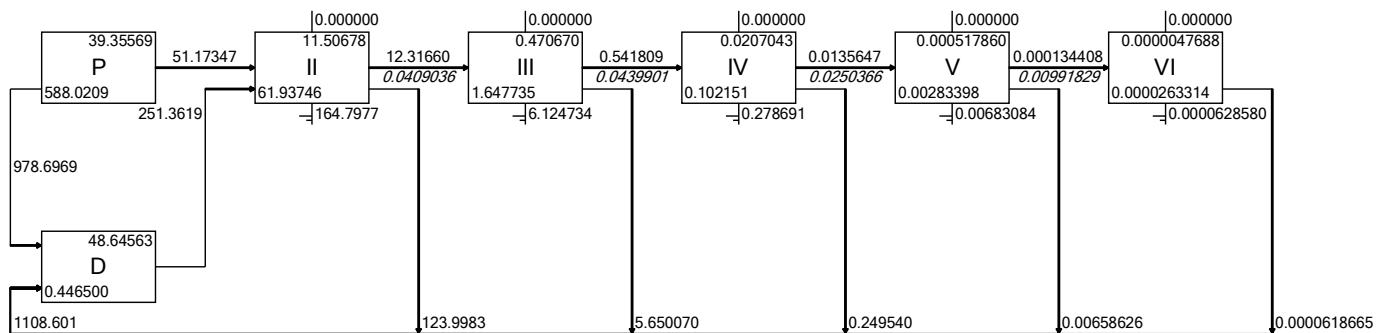
3.3.1 Characteristics of Ecosystem energy flow

According to the two balanced models, barren grounds and macroalgal forest states of Mediterranean sublittoral rocky ecosystems possess seven and six theoretical trophic levels (TLs), respectively. Most energy transfer occurs within the first three levels, accounting for over 99% of total system throughput (TST) in both ecosystem alternative states (Fig. 3.2.1). Biomass decreases as the trophic level increases, conforming to the vertex-up Eltonian pyramid model (Fig. 3.2.2). TL 1 includes detritus, macrophytes, phytoplankton, and microphytobenthos, while the higher TLs include macrofauna, megafauna, and fish. Carnivorous amphipods, the benthopelagic planktivorous fish *Boops boops*, the carnivorous sea star *Marthasterias glacialis*, and the benthic piscivorous *Muraena helena* exhibit higher values at TL 3 or above in both food webs. Energy flows in both models either derive directly from detritus or indirectly from primary production through detritus- and grazing-based food chains (Fig. 3.2.2). The Lindemann Spine illustrates a significant proportion of energy flow from the first to the second level and into the detritus pool. The total energy input into the detritus pool amounts to 452.75 and 1125.30 t km⁻² year⁻¹ in barren and forest ecosystems, respectively, with primary producers contributing 88.45% in forests and 69.86% in barren ecosystems, and TL II taxa contributing 11.02% and 28.92%, respectively. The total primary production (TPP) in macroalgal forest and barren ground ecosystems was 1046.09 and 446.98 t km⁻² year⁻¹, respectively, with 95.15% and 70.76% of this production flowing into detritus (Fig. 3.2.2). A total of 224 and 251 t km⁻² year⁻¹ of detritus was consumed by TL II, with 123 and 131 t km⁻² year⁻¹ returning to the detritus pool in barren and forest states, respectively.

Overall, the mean trophic efficiency (MTE) in the forest ecosystem (3.56%) was slightly lower than in the barren state (4.38%). These values are below the desired Lindeman efficiency of 10%, indicating low MTE values consistent with findings from extensive meta-analyses of marine ecosystem models (Heymans et al., 2014). The MTE from detritus was higher than that from primary producers in both ecosystems. Moreover, MTE from detritus was higher in the barren than in the forest state (4.98% vs.

3.70%), while MTE from primary producers showed low values in both ecosystems (2.52% and 2.54% in forest and barren models, respectively). Based on the Lindeman spine, the highest transfer efficiency was observed in TL II for both systems.

FOREST



BARREN

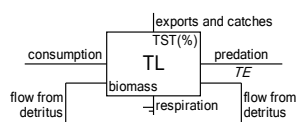
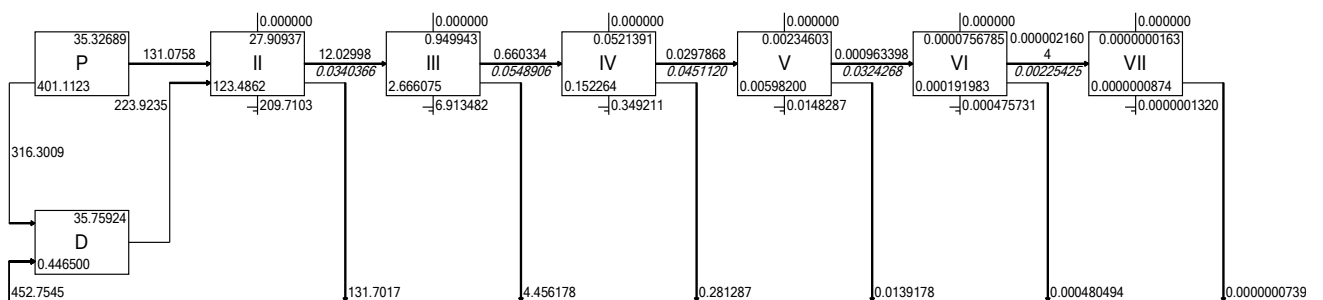


Fig. 3.3.1 Lindeman spine diagram at algae forest and barren grounds ecosystems of Mediterranean rocky reef

3.3.2 Differential Biomass and Production Distribution in Forest and Barren States

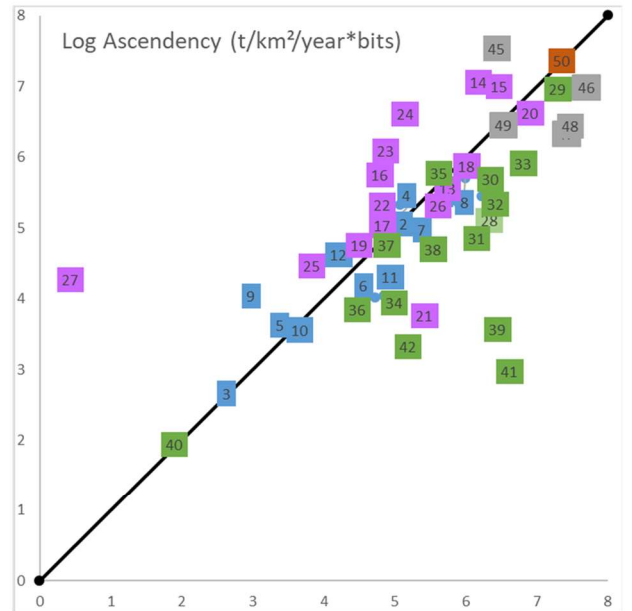
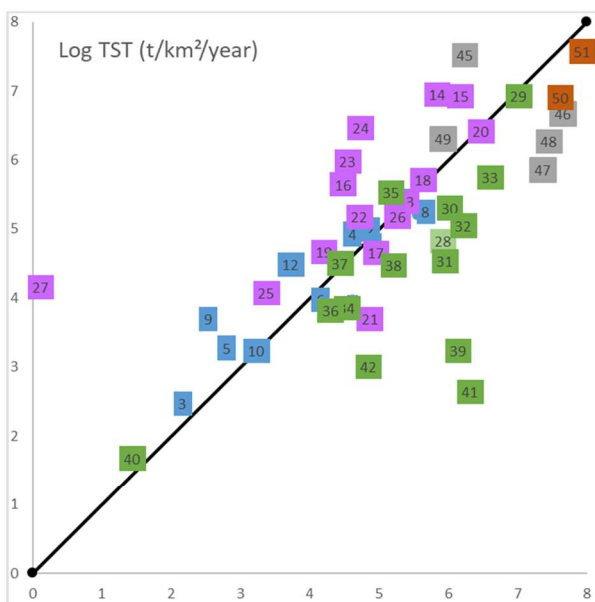
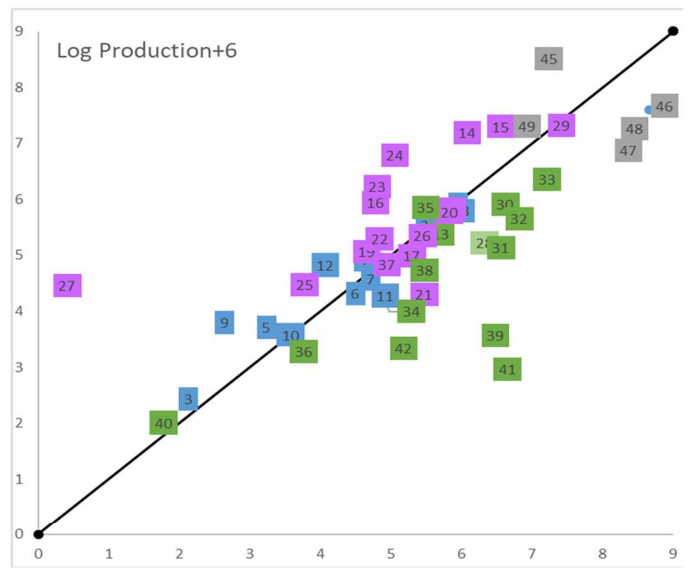
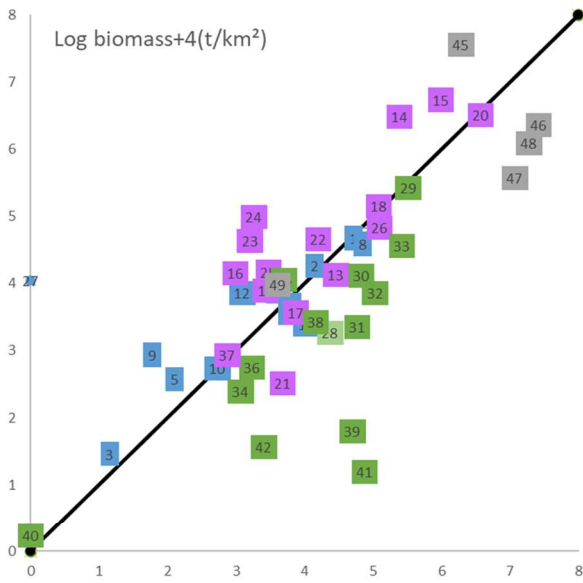
Macroalgal forest and barren ground states are characterized by distinct distributions of biomass and production among the groups considered in the two models. High amounts of erect algae in the forest state correlate with increased biomass and production of meiofauna and macrofauna, while large amounts of crustose algae in the barren state correspond to high biomass and production of megafauna (Tab. 3.2.3; Fig.3.3.2). Despite both states featuring the same trophic links, the differing biomass distributions lead to a reconfiguration of biomass-flow intensities, affecting the potential roles of various functional groups within each state.

Generally, system throughput (ST) and flow to detritus from encrusting algae, microphytobenthos, and megafauna are higher in the barren ground food web than in the macroalgal forest food web. Conversely, erect algae, meiofauna, and macrofauna exhibit higher values in the forest state (Figs. 3.3.2; 3.3.3; 3.3.4). Specifically, in the barren state, encrusting coralline algae (FG 45) display the highest values of both ST and relative ascendancy. In contrast, in the forest state, the highest values are observed for corticated algae (FG 47), leathery macrophytes (FG 48) and turf (FG 46) (Figs. 3.3.3 and 3.3.4). Regarding metazoans, omnivorous sea urchins *A. lixula* (FG 14) and *P. lividus* (FG 15), along with carnivorous sea stars (FG 27), show a notable increase in TST and relative ascendancy from the forest to the barren state. Conversely, polychaetes (FGs 30, 31, 32, 33) and amphipods (FGs 39, 41, 42) showed higher values in the macroalgal forest state (Fig. 3.3.3). Sipunculid worms (FG 29) and sponges (FG 20) maintain high values of ST and relative ascendancy in both states.

These trends indicate varying overall relative effects and keystone indices between the two alternative states. For example, megafauna such as omnivorous sea urchins (FGs 14 and 15), omnivorous and carnivorous starfish (FGs 26 and 27), scavengers *Hermodice carunculata* and *Hexaplex trunculus* (FGs 16 and 23), and bivalves (FG 24) exhibited higher values of overall relative effects in the barren state compared to the forest state (Fig. 3.3.3). In contrast, macrofauna groups (omnivores, herbivores, and detritivores) show an opposite trend (Fig. 3.3.3).

Among invertebrate groups, the fireworm *H. carunculata* (FG 16) and the sea urchin *P. lividus* (FG 15) showed the highest values of keystones in the barren ground food web, whereas brittle stars (FG 17) held that distinction in the macroalgal forest web (Fig. 3). Regarding fish, predators of adult sea urchins and benthopelagic carnivorous fish (FGs 1 and 8) showed high values of overall effect and keystone index in both food web models (Fig. 3.3.3).

BARREN



FOREST

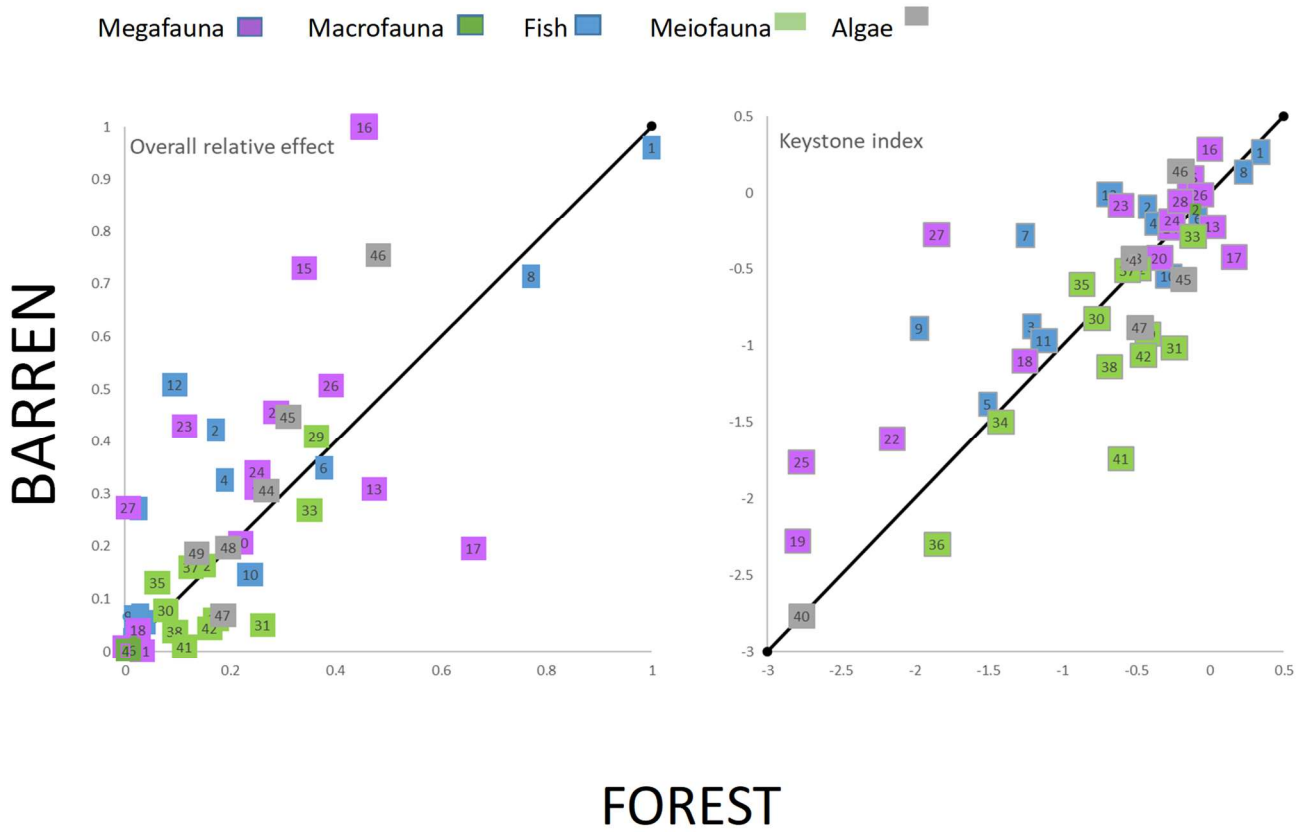


Fig. 3.3.2 - Comparison between food-web indicators of the macroalgae forest (on the horizontal axis) and barren grounds (on the vertical axis). Numbers refers to food groups (FGs) codes.

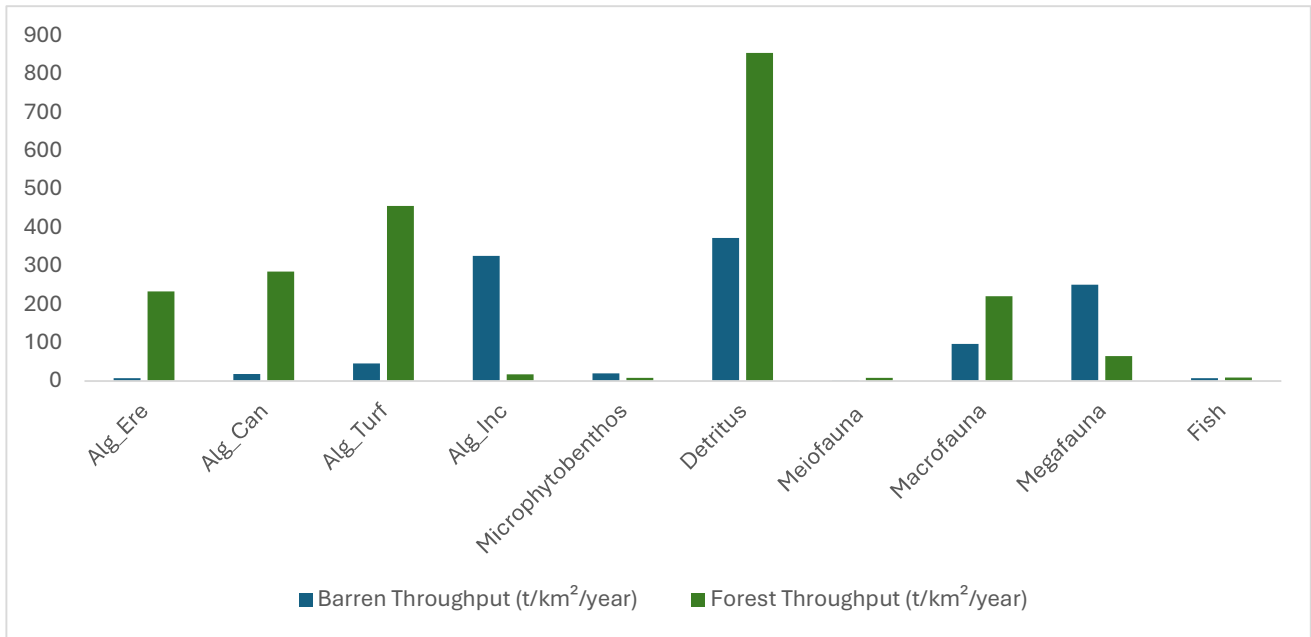


Fig.3.3.3 – System throughput in macroalgae forest and barren grounds in rocky sublittoral ecosystems of the Mediterranean Sea.

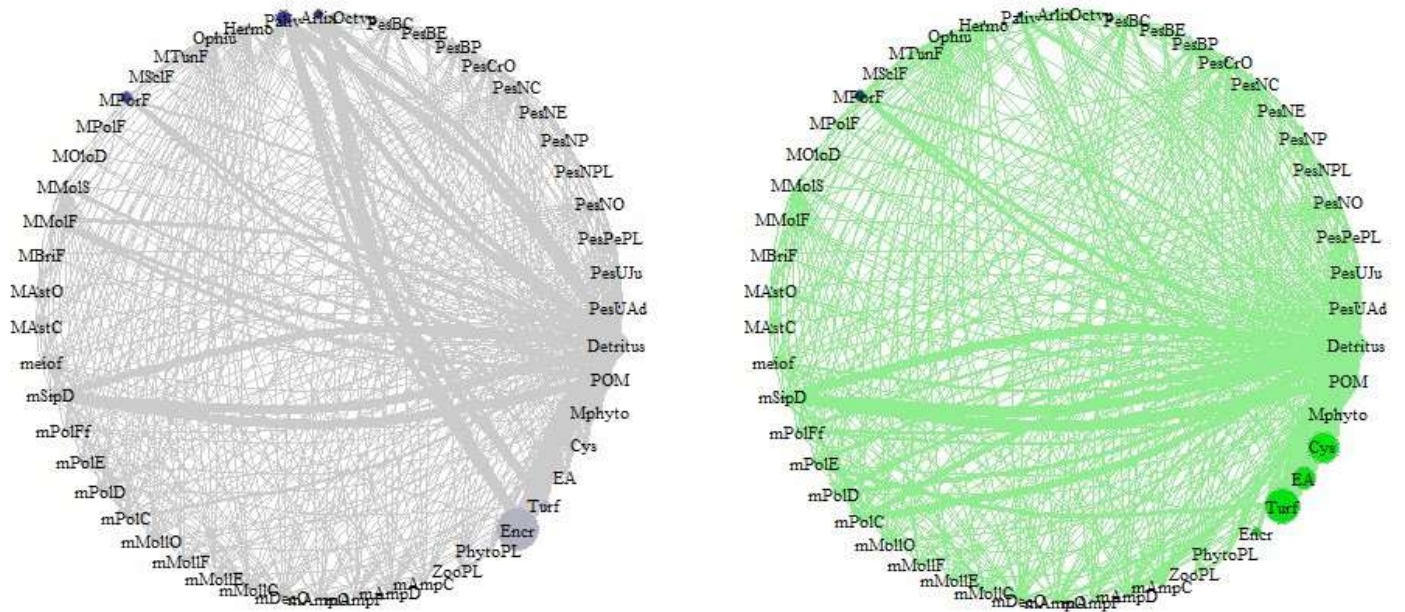


Fig. 3.3.4 - Comparison between biomass flows in the food webs of macroalgae forest and barren ground states of the Mediterranean subtidal rocky community.

3.3.3 Network flow indicators

Summary statistics and indicators of network flow and ecosystem structure for the food webs of each alternative state of Mediterranean rocky sublittoral communities are provided in Table 3.3.1. In the barren ground state, the Total System Throughput (TST) was $1266.42 \text{ t km}^{-2} \text{ year}^{-1}$, with Total Consumption (TC) contributing 29.04%, Total Exports (TEX) 18.07%, Total Respiration (TR) 17.13%, and Total Flow into Detritus (TDET) 35.76%. Conversely, in the macroalgal forest state, TST reached $2616.86 \text{ t km}^{-2} \text{ year}^{-1}$, with TC accounting for 12.05%, exports for 32.76%, respiration for 6.54%, and flow to detritus for 48.65%.

Although both food webs exhibited high TDET values, it was notably higher in the macroalgal forest state, indicating that recycling was the primary means of energy utilization in both states, with energy underutilization observed in both cases. The Total Primary Production/Total Respiration ratio (TPP/TR) was higher in the macroalgal forest than in the barren ground food web, while the Connectance Index (CI) and Omnivory Index were similar in both systems.

	Barren	Forest
Total consumption, TC	367.74	315.44
Total export, TEX	228.83	857.23
Total respiration, TR	216.99	171.21
Total flows into detritus, TDET	452.85	1272.98
Total system throughput, TST	1266.42	2616.86
Total production, TP	524.58	1111.02
Net system production, NSP	447.38	1029.87
Total primary production/total respiration, TPP/TR	2.06	6.02
Total biomass (excluding detritus)	527.42	651.71
Connectance Index	0.16	0.16
System Omnivory Index	0.09	0.09

Tab.3.3.1- Indicators of network flow and ecosystem structure for the food webs of the alternative states (either barren grounds or macroalgal forests) of the Mediterranean rocky sublittoral community.

3.4 Discussion

Two food-web models were constructed for each of the two alternative states of the Mediterranean rocky sublittoral community, based on *in situ* data: the macroalgal forest state dominated by erect algae and the barren ground state dominated by encrusting coralline algae. The distinct algal assemblages significantly influenced the total primary production, which was twice as large in the macroalgal forest state compared to the barren ground state, consequently impacting the structure and functioning of the entire community.

Both food web models were characterized by the predominance of consumers with low trophic levels (TLs), possibly due to the small size of the studied system (Heymans et al., 2014) and the relatively high standing crop of benthic macroalgae in each state (erect and encrusting macroalgae respectively in the forest and barren states) (Wu et al., 2016). The Lindemann spine analysis showed a large proportion of energy flowing into detritus from TL I in both food webs, although this proportion was higher in the macroalgal forest state by approximately 18%. In the macroalgal forest, a significant portion of the algae likely decays and settles on the seafloor, where it is decomposed by bacteria, providing energy to TL II through the detritus-based pathway (Schaal et al., 2010). Approximately half of the detritus consumed by TL II returned to the detritus pool in both models, indicating the significant role of TL II in system recycling. The mean transfer efficiency from detritus confirmed the importance of recycling in supporting the stability of both food web models (Vasconcellos et al., 1997).

Indicators revealed that the two food web models were supported by different functional groups: mega- and macro-fauna in the barren ground and macroalgal forest food web models, respectively. In the barren ground food web, sea urchins exhibited high values of biomass, total system throughput (TST), ascendancy, and overall effect. Omnivorous sea urchins may play a pivotal role in matter recycling, feeding on encrusting organisms, detritus, and microphytobenthos, and producing feces that, when degraded by bacteria, contribute to the detritus-based pathway (Krumhansl & Scheibling, 2012b; Mamelona & Pelletier, 2005). Similarly, sea urchins such as *Arbacia lixula* and *Paracentrotus lividus* can exploit resources present in the barren by grazing on corallines and consuming benthic organisms

(in the case of *A. lixula*) or feeding on drift algae and detritus (when it comes to *P. lividus*) (Agnetta et al., 2013), acting as energy hubs by providing food to suspension and deposit feeders in the barren ground web. In our study, the spiny starfish *M. glacialis* showed a high value of overall relative effect in the barren ground food web, indicating its potential role in controlling sea urchin populations there (Galasso et al., 2015). Other groups of benthic megafauna, such as omnivorous starfish, filter feeders (e.g. bivalves), and scavengers (e.g., *Hermodice carunculata* and *Hexaplex trunculus*), exhibited higher values of overall relative effects in the barren ground web compared to the macroalgal forest web. Conversely, the opposite trend was observed for benthic macrofauna groups, indicating their role in the functioning of the forest food web. An exception to this trend was sipunculids and sponges, whose indicators (TST, overall relative effects, and ascendancy) were high in both models. Sipunculids are worm-like invertebrates present in both reef states and are important detritivores in rocky reefs, contributing to the diet of many fishes and invertebrates (Murina, 1984; Hansen, 1978). Sponges are key components of rocky reef communities and potentially play significant ecological roles (e.g., benthopelagic coupling, food sources, and habitat provision for other organisms) in both macroalgal forest and barren ground states of rocky sublittoral communities (Bell, 2008; Di Trapani et al., 2020). Regarding the keystone roles of benthic organisms, we found high values for both turf algae and the fireworm *H. carunculata* in the barren ground food web model. The key role of turf algae is likely linked to that of *P. lividus*; erect macrophytes are an important component of *P. lividus*' diet (Agnetta et al., 2013 and references therein), and turf algae plausibly represent a significant resource for *P. lividus* within barren grounds. Interestingly, *H. carunculata* was found to be the main invertebrate keystone predator in the barren web model. *H. carunculata* is an amphinomid annelid capable of consuming a wide range of marine invertebrates, exploiting dorsal stinging chaetae and their eversible pharynx to capture even large, shielded prey (Simonini et al., 2017, 2018). The diet of *H. carunculata* includes sea urchins, starfish, tube worms, sea cucumbers, and sponges (Righi et al., 2020) and its predatory activity likely stabilizes barren grounds.

In the forest web, we found a high keystone value for brittle stars. It has been shown that brittle star biomass is positively correlated with the abundance of macrofauna and the percentage of sediment organic matter, indicating that brittle stars could enhance rates of benthopelagic coupling and play a key role in reef system functioning (Geraldi et al., 2017). Regarding fish, they are characterized by low values of biomass, productivity, TST, and ascendancy, likely due to the fact that the present study was conducted in a heavily fished area. Nevertheless, benthopelagic carnivorous fish and predators of adult sea urchins (i.e., *Diplodus vulgaris* and *D. sargus*) exhibited high values of overall effect and keystone-ness in both food webs, suggesting that these fish may impact the biomass of other functional groups, contributing to the stability of both food webs. In particular, the here presented results confirm that seabreams play a role in the top-down control of the sublittoral communities in Mediterranean rocky reefs (Guidetti, 2006).

As expected from the Total Primary Production (TPP) data, the Total Production (TP) of the macroalgal forest food web was twice as high as that of the barren ground food web, indicating a higher energy exportation from the forest to other systems. Conversely, we found a higher percentage of flows into detritus and exports in the forest state compared to the barren state, while the opposite trend was observed in respiration and consumption flows, with higher percentages in the barren food web. We found a high value of TPP/TR in both state webs. TPP/TR is an indicator of ecosystem maturity (Odum, 1986). When TPP/TR is close to one, all primary production is used for respiration, thereby leaving no residual production and indicating a mature system. In our study, we found values of TPP/TR higher than one, indicating that the two-food web models are incomplete, and the primary production cannot be fully utilized. This finding likely depends on the virtual absence of key components of the food web resulting from the heavy impact of fishing in the studied area (V. Macic personal communication). Interestingly, TPP/TR was even higher in the macroalgal forest food web, possibly due to the age of the barrens studied (several decades) and the different energy pathways characterizing the two states. We found similar values for the Connectance Index (CI) and System Omnivory Index (SOI), suggesting

that barren grounds and macroalgal forest systems are characterized by similar complexity of interspecies relationships and consequent stability.

In conclusion, our study confirmed that macroalgal forests productivity was higher than that of barren grounds, resulting in higher energy exportation from the macroalgal forests to other systems. However, we also found that energy is effectively stored in barren grounds and may host a diverse megafauna that covers different functional roles, supporting a stable food web, ultimately offsetting the significant reduction in biomass and biodiversity of meio- and macrofauna observed in this system.

4. Unravelling hidden predator-prey interactions among sea urchin juveniles and micropredators by prey DNA amplification

Abstract

Sublittoral rocky reefs may exist in two distinct, alternative states: macroalgal forests characterized by high abundance and biodiversity of macrofauna, and barrensgrounds consisting in an impoverished state dominated by encrusting algae and abundant sea urchins. The barren ground state may persist despite the recovery of adult sea urchin predators, suggesting the existence of additional stabilizing mechanisms. It has been observed that sea urchin settlers rapidly disappear in macroalgal forests but they persist in barren grounds, suggesting that post-settlement predation plays a crucial role in determining sea urchin population density. Visual assessment of predation events in the field is unfeasible due to the microscopic scale of both predators and preys and the complexity of the arena. In this study, specific primers for the detection of mtDNA were designed and tested for the Mediterranean sympatric sea urchin species *Paracentrotus lividus* and *Arbacia lixula* on degraded samples. By testing 379 invertebrates collected in algal forests during an urchin settling event, 44 (13%) potential predators of *P. lividus* settlers we identified, suggesting that micropredation may represent an important process in controlling sea urchin population density and maintaining the macroalgal forest state in temperate rocky reefs.

4.1 Introduction

Rocky reefs may exhibit two alternative, distinct states: Macroalgal forests and barren grounds. Macroalgal forests are characterized by complex architecture and high species diversity, whereas barren grounds are structurally simpler, hosting low diversity and dominated by both sea urchins and encrusting organisms (Ling et al., 2008.; Sala et al., 1998). Transitions from macroalgal forests to barren grounds occur globally due to various factors such as the loss of top-down control on sea urchins, destructive harvesting, or storms (Bonaviri et al., 2009; Jackson et al., 2001; Sala et al., 1998; Steneck et al., 2002). Once a given alternative state is in place, hysteresis mechanisms maintain such a state, even if the previous conditions are restored (Baskett & Salomon, 2010; Scheffer & Carpenter, 2003; Suding et al., 2004). Upon establishment, barren states often see high sea urchin density and biomass, further stabilizing the state (Bonaviri et al., 2017; Gianguzza et al., 2010; Knowlton, 2004; Ling et al., n.d.; Steneck et al., 2002). Research indicates that large predators of adult sea urchins can reverse the coralline barren grounds and sustain macroalgal forests (Ling et al., 2015; Clemente et al., 2009; Guidetti, 2006; Shears & Babcock, 2003; Jackson et al., 2001; Bernstein et al., 1981). However, despite the recovery of adult sea urchin predators, high sea urchin densities and barren communities can persist for years (Filbee-Dexter & Scheibling, 2014; Babcock et al., 2010; Pinnegar et al., 2000), suggesting additional stabilizing mechanisms.

Post-settlement mortality is likely the most important factor determining urchin population density (Andrew and Choat, 1985; Harrold et al., 1991; Jennings and Hunt, 2010, 2011; Pearse and Hines, 1987; Rowley, 1989). After the planktonic larval stage, settlement induction and recruitment, sea urchin density appears independent of community state or conspecific abundance, with young urchin settlers settling patchily equally in both macroalgal forest and barren grounds (Balch and Scheibling, 2000, 2001; Cameron and Schroeter, 1980; Hereu et al., 2004; Hernández et al., 2010; Prado et al., 2009; Privitera et al., 2011; Rowley, 1989). However, settler population rapidly drops in macroalgal forests, despite the presence of structural refuges in forests protects small urchins from predation by fishes. As

a result, adult sea urchins are typically rare in macroalgal forests but abundant in barren grounds. It has long been postulated that invertebrate micropredators are responsible for the control of urchin settlers. Predation is a significant cause of early benthic invertebrate mortality (Gosselin and Qian, 1997; Griffith and Gosselin, 2008; Hunt and Scheibling, 1997; Osman and Whitlatch, 1995, 2004; Osman et al., 1992; Sala and Graham, 2002). Macroalgal forests host a larger abundance and diversity of microfauna including micropredators, than the less complex barren grounds. Consequently, the absence of urchin settlers in macroalgal forests might be the result of substantive predation by some resident invertebrates. Experiments in aquaria showed that several decapod species were able to feed on urchin settlers, especially larger specimens (Bonaviri et al., 2012a; Fagerli et al., 2014). However, the number and variety of invertebrates tested was limited, and aquaria are artificial, oversimplified systems which poorly encompass the real trophic dynamics in the field. Traditional techniques for *in situ* identification of predation events involving marine invertebrates face paramount challenges, due to the small size of both predators and preys, presence of the algal canopy, frequent nocturnal activity, and disturbance by the observer. Mounting of cameras on the seabed may ease some of these problems, but it still presents a limited temporal and spatial arena, often deprived of canopy and other organisms, or where preys are tethered to the substratum. As a result, predation rates measured by visual scoring might be overestimated. Analysis of gut content is plenty of difficulties as well, since many invertebrates are fluid feeders, avoid consuming indigestible remains, or fully digest samples leaving no recognizable material.

In the last decade, several studies have employed environmental DNA (eDNA) to study the trophic interactions in invertebrates (Pompanon et al., 2012; Clare 2014; Cuff et al. 2022). Amplification of prey DNA by polymerase chain reaction (PCR) allows the detection of trace amounts of undigested prey material in predator guts content and in feces.

Here, we applied molecular techniques to untangle the trophic interactions involving sea urchin settlers in Mediterranean forests. In particular, we aimed to: (1) design specific primers for the detection of

DNA of the Mediterranean urchin species *P. lividus* and *Arbacia lixula* in degraded samples; (2) identify the invertebrates belonging to different taxa collected during the urchin settlement stage, by both visual assignment and molecular barcoding; and (3) detect potential consumers of urchin settlers.

The extent of micropredation as a process controlling urchin populations in temperate reefs is discussed.

4.2 Materials and methods

4.2.1 Sample collection

Weekly surveys by SCUBA diving along the coastline of the Montgrí massif (42.8160 N, 03.8130 E), Spain, northwestern Mediterranean Sea, and at one site on the Tyrrhenian coast of Sicily (38.1086 N, 13.5382 E), Italy, central Mediterranean Sea, were conducted in summer 2017 to detect the peak of sea urchin recruits abundance. In July, it was observed the largest number of sea urchin recruits on algal assemblages at between 5 and 8 m depth. Potential micropredators were collected by scraping an algae-covered rocky substrate by SCUBA diving, then sorted under a stereomicroscope in the laboratory the same day of collection. Specimens were individually stored in plastic tubes of 1 to 10 ml of capacity, depending on animal size, subsequently kept at -20 °C until processing. We paid attention to avoid cross-contamination between samples, by changing gloves and cleaning tweezers for each specimen.

Sea urchin juveniles were also collected in the same locations. To collect the small juveniles, the scraped material was placed in a salver containing a thin layer of seawater and covered with a plastic grid. After a few hours, the small sea urchins climbed actively out of the salver onto the surface of the plastic grid, probably in response to oxygen shortage. Sea urchins were then carefully collected with tweezers and individually stored as described above. As a precaution to avoid sea urchin DNA contamination with that of micropredators, the tubes containing sea urchins were stored separately in a different box, in a different freezer.

Adults of *P. lividus* and *A. lixula*, whose DNA was used as positive controls in primer tests, were collected at the Sicilian locality.

4.2.2 Taxonomic identification

Invertebrates were visually classified in two rounds: at the moment of collection, and before DNA extraction. Samples were individually visualized under a stereomicroscope in the laboratory and photographed. With the aid of manuals, we identified the specimens at the lowest possible taxonomic level (Table 4.2.1).

Sample code	Microscopy class	Microscopy family	Tentative identification	taxonomic level of identification	COI identification	% identity sequencing	COI Class	COI Family
86	Polychaeta		Polychaeta	class	Lepidonotus spiculus	82.8	Polychaeta	Polynoidae
87	Polychaeta		Polychaeta	class	Platynereis dumerilii	98.48	Polychaeta	Nereididae
88	Polychaeta		Polychaeta	class	Platynereis dumerilii	99.83	Polychaeta	Nereididae
89	Polychaeta		Polychaeta	class	Polynoidae sp.	83.76	Polychaeta	Polynoidae
90	Polychaeta		Polychaeta	class	Platynereis dumerilii	98.61	Polychaeta	Nereididae
91	Polychaeta		Polychaeta	class	Platynereis dumerilii	97.91	Polychaeta	Nereididae
92	Polychaeta		Polychaeta	class	Platynereis dumerilii	98.2	Polychaeta	Nereididae
93	Polychaeta		Polychaeta	class	Platynereis dumerilii	99.46	Polychaeta	Nereididae
94	Polychaeta		Polychaeta	class	Platynereis dumerilii	100	Polychaeta	Nereididae
215	Malacostraca		Decapoda	order	Pilumnus hirtellus	94.03	Malacostraca	Pilumnidae
216	Malacostraca		Decapoda	order	Austinoerga alayseae	80.18	Malacostraca	Bythograeidae
258	Malacostraca	Alpheidae	Alpheidae	family	Synalpheus gambarelloides	99.61	Malacostraca	Alpheidae
259	Malacostraca	Alpheidae	Alpheidae	family	Synalpheus gambarelloides	100	Malacostraca	Alpheidae
276	Malacostraca		Anomura	infraorder	Cestopagurus timidus	99.05	Malacostraca	Paguridae
385	Malacostraca	Paguridae	Pagurus anachoretus	species	Pagurus emmersoni	85.92	Malacostraca	Paguridae
386	Malacostraca	Paguridae	Pagurus anachoretus	species	Pagurus anachoretus	98.9	Malacostraca	Paguridae
418	Ophiuroidea		Ophiuroidea	class	Ophiothrix sp.	99.13	Ophiuroidea	Ophiotrichidae
419	Ophiuroidea		Ophiuroidea	class	Ophiothrix sp.	99.48	Ophiuroidea	Ophiotrichidae
420	Ophiuroidea		Ophiuroidea	class	Ophiothrix sp.	99.83	Ophiuroidea	Ophiotrichidae
421	Ophiuroidea		Ophiuroidea	class	Ophiothrix sp.	99.3	Ophiuroidea	Ophiotrichidae
95	Polychaeta		Polychaeta	class	Platynereis dumerilii	98.18	Polychaeta	Nereididae
96	Polychaeta		Polychaeta	class	Lepidonotus clava	87.29	Polychaeta	Polynoidae
97	Polychaeta		Polychaeta	class				
217	Malacostraca		Decapoda	order	Acanthonyx lunulatus	98.56	Malacostraca	Epialtidae
218	Malacostraca		Decapoda	order	Pilumnus hirtellus	100	Malacostraca	Pilumnidae
219	Malacostraca		Decapoda	order	Pilumnus villosissimus	98.57	Malacostraca	Pilumnidae
220	Malacostraca		Decapoda	order				
260	Malacostraca	Alpheidae	Alpheidae	family	Synalpheus gambarelloides	100	Malacostraca	Alpheidae
261	Malacostraca	Alpheidae	Alpheidae	family	Synalpheus gambarelloides	99.81	Malacostraca	Alpheidae
262	Malacostraca	Alpheidae	Alpheidae	family	Synalpheus gambarelloides	100	Malacostraca	Alpheidae
340	Malacostraca	Diogenidae	Calcinus tubularis	species	Calcinus tubularis	99.53	Malacostraca	Diogenidae
341	Malacostraca	Diogenidae	Calcinus tubularis	species	Calcinus tubularis	99.69	Malacostraca	Diogenidae
342	Malacostraca	Diogenidae	Calcinus tubularis	species	Pagurus anachoretus	98.54	Malacostraca	Paguridae
387	Malacostraca	Paguridae	Pagurus anachoretus	species	Calcinus tubularis	99.69	Malacostraca	Diogenidae
422	Ophiuroidea		Ophiuroidea	class	Ophiothrix sp.	99.48	Ophiuroidea	Ophiotrichidae

423	Ophiuroidea		Ophiuroidea	class	Ophiothrix sp.	99.65	Ophiuroidea	Ophiotrichidae
424	Ophiuroidea		Ophiuroidea	class	Ophiothrix sp.	99.47	Ophiuroidea	Ophiotrichidae
425	Ophiuroidea		Ophiuroidea	class	Ophiothrix sp.	99.47	Ophiuroidea	Ophiotrichidae
426	Ophiuroidea		Ophiuroidea	class	Ophiothrix sp.	99.65	Ophiuroidea	Ophiotrichidae
427	Ophiuroidea		Ophiuroidea	class	Ophiothrix sp.	99.14	Ophiuroidea	Ophiotrichidae
428	Ophiuroidea		Ophiuroidea	class	Ophiothrix sp.	99.65	Ophiuroidea	Ophiotrichidae
540	Malacostraca		Decapoda	order	Acanthonyx lunulatus	98.38	Malacostraca	Epialtidae
541	Malacostraca		Amphipoda	order	Ampithoe rubricata	88.64	Malacostraca	Ampithoidea
542	Malacostraca	Galatheidae	Galathea	genus	Galathea intermedia	88.94	Malacostraca	Galatheidae
543	Polychaeta	Nereididae	Nereididae	family	Perinereis sp.	88.43	Polychaeta	Nereididae
544	Polychaeta		Polychaeta	class	Harmothoe spinifera	99.18	Polychaeta	Polynoidae
98	Polychaeta		Polychaeta	class	Platynereis dumerilii	98.04	Polychaeta	Nereididae
99	Polychaeta		Polychaeta	class	Lepidonotus clava	85.13	Polychaeta	Polynoidae
100	Polychaeta		Polychaeta	class	Phyllodoce madeirensis	99.01	Polychaeta	Phyllococidae
101	Polychaeta		Polychaeta	class	Platynereis dumerilii	98.19	Polychaeta	Nereididae
102	Polychaeta		Polychaeta	class	Polynoidae sp	89.92	Polychaeta	Polynoidae
103	Polychaeta		Polychaeta	class	Platynereis dumerilii	98.33	Polychaeta	Nereididae
106	Polychaeta		Polychaeta	class	Platynereis dumerilii	99.39	Polychaeta	Nereididae
107	Polychaeta		Polychaeta	class	Lepidonotus clava	87.03	Polychaeta	Polynoidae
108	Polychaeta		Polychaeta	class	Leodice harassii	99.32	Polychaeta	Eunicidae
109	Polychaeta		Polychaeta	class	Lepidonotus clava	86.86	Polychaeta	Polynoidae
111	Polychaeta		Polychaeta	class	Lysidice ninetta	97.53	Polychaeta	Eunicidae
112	Polychaeta		Polychaeta	class	Lysidice ninetta	97.83	Polychaeta	Eunicidae
114	Polychaeta		Polychaeta	class	Lysidice ninetta	97.83	Polychaeta	Eunicidae
115	Polychaeta		Polychaeta	class	Lysidice ninetta	97.83	Polychaeta	Eunicidae
128	Polychaeta		Polychaeta	class	Harmothoe spinifera	99	Polychaeta	Polynoidae
129	Polychaeta		Polychaeta	class	Hediste astae	80.62	Polychaeta	Nereididae
130	Polychaeta		Polychaeta	class	Harmothoe bathydomus	83.56	Polychaeta	Polynoidae
131	Polychaeta		Polychaeta	class	Harmothoe spinifera	99.56	Polychaeta	Polynoidae
132	Polychaeta		Polychaeta	class	Hediste astae	80.74	Polychaeta	Nereididae
133	Polychaeta		Polychaeta	class	Harmothoe bathydomus	83.24	Polychaeta	Polynoidae
141	Polychaeta		Polychaeta	class	Eunicidae sp/Palola	82.59	Polychaeta	Eunicidae
142	Polychaeta		Polychaeta	class	Polynoidae/Gattyana cirrhosa	85.62	Polychaeta	Polynoidae
143	Polychaeta		Polychaeta	class				
144	Polychaeta		Polychaeta	class	Lepidonotus clava	86.99	Polychaeta	Polynoidae
145	Polychaeta		Polychaeta	class	Eunicidae sp/Palola	82.59	Polychaeta	Eunicidae
146	Polychaeta		Polychaeta	class	Eunicidae sp/Palola	82.59	Polychaeta	Eunicidae
147	Polychaeta		Polychaeta	class				
148	Polychaeta		Polychaeta	class	Hediste diversicolor	82.57	Polychaeta	Nereididae
149	Polychaeta		Polychaeta	class	Harmothoe bathydomus/Polynoidae sp	83.23	Polychaeta	Polynoidae
150	Polychaeta		Polychaeta	class	Polynoidae sp/Gattyana cirrhosa/Harmothoe	85.16	Polychaeta	Polynoidae
151	Polychaeta		Polychaeta	class	Lumbrineris sp.	75.15	Polychaeta	Lumbrineridae
152	Polychaeta		Polychaeta	class	Hediste diversicolor	82.53	Polychaeta	Nereididae
154	Polychaeta		Polychaeta	class	Polynoidae sp/Gattyana cirrhosa/Harmothoe	84.71	Polychaeta	Polynoidae
156	Polychaeta		Polychaeta	class	Ampithoe rubricata	88.23	Polychaeta	Nereididae

157	Polychaeta		Polychaeta	class	Perinereis cultrifera/Nereis falsa/Hediste diversicolor	85.8	Polychaeta	Nereididae
163	Polychaeta	Terebellidae	Terebellidae	family	Thelepus hamatus	88.96	Polychaeta	Terebellidae
170	Polychaeta	Terebellidae	Terebellidae	family	Thelepus hamatus	89.05	Polychaeta	Terebellidae
171	Polychaeta	Terebellidae	Terebellidae	family	Thelepus hamatus	89.06	Polychaeta	Terebellidae
172	Polychaeta	Terebellidae	Terebellidae	family				
173	Polychaeta	Terebellidae	Terebellidae	family	Thelepus hamatus	89.06	Polychaeta	Terebellidae
174	Polychaeta	Terebellidae	Terebellidae	family	Perinereis sp.	88.13	Polychaeta	Nereididae
195	Malacostraca		Amphipoda	order	Ampithoe rubricata	88.24	Malacostraca	Ampithoidea
200	Malacostraca		Amphipoda	order	Ampithoe rubricata	88.26	Malacostraca	Ampithoidea
201	Malacostraca		Amphipoda	order	Ampithoe ramondi	91.06	Malacostraca	Ampithoidea
202	Malacostraca		Amphipoda	order				
209	Sipuncula		Sipuncula	order	Phascolosoma granulatum	99.21	Sipuncula	Phascolosomatidae
210	Sipuncula		Sipuncula	order	Phascolosoma granulatum	98.89	Sipuncula	Phascolosomatidae
211	Sipuncula		Sipuncula	order	Phascolosoma granulatum	99.68	Sipuncula	Phascolosomatidae
212	Sipuncula		Sipuncula	order	Phascolosoma granulatum	99.21	Sipuncula	Phascolosomatidae
213	Sipuncula		Sipuncula	order	Phascolosoma granulatum	99.02	Sipuncula	Phascolosomatidae
214	Sipuncula		Sipuncula	order	Phascolosoma granulatum	98.12	Sipuncula	Phascolosomatidae
221	Malacostraca		Decapoda	order	Pilumnus hirtellus	99.68	Malacostraca	Pilumnidae
227	Malacostraca		Decapoda	order	Inachus aguiarii	88.19	Malacostraca	Inachidae
238	Malacostraca		Decapoda	order	Pilumnus villosissimus	98.88	Malacostraca	Pilumnidae
239	Malacostraca		Decapoda	order				
240	Malacostraca	Inachidae	Macropodia longirostris	species	Macropodia rostrata	95.14	Malacostraca	Inachidae
241	Malacostraca	Inachidae	Achaeus cranchii	species	Inachus aguiarii	88.03	Malacostraca	Inachidae
243	Malacostraca	Inachidae	Achaeus cranchii	species	Inachus aguiarii	88.1	Malacostraca	Inachidae
244	Malacostraca	Inachidae	Achaeus cranchii	species	Inachus aguiarii	88.19	Malacostraca	Inachidae
245	Malacostraca	Inachidae	Achaeus cranchii	species	Inachus aguiarii	88.19	Malacostraca	Inachidae
246	Malacostraca	Inachidae	Achaeus cranchii	species	Inachus dorsettensis	87.7	Malacostraca	Inachidae
247	Malacostraca	Majoidea	Majoidea	superfamily	Inachus aguiarii	88.03	Malacostraca	Inachidae
248	Malacostraca	Majoidea	Majoidea	family	Herbstia condyliata	99.36	Malacostraca	Majoidea
249	Malacostraca	Galatheidae	Galathea	genus	Galathea intermedia	88.98	Malacostraca	Galatheidae
254	Malacostraca	Porcellanidae	Pisidia longicornis	species	Synalpheus gambarelloides	100	Malacostraca	Alpheidae
256	Malacostraca	Galatheidae	Galathea	genus	Galathea intermedia	88.47	Malacostraca	Galatheidae
257	Malacostraca	Galatheidae	Galathea	genus	Galathea intermedia	88.92	Malacostraca	Galatheidae
263	Malacostraca	Alpheidae	Alpheus dentipes	species	Synalpheus gambarelloides	99.81	Malacostraca	Alpheidae
264	Malacostraca	Alpheidae	Alpheus dentipes	species	Synalpheus gambarelloides	99.61	Malacostraca	Alpheidae
265	Malacostraca	Alpheidae	Alpheus	genus	Synalpheus gambarelloides	100	Malacostraca	Alpheidae
267	Malacostraca	Alpheidae	Alpheidae	family	Alpheidae sp.	83.91	Malacostraca	Alpheidae
268	Malacostraca	Alpheidae	Alpheidae	family	Synalpheus gambarelloides	99.81	Malacostraca	Alpheidae
269	Malacostraca	Alpheidae	Alpheidae	family	Synalpheus gambarelloides	100	Malacostraca	Alpheidae
270	Malacostraca	Alpheidae	Alpheidae	family	Alpheidae sp.	84.05	Malacostraca	Alpheidae
271	Malacostraca	Alpheidae	Alpheidae	family				
272	Malacostraca	Alpheidae	Alpheidae	family	Synalpheus gambarelloides	100	Malacostraca	Alpheidae
274	Malacostraca		Decapoda	order	Synalpheus gambarelloides	100	Malacostraca	Alpheidae
275	Malacostraca		Decapoda	order	Synalpheus gambarelloides	99.19	Malacostraca	Alpheidae
282	Malacostraca	Paguridae	Pagurus anachoretus	species	Anapagurus breviaculeatus	98.62	Malacostraca	Paguridae

285	Malacostraca	Paguridae	Panachoretus	species	Pagurus cuanensis	99.84	Malacostraca	Paguridae
286	Malacostraca		Anomura	infraorder	Anapagurus breviculeatus	99.53	Malacostraca	Paguridae
347	Malacostraca	Diogenidae	Calcinus tubularis	species	Calcinus tubularis	99.68	Malacostraca	Diogenidae
348	Malacostraca	Diogenidae	Calcinus tubularis	species				
349	Malacostraca	Diogenidae	Calcinus tubularis	species	Calcinus tubularis	99.38	Malacostraca	Diogenidae
351	Malacostraca	Diogenidae	Calcinus tubularis	species	Calcinus tubularis	88.86	Malacostraca	Diogenidae
353	Malacostraca	Calcinidae	Calcinus tubularis	species	no homology			
354	Malacostraca	Diogenidae	Calcinus tubularis	species	Calcinus tubularis	99.69	Malacostraca	Diogenidae
365	Malacostraca	Calcinidae	Calcinus tubularis	species	no homology			
366	Malacostraca	Calcinidae	Calcinus tubularis	species				
367	Malacostraca	Calcinidae	Calcinus tubularis	species				
377	Malacostraca	Diogenidae	Calcinus tubularis	species	Calcinus tubularis	97.78	Malacostraca	Diogenidae
378	Malacostraca	Diogenidae	Calcinus tubularis	species	Calcinus tubularis	99.53	Malacostraca	Diogenidae
379	Malacostraca	Diogenidae	Calcinus tubularis	species	Calcinus tubularis	99.34	Malacostraca	Diogenidae
380	Malacostraca	Calcinidae	Calcinus tubularis	species				
381	Malacostraca	Calcinidae	Calcinus tubularis	species				
382	Malacostraca	Diogenidae	Calcinus tubularis	species	Calcinus tubularis	98.58	Malacostraca	Diogenidae
383	Malacostraca	Diogenidae	Calcinus tubularis	species	Calcinus tubularis	99.11	Malacostraca	Diogenidae
384	Malacostraca	Diogenidae	Calcinus tubularis	species	Calcinus tubularis	99.69	Malacostraca	Diogenidae
390	Malacostraca	Paguridae	Pagurus anachoretus	species				
391	Malacostraca	Paguridae	Pagurus anachoretus	species	Pagurus emmersoni	86.08	Malacostraca	Paguridae
392	Malacostraca	Paguridae	Pagurus anachoretus	species	Pagurus anachoretus	100	Malacostraca	Paguridae
394	Malacostraca	Paguridae	Pagurus anachoretus	species	Pagurus anachoretus	98.9	Malacostraca	Paguridae
395	Malacostraca	Paguridae	Pagurus anachoretus	species	Pagurus anachoretus	98.72	Malacostraca	Paguridae
400	Ophiuroidea	Ophiodermatidae	Ophioderma longicauda	species	Ophioderma longicauda	98.93	Ophiuroidea	Ophiodermatidae
402	Ophiuroidea	Ophiodermatidae	Ophioderma longicauda	species	Ophioderma longicauda	98.62	Ophiuroidea	Ophiodermatidae
403	Ophiuroidea	Ophiodermatidae	Ophioderma longicauda	species	Ophioderma longicauda	99.08	Ophiuroidea	Ophiodermatidae
404	Ophiuroidea	Ophiodermatidae	Ophioderma longicauda	species	Ophioderma longicauda	98.18	Ophiuroidea	Ophiodermatidae
407	Ophiuroidea	Ophiotrichidae	Ophiotrix sp.	genus	Ophiotrix sp.	99.83	Ophiuroidea	Ophiotrichidae
408	Ophiuroidea	Ophiotrichidae	Ophiotrix sp.	genus	Ophiotrix sp.	99.83	Ophiuroidea	Ophiotrichidae
409	Ophiuroidea	Ophiotrichidae	Ophiotrix sp.	genus	Ophiotrix sp.	99.13	Ophiuroidea	Ophiotrichidae
410	Ophiuroidea	Ophiotrichidae	Ophiotrix sp.	genus	Ophiotrix sp.	99.65	Ophiuroidea	Ophiotrichidae
411	Ophiuroidea	Ophiotrichidae	Ophiotrix sp.	genus	Ophiotrix sp.	99.83	Ophiuroidea	Ophiotrichidae
412	Ophiuroidea	Ophiotrichidae	Ophiotrix sp.	genus	Ophiotrix sp.	99.65	Ophiuroidea	Ophiotrichidae
413	Ophiuroidea	Ophiotrichidae	Ophiotrix sp.	genus	Ophiotrix sp.	99.48	Ophiuroidea	Ophiotrichidae
414	Ophiuroidea	Ophiotrichidae	Ophiotrix sp.	genus	Ophiotrix sp.	99.48	Ophiuroidea	Ophiotrichidae
415	Ophiuroidea	Ophiotrichidae	Ophiotrix sp.	genus	Ophiotrix sp.	99.31	Ophiuroidea	Ophiotrichidae
416	Ophiuroidea	Ophiotrichidae	Ophiotrix sp.	genus	Ophiotrix sp.	99.65	Ophiuroidea	Ophiotrichidae
417	Ophiuroidea	Ophiotrichidae	Ophiotrix sp.	genus	Ophiotrix sp.	99.65	Ophiuroidea	Ophiotrichidae
429	Ophiuroidea		Ophiuroidea	class				
430	Ophiuroidea		Ophiuroidea	class	Ophiotrix sp.	99.48	Ophiuroidea	Ophiotrichidae
431	Ophiuroidea		Ophiuroidea	class	Ophiotrix sp.	99.65	Ophiuroidea	Ophiotrichidae
441	Ophiuroidea	Amphiuridae	Amphiuridae	family	Amphipholis squamata	98.9	Ophiuroidea	Amphiuridae
442	Ophiuroidea	Amphiuridae	Amphiuridae	family	Ophiotrix fragilis	83.27	Ophiuroidea	Ophiotrichidae
443	Ophiuroidea	Amphiuridae	Amphiuridae	family	Amphipholis squamata	94.29	Ophiuroidea	Amphiuridae

445	Ophiuroidea	Amphiuridae	Amphiuridae	family	Amphipholis squamata	94.08	Ophiuroidea	Amphiuridae
446	Ophiuroidea	Amphiuridae	Amphiuridae	family	Amphipholis squamata	93.98	Ophiuroidea	Amphiuridae
447	Ophiuroidea	Amphiuridae	Amphiuridae	family	Amphipholis squamata	92.75	Ophiuroidea	Amphiuridae
448	Ophiuroidea	Amphiuridae	Amphiuridae	family	Amphipholis squamata	99.38	Ophiuroidea	Amphiuridae
450	Ophiuroidea	Amphiuridae	Amphiuridae	family	Amphipholis squamata	94.14	Ophiuroidea	Amphiuridae
451	Ophiuroidea	Amphiuridae	Amphiuridae	family	Ophiothrix fragilis	99.53	Ophiuroidea	Ophiotrichidae
454	Ophiuroidea	Amphiuridae	Amphiuridae	family	Amphipholis squamata	93.62	Ophiuroidea	Amphiuridae
455	Ophiuroidea	Ophiotrichidae	Ophiothrix sp.	genus	Ophiothrix fragilis	98.74	Ophiuroidea	Ophiotrichidae
456	Ophiuroidea	Ophiotrichidae	Ophiothrix sp.	genus	Ophiothrix fragilis	99.37	Ophiuroidea	Ophiotrichidae
457	Ophiuroidea	Ophiotrichidae	Ophiothrix sp.	genus	Ophiothrix fragilis	97.64	Ophiuroidea	Ophiotrichidae
458	Ophiuroidea	Ophiotrichidae	Ophiothrix sp.	genus	Ophiothrix fragilis	99.37	Ophiuroidea	Ophiotrichidae
459	Ophiuroidea	Ophiotrichidae	Ophiothrix sp.	genus	Ophiothrix fragilis	97.96	Ophiuroidea	Ophiotrichidae
460	Ophiuroidea	Ophiotrichidae	Ophiothrix sp.	genus	Ophiothrix fragilis	98.9	Ophiuroidea	Ophiotrichidae
461	Ophiuroidea	Ophiotrichidae	Ophiothrix sp.	genus	Ophiothrix fragilis	99.21	Ophiuroidea	Ophiotrichidae
462	Ophiuroidea	Ophiotrichidae	Ophiothrix sp.	genus	Ophiothrix fragilis	98.89	Ophiuroidea	Ophiotrichidae
463	Ophiuroidea	Ophiotrichidae	Ophiothrix sp.	genus	Ophiothrix fragilis	99.53	Ophiuroidea	Ophiotrichidae
464	Ophiuroidea		Ophiuroidea	class	Amphipholis squamata	99.09	Ophiuroidea	Amphiuridae
465	Ophiuroidea		Ophiuroidea	class	Ophiothrix fragilis	92.88	Ophiuroidea	Ophiotrichidae
466	Ophiuroidea	Ophiotrichidae	Ophiothrix sp.	genus	Amphipholis squamata	99.01	Ophiuroidea	Ophiotrichidae
467	Ophiuroidea		Ophiuroidea	class	Amphipholis squamata	99.01	Ophiuroidea	Amphiuridae
468	Ophiuroidea		Ophiuroidea	class	Amphipholis squamata	93.22	Ophiuroidea	Amphiuridae
469	Ophiuroidea		Ophiuroidea	class	Amphipholis squamata	93.52	Ophiuroidea	Amphiuridae
470	Ophiuroidea		Ophiuroidea	class	Amphipholis squamata	93.97	Ophiuroidea	Amphiuridae
471	Ophiuroidea		Ophiuroidea	class	Amphipholis squamata	93.55	Ophiuroidea	Amphiuridae
472	Ophiuroidea	Ophiotrichidae	Ophiothrix sp.	genus	Amphipholis squamata	93.85	Ophiuroidea	Amphiuridae
473	Ophiuroidea	Ophiotrichidae	Ophiothrix sp.	genus	Ophiothrix fragilis	99.06	Ophiuroidea	Ophiotrichidae
474	Ophiuroidea	Ophiotrichidae	Ophiothrix sp.	genus	Ophiothrix fragilis	99.53	Ophiuroidea	Ophiotrichidae
475	Ophiuroidea	Ophiotrichidae	Ophiothrix sp.	genus	Ophiothrix fragilis	99.21	Ophiuroidea	Ophiotrichidae
487	Ophiuroidea		Ophiuroidea	class	Amphipholis squamata	93.43	Ophiuroidea	Amphiuridae
488	Ophiuroidea		Ophiuroidea	class	Amphipholis squamata	91.03	Ophiuroidea	Amphiuridae
489	Ophiuroidea		Ophiuroidea	class	Amphipholis squamata	99.23	Ophiuroidea	Amphiuridae
490	Ophiuroidea		Ophiuroidea	class	Amphipholis squamata	87.23	Ophiuroidea	Amphiuridae
491	Ophiuroidea		Ophiuroidea	class	Amphipholis squamata	94.18	Ophiuroidea	Amphiuridae
493	Malacostraca		Amphipoda	order	Ampithoe rubricata	88.66	Malacostraca	Ampithoidae
494	Malacostraca		Amphipoda	order	Ampithoe rubricata	89.2	Malacostraca	Ampithoidae
495	Malacostraca		Amphipoda	order	Ampithoe rubricata	88.75	Malacostraca	Ampithoidae
496	Malacostraca		Amphipoda	order	Ampithoe rubricata	89.04	Malacostraca	Ampithoidae
498	Malacostraca	Paguridae	Paguridae	family	Cestopagurus timidus	99	Malacostraca	Paguridae
499	Malacostraca	Paguridae	Paguridae	family	Cestopagurus timidus	99.07	Malacostraca	Paguridae
500	Malacostraca	Paguridae	Pagurus anachoretus	species	Pagurus anachoretus	98.15	Malacostraca	Paguridae
501	Malacostraca	Paguridae	Pagurus anachoretus	species	Pagurus anachoretus	97.98	Malacostraca	Paguridae
518	Ophiuroidea	Amphiuridae	Amphipholis squamata	species				
519	Ophiuroidea	Amphiuridae	Amphipholis squamata	species				
520	Ophiuroidea	Amphiuridae	Amphipholis squamata	species	Amphipholis squamata	99.23	Ophiuroidea	Amphiuridae
521	Ophiuroidea	Amphiuridae	Amphipholis squamata	species	Amphipholis squamata	99.24	Ophiuroidea	Amphiuridae

522	Ophiuroidea	Amphiuridae	Amphipholis squamata	species				
523	Malacostraca	Idoteidae	Idoteidae	family	Macropodia czernjawskii	99.53	Malacostraca	Inachidae
524	Ophiuroidea	Amphiuridae	Amphipholis squamata	species	Amphipholis squamata	93.44	Ophiuroidea	Amphiuridae
525	Ophiuroidea	Amphiuridae	Amphipholis squamata	species	Amphipholis squamata	89.8	Ophiuroidea	Amphiuridae
526	Malacostraca	Calcinidae	Calcinus tubularis	species				
528	Ophiuroidea	Amphiuridae	Amphiuridae	family	Amphipholis squamata	99.54	Ophiuroidea	Amphiuridae
529	Ophiuroidea	Amphiuridae	Amphiuridae	family	Amphipholis squamata	99.23	Ophiuroidea	Amphiuridae
530	Ophiuroidea	Amphiuridae	Amphiuridae	family	Amphipholis squamata	96.39	Ophiuroidea	Amphiuridae
531	Ophiuroidea	Amphiuridae	Amphiuridae	family	Amphipholis squamata	93.43	Ophiuroidea	Amphiuridae
532	Ophiuroidea	Ophiotrichidae	Ophiotrix sp.	genus	Ophiotrix sp.	98.93	Ophiuroidea	Ophiotrichidae
533	Ophiuroidea	Ophiotrichidae	Ophiotrix	genus	Amphipholis squamata	96.04	Ophiuroidea	Amphiuridae
534	Ophiuroidea	Ophiotrichidae	Ophiotrix sp.	genus	Ophiotrix fragilis	98.9	Ophiuroidea	Ophiotrichidae
535	Ophiuroidea	Amphiuridae	Amphiuridae	family	Amphipholis squamata	98.94	Ophiuroidea	Amphiuridae
536	Ophiuroidea	Amphiuridae	Amphiuridae	family	Amphipholis squamata	98.36	Ophiuroidea	Amphiuridae
537	Ophiuroidea	Amphiuridae	Amphiuridae	family	Amphipholis squamata	88.93	Ophiuroidea	Amphiuridae
545	Malacostraca	Paguridae	Paguroidea	superfamily	Calcinus tubularis	99.39	Malacostraca	Diogenidae
546	Malacostraca	Idoteidae	Idoteidae	family	Photobaterium sp.	82.14		
566	Malacostraca	Paguridae	Paguridae	family	Cestopagurus timidus	98.78	Malacostraca	Paguridae
567	Malacostraca	Paguridae	Paguridae	family	Cestopagurus timidus	98.93	Malacostraca	Paguridae
568	Malacostraca	Paguridae	Paguridae	family	Cestopagurus timidus	98.62	Malacostraca	Paguridae
569	Malacostraca	Paguridae	Paguridae	family	Cestopagurus timidus	100	Malacostraca	Paguridae
570	Malacostraca	Paguridae	Paguridae	family	Cestopagurus timidus	98.74	Malacostraca	Paguridae
571	Malacostraca	Paguridae	Paguridae	family	Cestopagurus timidus	99.08	Malacostraca	Paguridae
572	Malacostraca	Paguridae	Paguridae	family	Cestopagurus timidus	98.62	Malacostraca	Paguridae
573	Malacostraca	Paguridae	Paguridae	family	Cestopagurus timidus	99.23	Malacostraca	Paguridae
574	Malacostraca	Paguridae	Paguridae	family	Cestopagurus timidus	98.78	Malacostraca	Paguridae
576	Malacostraca	Calcinidae	Calcinus tubularis	species				
577	Malacostraca	Paguridae	Paguridae	family	Cestopagurus timidus	98.47	Malacostraca	Paguridae
578	Polychaeta	Terebellidae	Terebellidae	family	Thelepus hamatus	88.82	Polychaeta	Terebellidae
182	Malacostraca		Amphipoda	order	Ampithoe sp.	88.48	Malacostraca	Ampithoidae
183	Malacostraca		Amphipoda	order	Ampithoe rubricata	88.17	Malacostraca	Ampithoidae
184	Malacostraca		Amphipoda	order	Ampithoe sp.	88.52	Malacostraca	Ampithoidae
186	Malacostraca		Amphipoda	order				
345	Malacostraca	Diogenidae	Calcinus tubularis	species	Calcinus tubularis	99.04	Malacostraca	Diogenidae
396	Gastropoda	Cerithiidae	Cerithium	genus	Alvania sp.	87.27	Gastropoda	Rissoidae
397	Gastropoda	Cerithiidae	Cerithium	genus	Alvania sp.	86.73	Gastropoda	Rissoidae
432	Ophiuroidea		Ophiuroidea	class	Ophiotrix sp.	99.48	Ophiuroidea	Ophiotrichidae
502	Malacostraca	Paguridae	Paguridae	family	Cestopagurus timidus	98.77	Malacostraca	Paguridae
503	Malacostraca	Paguridae	Paguridae	family	Cestopagurus timidus	98.93	Malacostraca	Paguridae
438	Ophiuroidea		Ophiuroidea	class	Ophiotrix sp.	99.48	Ophiuroidea	Ophiotrichidae
439	Ophiuroidea		Ophiuroidea	class	Ophiotrix sp.	99.65	Ophiuroidea	Ophiotrichidae
104	Polychaeta		Polychaeta	class	Hediste diversicolor	82.53	Polychaeta	Nereididae
222	Malacostraca		Decapoda	order	Photobacterium sp	86.78		
440	Ophiuroidea		Ophiuroidea	class	Ophiotrix sp.	99.37	Ophiuroidea	Ophiotrichidae
105	Polychaeta		Polychaeta	class	Lepidonotus clava	87.12	Polychaeta	Polynoidea

122	Polychaeta		Polychaeta	class	<i>Lysidice ninetta</i>	97.99	Polychaeta	Eunicidae
123	Polychaeta		Polychaeta	class	<i>Platynereis dumerilii</i>	98.94	Polychaeta	Nereididae
124	Polychaeta		Polychaeta	class	<i>Nereis aff. zonata</i>	98.93	Polychaeta	Nereididae
125	Polychaeta		Polychaeta	class	<i>Cheilonereis cyclurus</i>	82.83	Polychaeta	Nereididae
126	Polychaeta		Polychaeta	class	<i>Nereis aff. Zonata</i>	99.41	Polychaeta	Nereididae
127	Polychaeta		Polychaeta	class	<i>Platynereis sp</i>	99.07	Polychaeta	Nereididae
134	Polychaeta		Polychaeta	class	<i>Eunice roussaei</i>	98.45	Polychaeta	Eunicidae
135	Polychaeta		Polychaeta	class	<i>Palola siciliensis</i>	99.19	Polychaeta	Eunicidae
136	Polychaeta		Polychaeta	class	<i>Hediste diversicolor</i>	82.82	Polychaeta	Nereididae
137	Polychaeta		Polychaeta	class	<i>Dendronereides sp/Pseudonereis variegata</i>	80.36	Polychaeta	Nereididae
138	Polychaeta		Polychaeta	class	<i>Lepidonotus clava</i>	86.54	Polychaeta	Polynoidae
159	Polychaeta	Terebellidae	Terebellidae	family	<i>Thelepus hamatus</i>	89.22	Polychaeta	Terebellidae
160	Polychaeta	Terebellidae	Terebellidae	family	<i>Thelepus hamatus</i>	89.03	Polychaeta	Terebellidae
161	Polychaeta	Terebellidae	Terebellidae	family	<i>Thelepus hamatus</i>	89.06	Polychaeta	Terebellidae
162	Polychaeta	Terebellidae	Terebellidae	family	<i>Thelepus hamatus</i>	88.91	Polychaeta	Terebellidae
164	Polychaeta	Terebellidae	Terebellidae	family	<i>Thelepus hamatus</i>	89.06	Polychaeta	Terebellidae
165	Polychaeta	Terebellidae	Terebellidae	family	<i>Thelepus hamatus</i>	89.06	Polychaeta	Terebellidae
166	Polychaeta	Terebellidae	Terebellidae	family	<i>Thelepus hamatus</i>	89.06	Polychaeta	Terebellidae
167	Polychaeta	Terebellidae	Terebellidae	family	<i>Thelepus hamatus</i>	89.06	Polychaeta	Terebellidae
168	Polychaeta	Terebellidae	Terebellidae	family	<i>Thelepus hamatus</i>	89.06	Polychaeta	Terebellidae
169	Polychaeta	Terebellidae	Terebellidae	family	<i>Thelepus hamatus</i>	89.03	Polychaeta	Terebellidae
192	Malacostraca		Amphipoda	order	<i>Ampithoe rubricata</i>	88.65	Malacostraca	Ampithoidae
193	Malacostraca		Amphipoda	order	<i>Ampithoe rubricata</i>	88.52	Malacostraca	Ampithoidae
194	Malacostraca		Amphipoda	order	<i>Ampithoe ramondi</i>	74.63	Malacostraca	Ampithoidae
197	Malacostraca		Amphipoda	order	<i>Ampithoe rubricata</i>	88.4	Malacostraca	Ampithoidae
203	Sipuncula		Sipuncula	order	<i>Phascolosoma granulatum</i>	99.47	Sipuncula	Phascolosomatidae
204	Sipuncula		Sipuncula	order	<i>Phascolosoma granulatum</i>	98.04	Sipuncula	Phascolosomatidae
205	Sipuncula		Sipuncula	order	<i>Phascolosoma granulatum</i>	98.58	Sipuncula	Phascolosomatidae
206	Sipuncula		Sipuncula	order	<i>Phascolosoma granulatum</i>	99.36	Sipuncula	Phascolosomatidae
207	Sipuncula		Sipuncula	order	<i>Phascolosoma granulatum</i>	98.72	Sipuncula	Phascolosomatidae
208	Sipuncula		Sipuncula	order	<i>Phascolosoma granulatum</i>	99.52	Sipuncula	Phascolosomatidae
229	Malacostraca	Majoidea	Majoidea	family	<i>Pisa tetraodon</i>	99.07	Malacostraca	Epialtidae
230	Malacostraca	Eriphiidae	<i>Eriphia verrucosa</i>	species				
231	Malacostraca		Decapoda	order	<i>Inachus dorsettensis</i>	88.17	Malacostraca	Inachidae
232	Malacostraca	Xanthidae	<i>Xantho poressa</i>	species	<i>Pilumnus villosissimus</i>	99.05	Malacostraca	Pilumnidae
233	Malacostraca	Pilumnidae	<i>Pilumnus hirtellus</i>	species				
234	Malacostraca	Pilumnidae	<i>Pilumnus hirtellus</i>	species	<i>Pilumnus villosissimus</i>	99.84	Malacostraca	Pilumnidae
235	Malacostraca	Pilumnidae	<i>Pilumnus hirtellus</i>	species	<i>Pilumnus hirtellus</i>	99.84	Malacostraca	Pilumnidae
236	Malacostraca	Xanthidae	<i>Xantho poressa</i>	species	<i>Lophozozymus incisus</i>	99.01	Malacostraca	Xanthidae
242	Malacostraca	Inachidae	<i>Inachus dorsettensis</i>	species	<i>Inachus aguiarii</i>	87.77	Malacostraca	Inachidae
251	Malacostraca	Inachidae	<i>Achaeus cranchii</i>	species	<i>Photobacterium damsela</i>	78.06		
252	Malacostraca	Galatheidae	<i>Galathea</i>	genus	<i>Galathea intermedia</i>	95.08	Malacostraca	Galatheidae
253	Malacostraca	Galatheidae	<i>Galathea</i>	genus	<i>Galathea intermedia</i>	99.83	Malacostraca	Galatheidae
266	Malacostraca	Alpheidae	<i>Alpheus dentipes</i>	species	<i>Anapagurus breviculeatus</i>	98.89	Malacostraca	Paguridae
273	Malacostraca	Alpheidae	<i>Athanas nitescens</i>	species	<i>Athanas nitescens</i>	99.85	Malacostraca	Alpheidae

287	Malacostraca		Anomura	infraorder	Cestopagurus timidus	98.26	Malacostraca	Paguridae
288	Malacostraca		Anomura	infraorder	Cestopagurus timidus	98.89	Malacostraca	Paguridae
356	Malacostraca	Diogenidae	Calcinus tubularis	species	Calcinus tubularis	99.05	Malacostraca	Diogenidae
357	Malacostraca	Calcinidae	Calcinus tubularis	species				
358	Malacostraca	Calcinidae	Calcinus tubularis	species	Calcinus tubularis	86.61	Malacostraca	Diogenidae
359	Malacostraca	Diogenidae	Calcinus tubularis	species	Calcinus tubularis	99.84	Malacostraca	Diogenidae
360	Malacostraca	Diogenidae	Calcinus tubularis	species	Calcinus tubularis	99.69	Malacostraca	Diogenidae
362	Malacostraca	Diogenidae	Calcinus tubularis	species	Calcinus tubularis	99.32	Malacostraca	Diogenidae
363	Malacostraca	Diogenidae	Calcinus tubularis	species	Calcinus tubularis	99.01	Malacostraca	Diogenidae
364	Malacostraca	Diogenidae	Calcinus tubularis	species	Calcinus tubularis	97.01	Malacostraca	Diogenidae
368	Malacostraca	Diogenidae	Calcinus tubularis	species	Cestopagurus timidus	99.37	Malacostraca	Paguridae
370	Malacostraca	Calcinidae	Calcinus tubularis	species				
371	Malacostraca	Diogenidae	Calcinus tubularis	species	Calcinus tubularis	99.32	Malacostraca	Diogenidae
372	Malacostraca	Calcinidae	Calcinus tubularis	species				
373	Malacostraca	Diogenidae	Calcinus tubularis	species	Calcinus tubularis	99.68	Malacostraca	Diogenidae
401	Ophiuroidea	Ophiodermatidae	Ophioderma longicauda	species	Ophioderma longicauda	97.8	Ophiuroidea	Ophiodermatidae
405	Ophiuroidea	Ophiotrichidae	Ophiothrix sp.	genus	Ophiothrix sp.	99.83	Ophiuroidea	Ophiotrichidae
406	Ophiuroidea	Ophiotrichidae	Ophiothrix sp.	genus	Ophiothrix fragilis	97.8	Ophiuroidea	Ophiotrichidae
479	Ophiuroidea	Ophiotrichidae	Ophiothrix sp.	genus	Ophiothrix fragilis	99.53	Ophiuroidea	Ophiotrichidae
480	Ophiuroidea	Ophiotrichidae	Ophiothrix sp.	genus	Ophiothrix fragilis	99.21	Ophiuroidea	Ophiotrichidae
481	Ophiuroidea	Ophiotrichidae	Ophiothrix sp.	genus				
482	Ophiuroidea	Ophiotrichidae	Ophiothrix sp.	genus	Ophiothrix fragilis	97.48	Ophiuroidea	Ophiotrichidae
483	Ophiuroidea	Ophiotrichidae	Ophiothrix sp.	genus	Ophiothrix fragilis	99.37	Ophiuroidea	Ophiotrichidae
484	Ophiuroidea	Ophiotrichidae	Ophiothrix sp.	genus				
485	Ophiuroidea	Ophiotrichidae	Ophiothrix sp.	genus	Ophiothrix fragilis	97.96	Ophiuroidea	Ophiotrichidae
486	Ophiuroidea	Ophiotrichidae	Ophiothrix sp.	genus	Ophiothrix fragilis	97.64	Ophiuroidea	Ophiotrichidae
527	Malacostraca	Paguridae	Paguridae	family	Cestopagurus timidus	99.69	Malacostraca	Paguridae
538	Polychaeta	Terebellidae	Terebellidae	family	Thelepus hamatus	89.05	Polychaeta	Terebellidae
539	Polychaeta	Terebellidae	Terebellidae	family	Thelepus hamatus	89.21	Polychaeta	Terebellidae
116	Polychaeta		Polychaeta	class				
117	Polychaeta		Polychaeta	class	Arabella iricolor	84.56	Polychaeta	Oeonidae
118	Polychaeta		Polychaeta	class	Lepidonotus clava	87.58	Polychaeta	Polynoidae
119	Polychaeta		Polychaeta	class	Arabella iricolor	84.69	Polychaeta	Oeonidae
120	Polychaeta		Polychaeta	class	Nereis aff. Zonata	99.08	Polychaeta	Nereididae
121	Polychaeta		Polychaeta	class	Platynereis dumerilii	98.05	Polychaeta	Nereididae
189	Malacostraca		Amphipoda	order	Ampithoe rubricata	88.65	Malacostraca	Ampithoidae
190	Malacostraca		Amphipoda	order	Ampithoe sp.	88.58	Malacostraca	Ampithoidae
250	Malacostraca	Galatheidae	Galathea	genus	Galathea intermedia	88.82	Malacostraca	Galatheidae
284	Malacostraca		Anomura	infraorder	Calcinus tubularis	99.84	Malacostraca	Diogenidae
355	Malacostraca	Diogenidae	Calcinus tubularis	species	Calcinus tubularis	99.69	Malacostraca	Diogenidae
504	Ophiuroidea		Ophiuroidea	class	Amphipholis sp.	92.31	Ophiuroidea	Amphipholidae
505	Ophiuroidea	Ophiotrichidae	Ophiothrix sp.	genus	Ophiothrix fragilis	99.54	Ophiuroidea	Ophiotrichidae
506	Ophiuroidea	Ophiotrichidae	Ophiothrix sp.	genus	Ophiothrix fragilis	99.38	Ophiuroidea	Ophiotrichidae
507	Ophiuroidea	Ophiotrichidae	Ophiothrix sp.	genus	Ophiothrix fragilis	98.92	Ophiuroidea	Ophiotrichidae
508	Ophiuroidea	Ophiotrichidae	Ophiothrix sp.	genus	Ophiothrix fragilis	98.93	Ophiuroidea	Ophiotrichidae

509	Ophiuroidea	Ophiotrichidae	Ophiotrix sp.	genus	Ophiotrix fragilis	98.92	Ophiuroidea	Ophiotrichidae
510	Ophiuroidea	Ophiotrichidae	Ophiotrix sp.	genus	Ophiotrix fragilis	99.08	Ophiuroidea	Ophiotrichidae
511	Ophiuroidea	Ophiotrichidae	Ophiotrix sp.	genus	Ophiotrix fragilis	99.21	Ophiuroidea	Ophiotrichidae
512	Ophiuroidea	Ophiotrichidae	Ophiotrix sp.	genus	Ophiotrix fragilis	98.91	Ophiuroidea	Ophiotrichidae
513	Ophiuroidea	Ophiotrichidae	Ophiotrix sp.	genus	Ophiotrix fragilis	99.06	Ophiuroidea	Ophiotrichidae
514	Ophiuroidea	Ophiotrichidae	Ophiotrix sp.	genus	Ophiotrix fragilis	98.6	Ophiuroidea	Ophiotrichidae
515	Ophiuroidea	Ophiotrichidae	Ophiotrix sp.	genus	Ophiotrix fragilis	99.53	Ophiuroidea	Ophiotrichidae
516	Ophiuroidea	Amphiuridae	Amphiuridae	family	no homology			
517	Ophiuroidea	Amphiuridae	Amphiuridae	family	Amphipholis squamata	91.31	Ophiuroidea	Amphiuridae
547	Gastropoda		Gastropoda	class	Hexaplex trunculus	99.54	Gastropoda	Muricidae
548	Gastropoda		Gastropoda	class	Conus ventricosus	98.34	Gastropoda	Conidae
549	Gastropoda		Gastropoda	class	Euthria cornea	98.63	Gastropoda	Tudicidae
550	Gastropoda		Gastropoda	class	Nassarius incrassatus	97.85	Gastropoda	Nassariidae
551	Gastropoda	Cerithiidae	Cerithium	genus	Alvania sp.	86.76	Gastropoda	Rissoidae
552	Malacostraca	Paguridae	Pagurus anachoretus	species	Pagurus cuanensis	100	Malacostraca	Paguridae
553	Gastropoda	Cerithiidae	Cerithium	genus	Alvania sp.	86.31	Gastropoda	Rissoidae
554	Gastropoda	Cerithiidae	Cerithium	genus	Alvania sp.	87.54	Gastropoda	Rissoidae
555	Gastropoda	Cerithiidae	Cerithium	genus	Alvania sp.	86.98	Gastropoda	Rissoidae
556	Malacostraca		Decapoda	order	Liocarcinus navigator	99.23	Malacostraca	Polybiidae
557	Malacostraca	Paguridae	Pagurus anachoretus	species	Pagurus cuanensis	99.54	Malacostraca	Paguridae
558	Gastropoda	Cerithiidae	Cerithium	genus	Alvania sp.	87.84	Gastropoda	Rissoidae
559	Gastropoda	Cerithiidae	Cerithium	genus	Alvania sp.	87.29	Gastropoda	Rissoidae
560	Gastropoda	Cerithiidae	Cerithium	genus	Alvania sp.	87.04	Gastropoda	Rissoidae
561	Malacostraca		Decapoda	order	Acanthonyx lunulatus	96.62	Malacostraca	Epialtidae
562	Malacostraca		Decapoda	order	Prostheceraeus roseus	89.71	Malacostraca	Euryleptidae
563	Gastropoda	Muricidae	Hexaplex trunculus	species	Hexaplex trunculus	99.54	Gastropoda	Muricidae
564	Gastropoda	Muricidae	Hexaplex trunculus	species	Hexaplex trunculus	99.24	Gastropoda	Muricidae
565	Polychaeta		Polychaeta	class	Perinereis wilsoni	79.6	Polychaeta	Nereididae
376	Malacostraca	Diogenidae	Calcinus tubularis	species	Calcinus tubularis	99.06	Malacostraca	Diogenidae

Table 4.2.1- Specimens of invertebrates found and used in the study.

For molecular taxonomic identification of both urchin juveniles and predators by DNA barcoding, we used the “universal” cytochrome oxidase subunit 1 (COI1) degenerate primer pair jgLCO1490/ jgHCO2198 (Table 4.2.2) described by Geller et al., which is particularly effective for identifying marine invertebrates (Geller et al.,2013)

Locus	Name of primer	Sequence (5'-3')	Amplicon size	Reference
COII	jgLCOI1490	titciaciaaycayaargayattgg		(Geller et al., 2013)
	jgHCO2198	taiacytciggrtgicraaraayca		
COII	Pl-COI-Cterm-for	actaccggatttggaatgatt	63	This study
	Pl-COI-Cterm-rev	aaaggttctctgcttcctga		
COII	Pl-COI-Nterm-for	ttctcactccatcttgcggg	93	This study
	Pl-COI-nterm-rev	aaaagacattcccggcgcttc		
COII	Pliv-COI-C-for	actatgcttctaacagaccgt	178	This study
	Pliv-COI-C-rev	tctcgcttcctgagtagtg		
COII	Pliv-COI1-Nfor	gcaccagatagggccttccc	103	This study
	Pliv-COI1-Nrev	cggctccttttctactcctg		
COII	Pliv-COI1-Mfor	gaacgccgggaatgtctttt	173	This study
	Pliv-COI1-Mrev	aattgggtctcctcctcctg		
16S	Pliv-16S-for	aggcggagggtaaaatcggt	161	This study
	Pliv-16S-rev	gcttctttactccgggtt		
CYT-b	Pliv-cytb-Nfor	tctggtggaattcgctct	155	This study
	Pliv-cytb-Nrev	tcgaagcagtcaccgtaat		
CYT-b	Pliv-cytb-Cfor	ttccgtcccctatctcaagc	86	This study
	Pliv-cytb-Crev	ggaagccaacctgtagaaca		
CYT-b	Pliv-cytb-Mfor	agacaatgccactctaactcg	119	This study
	Pliv-cytb-Mrev	cctactgggttfttgctcc		
COII	Al-COI-Nterm-for	atgctgggaagagagaacca	97	This study
	Al-COI-Nterm-rev	aacatgtggtgggctcaaac		
COII	Al-COI-Cterm-for	tgggagcagttctcgctatt	76	This study
	Al-COI-Cterm-rev	agtgggtggaagctgtatcc		
COII	Alix-COI1-Nfor	cccctaatgattggtgcccc	112	This study
	Alix-COI1-Nrev	ctcttctacccggcagaa		
COII	Alix-COI1-Cfor	cagcagtgaggagagacc	137	This study
	Alix-COI1-Crev	tggttctcttcccagcat		
COII	Alix-COI1-Mfor	ccggtgctcttccatctt	89	This study
	Alix-COI1-Mrev	ggcaaacggcaaaagaga		
16S	Alix-16sC-for	tgtgaccgcttatttaggc	153	This study
	Alix-16sC-rev	acagaccaaccctaaaagct		
16S	Alix-16sM-for	ggcaaccacggagaaaataa	110	This study
	Alix-16sM-rev	gcctaaataagcgggtcaca		

Table 4.2.2 - Primers used in this study

4.2.2 DNA extraction

For DNA extraction from both the predators and sea urchins, we used the Tissue DNA Kit by Ezna (VWR). Samples were removed from the ethanol bath, weighted, and rinsed in 1 to 10 mL of distilled water, depending on the animal size. For animals weighting more than 100 mg, we chopped the sample in several pieces by using a disposable blade and processed the parts independently. Legs and claws were also removed from larger animals, whenever possible, in order to minimize the amount of host

DNA recovered. Each sample was put in a 2 mL plastic tube with 3 tungsten beads and homogenized by shaking 15 s at 300 rpm at room temperature in the TissueLyser machine (Qiagen). Immediately after shaking, we added TL buffer and proceeded according to the indications provided by the kit protocol for processing the tissue. DNA was resuspended in 10 mM Tris buffer at pH 9.0. DNA concentration and extraction quality were measured with a fluorometer (Synergy H1, Biotek). DNA integrity was checked by electrophoretic run in a 1% agarose gel.

4.2.3 Primer design

For molecular identification of potential micropredators of sea urchins, we designed several primer pairs spanning different regions of the mitochondrial gene cytochrome oxidase subunit 1 (COI1), commonly used in similar studies since it is highly polymorphic among different species. Due to the high polymorphism of the gene, we were concerned about the possibility that different urchin accessions might also show sequence variations. In order to design primers that would work for any *P. lividus* and *A. lixula* sequence, we aligned by ClustalW (BioEdit) 254 COI1 sequences available on NCBI, including the complete mitochondrial genome for *P. lividus* (accessions 49036145-49036397; 1028338044-1028338084; 365735528-365735742; 564282614; 564282618; J04815.1) and 328 COI1 sequences available of the sympatric sea urchin species *Arbacia lixula* (JQ745096.1-JQ745256.1; JN603630.1-JN603633.1; AF030998.1-AF031011.1; JF772935.1-JF773074.1; KU172486.1-KU172488.1; HE800533.1-HE800538.1). In the alignment, we also included the COI1 sequences of marine invertebrate representatives of the major taxonomic groups found in this survey: *Alpheus dentipes* (AF309893.1); *Amphipholis squamata* (NSECH002-13); *Ampithoe ramondi* (GBCM8446-17); *Dorvillea sp* (BAMPOL0439); *Galathea intermedia* (BNSC183-10); *Lysidice ninetta*; *Nereis pelagica*; *Ophiothrix fragilis* (LOBO010-12); *Pagurus prideaux* (JSDUK158); *Palola cf. siciliensis* (USNM1120744); *Pilumnus villosissimus* (GBCMD18798-19); *Platynereis dumerilii* (GBAN12514-19); *Synalpheus gambarelloides* (GBCDA161-12); *Thelepus cincinnatus* (HUNTSPOL0372) in order

to avoid conserved regions during primer design. Likewise, we designed primers for the mitochondrial loci 16S and cytochrome b. We designed nine different primer pairs for *P. lividus* and seven for *A. lixula*, spanning from the 5' end to the 3' end of the gene, and comprising a region ranging from 63 to 178 base pairs (bp) in size. We intentionally selected small amplification sizes in order to maximize chances of recovery of digested and fragmented prey DNA in the guts. Details of the primers are given in Table 4.2.2.

As a test for DNA quality of the sample, we also used the primer pair jgLCO1490/ jgHCO2198 (Table 4.2.2), which robustly amplify a large range of marine invertebrate taxa.

4.2.4 Amplification

In order to minimize the risk of cross-contamination, pre-packed, aerosol-resistant and DNA-free pipette tips were used for assembling PCR reactions and loading samples in gels. Different pipette sets and laboratory rooms were used when handling urchin specimens, as well as the rest of sampled invertebrates and their DNA. Pre-PCR and post-PCR setups were located in different rooms.

PCR reactions were assembled with 0.4 μ M each primer, 1% w/v BSA and 2 units MyTaq polymerase (Bioline) and 5 μ L 5X buffer that includes dNTPs and Mg²⁺ in a reaction volume of 25 μ L. Amplifications were performed in 96 well plates. PCR conditions were: initial denaturation 3 min at 95°C, followed by 35 cycles of denaturation 60 sec at 95 °C, annealing 30 sec at 56 °C, extension 25 sec at 72 °C; a final extension step was set for 10 min at 72 °C. Templates in the specificity test PCR included DNA extracted from gonads of adult *P. lividus* and *A. lixula* (0.1 ng), and from invertebrates of different taxonomic groups (100 ng). In particular, we extracted DNA from the Sipunculid *Phascolosoma granulatum*; the crab *Pilumnus hirtellus*; the shrimp *Synalpheus gambarelloides*; the Ophiuridae *Amphipholis squamata*; from a Polychaete Terebellidae; the whelk *Euthria cornea*. Except for Ophiuridae and Polychete, either too small or unstructured to be dissected, we extracted DNA from appendices of invertebrate samples, with the aim to minimize contamination with DNA from other

species contained in the gut. Templates in the sensitivity tests consisted of DNA from adults of either *P. lividus* or *A. lixula*, diluted in water from 1 ng to 10 fg (105 folds dilution). For PCRs testing the inhibition effect of excess predator DNA, templates contained 0.1 ng urchin DNA and 100 ng (1,000 fold) of predator DNA. For screening all samples for presence of urchin DNA, we used 50 ng DNA as template in each reaction. Each reaction plate contained one positive control (0.1 ng *P. lividus* DNA) and 4-5 negative controls (reaction mixture with no template).

PCR products were loaded in 2% agarose gel and visualized by GelRed (Biotium) staining. Bands intensities were quantified by ImageJ software, after background subtraction for each plate. Samples were considered positive when band intensity scored higher than 65,000. Positive controls scored around 150,000.

4.2.5 COI-1 barcoding

For COI1 amplification with Geller's universal primers jgLCO1490/ jgHCO2198, PCR conditions were: initial denaturation 3 min at 95°C, followed by a touch down setup with 35 cycles of denaturation 60 sec at 95 °C, annealing 60 sec at 52-48 °C (-1 °C /cycle for the first four cycles, followed by 48 °C for 31 cycles), extension 60 sec at 72 °C; a final extension step was set for 10 min at 72 °C. Bands amplified by primers were manually excised from the gels and the DNA extracted by using the Gel Extraction Kit (Ezra, VWR) according to the manufacturer's instructions. For urchin settlers, DNA was subcloned into the pGem-Teasy vector (Promega) and propagated in *E. coli*. Plasmids from randomly selected positive, white colonies were extracted by the Plasmid Mini kit (Ezra, VWR), according to the manufacturer's instructions. The inserts were sequenced in both directions by using the T7 and SP6 primers (sites present in the vector backbone adjacent to the insertion site). For the collected invertebrate samples, the extracted DNA was directly sequenced by jgLCO1490. Sanger sequencing was performed by Eurofins Genomics (Germany). The resulting sequences were blasted in the NCBI database (BLASTn) to retrieve the identity of the specimens.

4.3 Results

4.3.1 Invertebrate assemblages

A total of 379 potential invertebrate predators were collected and visualized at a stereomicroscope for taxonomic identification (Table 4.2.1). Only for 23% of specimen we were confident enough to assign the identification at the species level, especially for crustaceans. For other samples, we only reached the Genus (17%), Family (19%), Order (14%) or even just the Class (27%) taxonomic level. Overall, most of the collected invertebrates were crustaceans (Malacostraca, 41%). Serpentine stars (Ophiuroidea) and worms (Polychaeta) were also abundant (29% and 23% of samples, respectively). The other invertebrates belonged to Gastropoda (4%) and Sipuncula (3%) (Fig. 4.3.1).

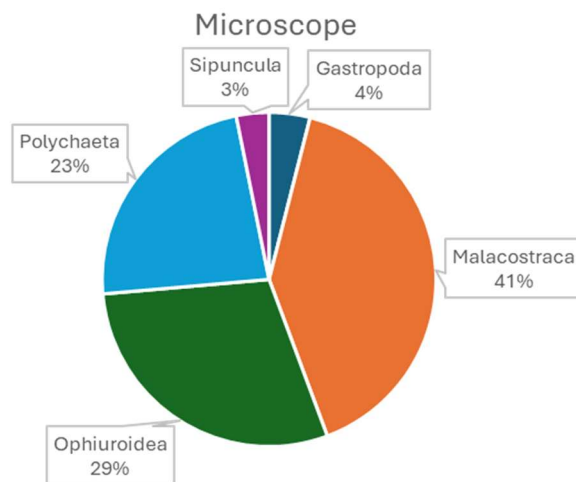


Fig. 4.3.1- Percentage of potential invertebrate predators collected and identified by visual assessment at the microscope

4.3.2 DNA quality and barcoding

To check for integrity of the DNA extracted from preserved invertebrate samples, we analyzed a subset of four randomly selected samples by electrophoresis. All samples showed an extended smear of low molecular weight DNA, indicative of degradation (Fig. 4.3.2).

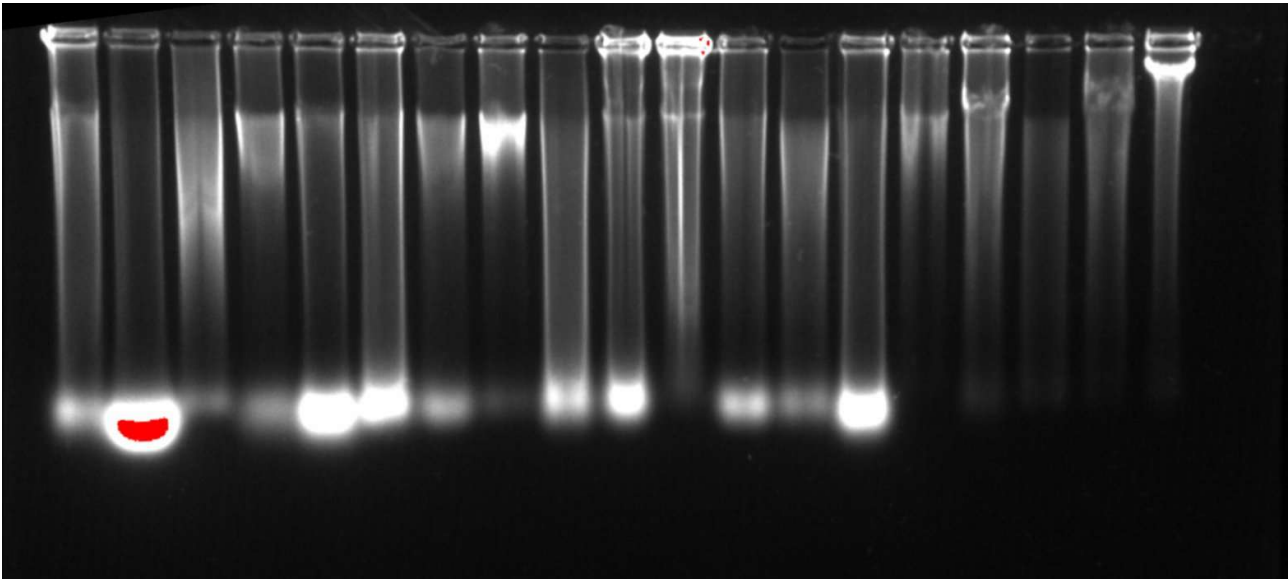
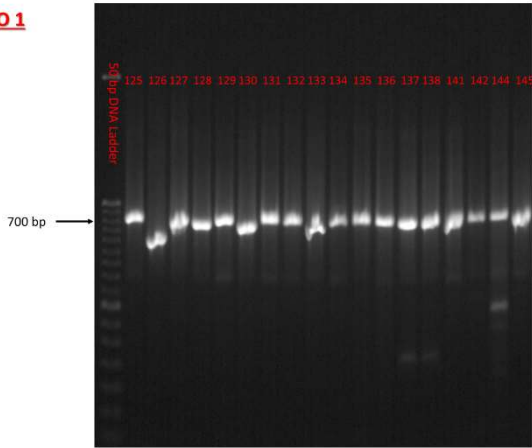


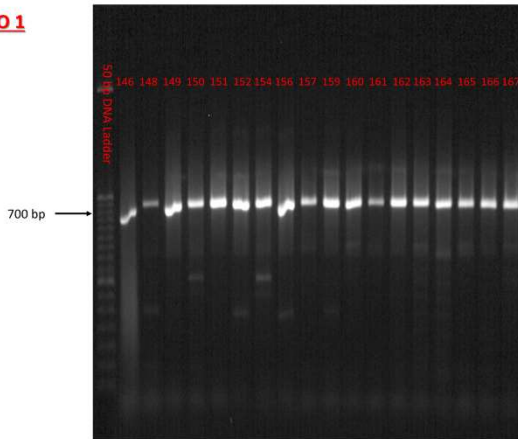
Fig. 4.3.2- Representative image of extract DNA showing a SMEAR of degradation.

Very little high molecular weight genomic DNA was visible. Degradation was likely a result of sample storage and handling during the extraction protocol. Concerned about the quality of the samples, we first tested all 379 potential predators for their ability to support PCR amplification. To that aim, we used Geller’s “universal” COI primer pair that had been shown to amplify a wide range of invertebrate taxa (Geller et al., 2013). Accordingly, the vast majority (92%) of samples gave a clear and strong band, indicating that the handling and storage of the animal and the extraction protocol did not affect the ability of the DNA to amplify (Examples in Fig. 4.3.3).

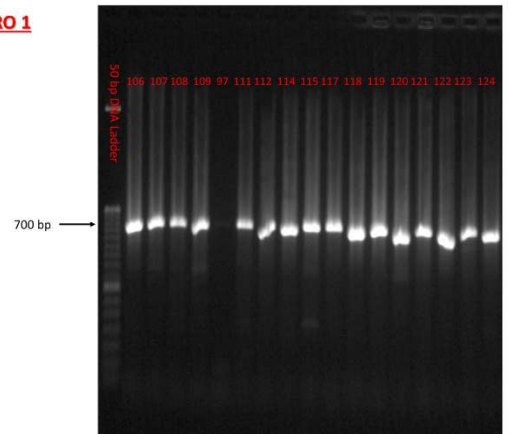
MICRO 1



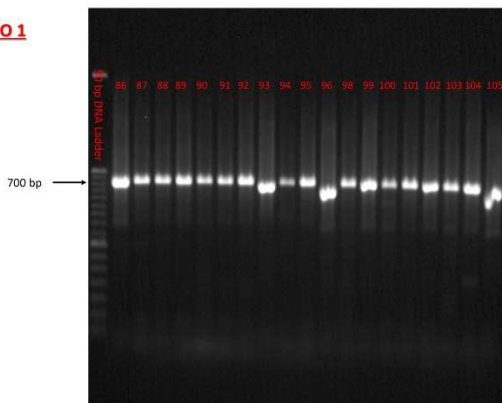
MICRO 1



MICRO 1



MICRO 1



MICRO 1

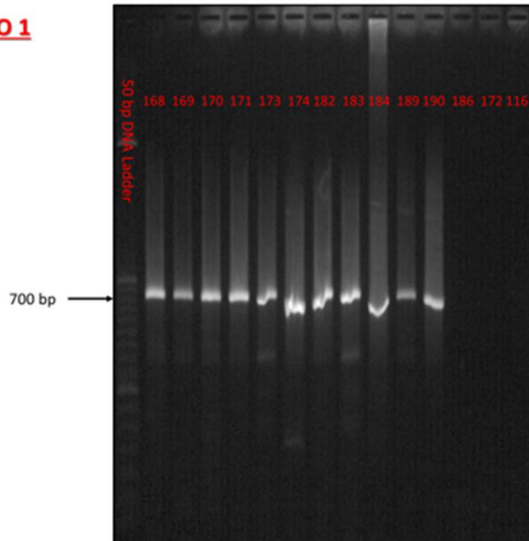


Fig.4.3.3 – Representative images of samples amplified with universal PRIMERS

Only 29 invertebrate samples failed to amplify. We exclude that the PCR failure was due to incompatibility of the primer set with the sample species, since other members of the same species showed a clear band in other reactions. More likely, the negative result for these 29 sample was due to the presence of PCR inhibitors, or to insufficient DNA quality. In all the other 350 invertebrate samples, the size of the amplicons varied, as expected in animals belonging to different taxa, yet it was generally comprised between 400 and 1,000 bp, indicating that the recovered DNA was not fully degraded, and that sufficient amount of nucleic acid was long enough to serve as template. Since the primers for prey identification were designed on a much smaller region (< 200 bp) and for a gene encoded in the mtDNA, present in high copy number, we were confident that our strategy had the potential to work even when the target DNA was present in trace amounts.

The bands amplified in the COI region by Geller's primers were purified and sequenced to serve as barcode for molecular identification of invertebrates and urchins. Out of 350 invertebrate sequences, six failed to provide a reliable identification, due to no significant homologies (three sequences) and misassignment to Bacteria (three sequences). Table 4.3.1 reports the names of species most closely related to sequences for each sample and the identity scores. Most of sequences (63%) retrieved a high

confidence hit (identity $\geq 95\%$). Samples with the lowest identity confidence (75-85%) were especially abundant among Polychaeta. Overall, molecular barcoding confirms the coarse visual assignment and provides a finer labelling. At the Class level, the molecular identification agreed with visual assignment for all samples. At the Family level, 14 samples (6%) showed a disagreement between COI sequencing and visual assignment. Class distribution was like the one obtained by visual assignment (Fig 4.3.4); minor deviations were due to the 35 specimen that failed to provide a valuable barcode sequence.

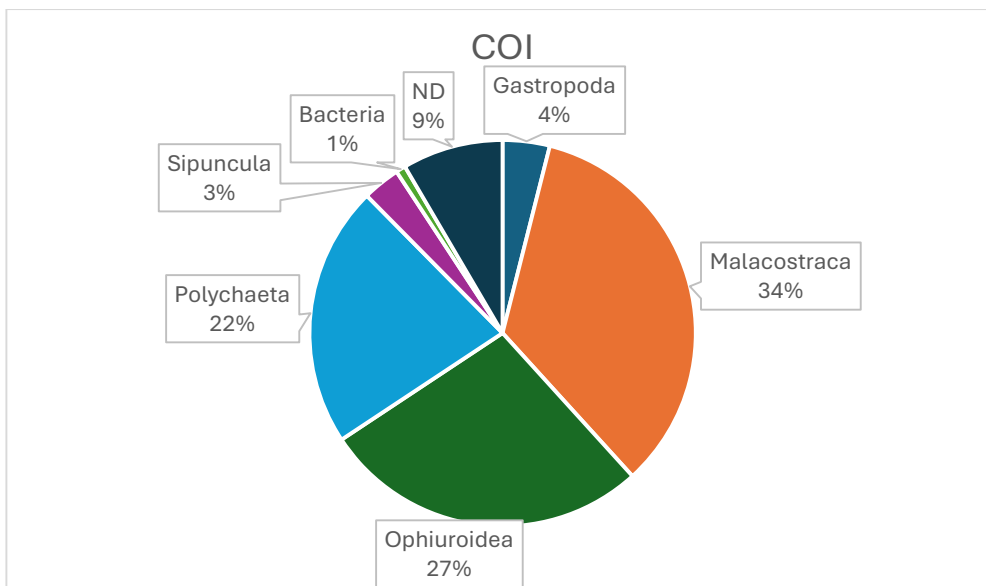


Fig. 4.3.4 – Percentage of potential invertebrate predators collected and identified by molecular barcoding. N.D. (non determined)

4.3.4 Barcoding of urchin juveniles

In the study area, the two most abundant sea urchin species are *P. lividus* and *A. lixula*. Adults are easily recognized by color, form and behavior. However, small juveniles (< 5 mm) are hardly distinguishable, since spines are still colorless, and the shape of the urchin is uniform. In our surveys we collected 55 sea urchin juveniles. Most of them (45, ~82%) were smaller than 1 mm, the rest being sized between 1 and 5 mm. In order to identify the urchin species, we sequenced the COI1 loci of a subset of 11 urchins, randomly picked. Only one sample provided an unreliable sequencing, assigned to Bacteria. The

remaining 10 juveniles were related to *P. lividus* (identity \geq 98.9%), suggesting that the settlement event that spanned our surveys was ascribed to that species.

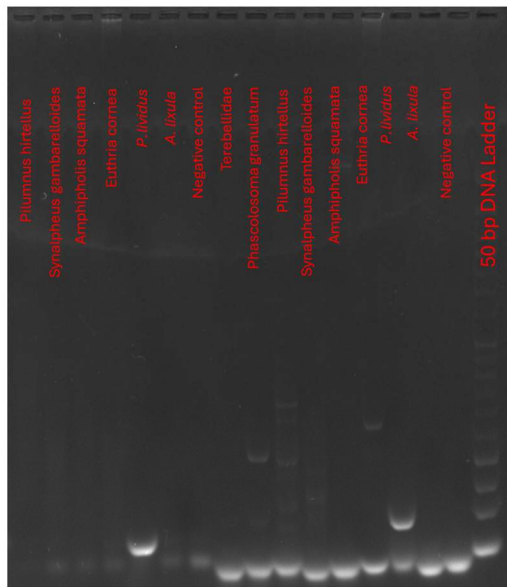
4.3.5 Primer efficiency

Ideal primer sets for assessing predator-prey interaction strongly amplify the prey DNA but not other organisms' DNA. In order to design primers specific for *P. lividus*, yet able to amplify *P. lividus* accessions from different Mediterranean regions, we aligned 254 sequences of *P. lividus* from different Mediterranean areas. To ensure specificity, the alignment included 328 sequences of the sympatric sea urchin species *A. lixula* and also those of other potentially occurring invertebrates from different taxonomic groups. We then selected the genetic regions that were conserved within the same species, but that differed between the two sea urchin species, and also with other invertebrates. In particular, for *P. lividus* we designed five primer pairs for the subunit 1 of the cytochrome oxidase c (COI1), three pairs for the cytochrome oxidase b (CYTb) and one pair for the 16S locus; for *A. lixula*, we designed five pairs for COI1 and two pairs for 16S (Table 4.2.2). Each primer pair was tested for specificity of amplification in a panel comprising positive controls (*i.e.* genomic DNA of adult *P. lividus* urchin and *A. lixula*) and negative controls (*i.e.* chosen among potential predator taxa). The expected band sizes were estimated to occur in the 63-178 bp range as the result of the amplification of degraded DNA.

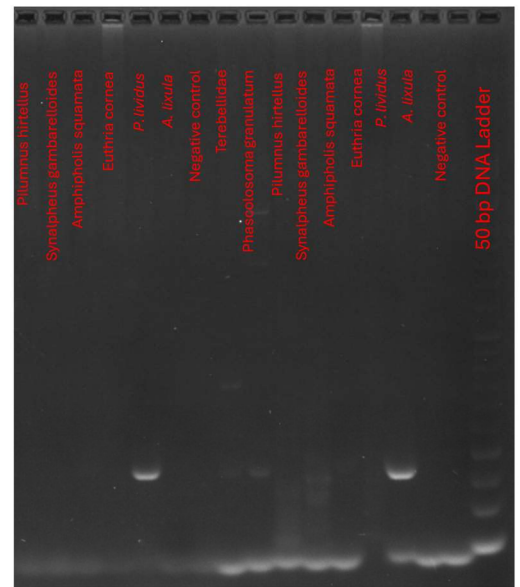
Primer sets amplified urchin DNA with different efficiencies, as observed by band intensity (Fig. 4.3.5). Pertaining *P. lividus* specific primers, all primers produced a strong band with *P. lividus* DNA, with the exception of Pliv-cytb-C, which failed to amplify. Pliv-COI1-N, Pliv-COI1-M and Pliv-cytb-M showed unspecific bands in the predator samples. Conversely, Pliv-COI1-C, Pl-COI-Nterm, Pliv-16S and Pliv-cytb-N only showed the specific band when *P. lividus* DNA was present in the template. For *A. lixula*, all primers produced a band in presence of *A. lixula* DNA. However, Al-COI-Nterm, Alix-COI1-C, Alix-COI1-M and Alix-16sM also produced unspecific bands in presence of predator DNA. Only Al-COI-Cterm, Alix-COI1-N and Alix-16sC were specific. On the basis of the specificity of primer sets in the

reaction, and considering the different targeting that might likely maximize the chances of recovery of amplifiable DNA in predator guts, we selected primers Pliv-16S, Pliv-cytb-N and Pl-COI-Nterm as *P. lividus* specific primers, and Alix-COI1-N and Alix-16sC as *A. lixula* specific primers in all subsequent experiments

Pl-COI-Cterm: 63 bp Pliv-COI1-N: 103 bp



Pliv-COI1-C: 178 bp Pliv-COI1-M: 173 bp



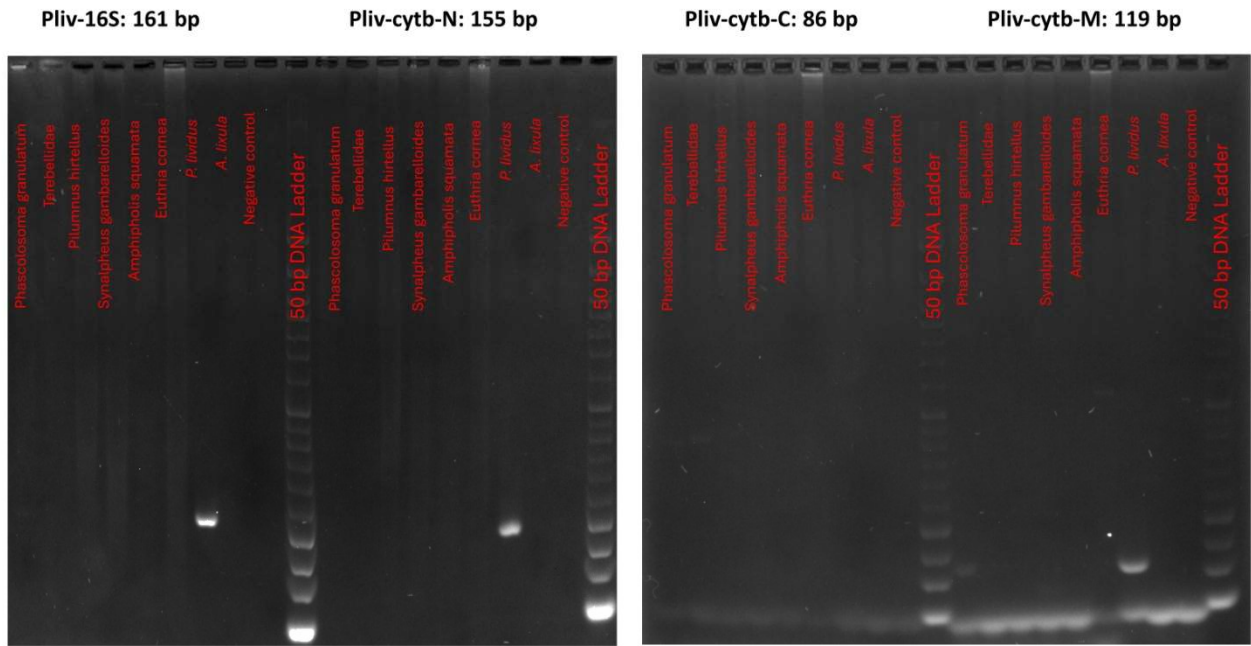


Fig. 4.3.5-Specificity test



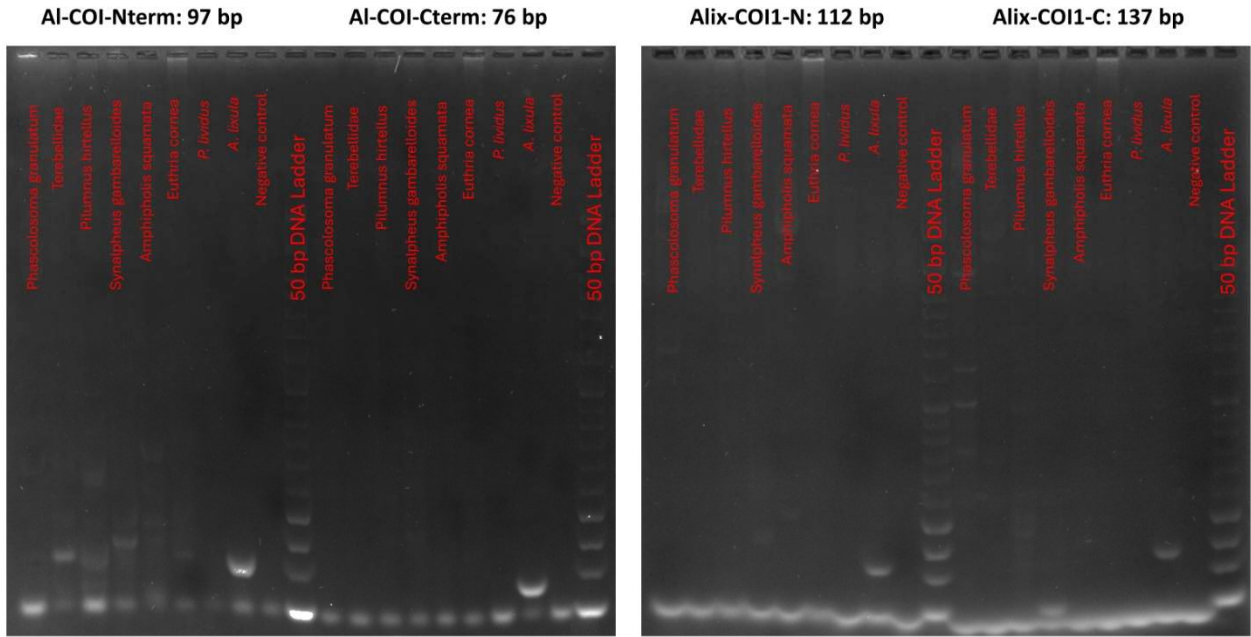


Fig. 4.3.5-Specificity test

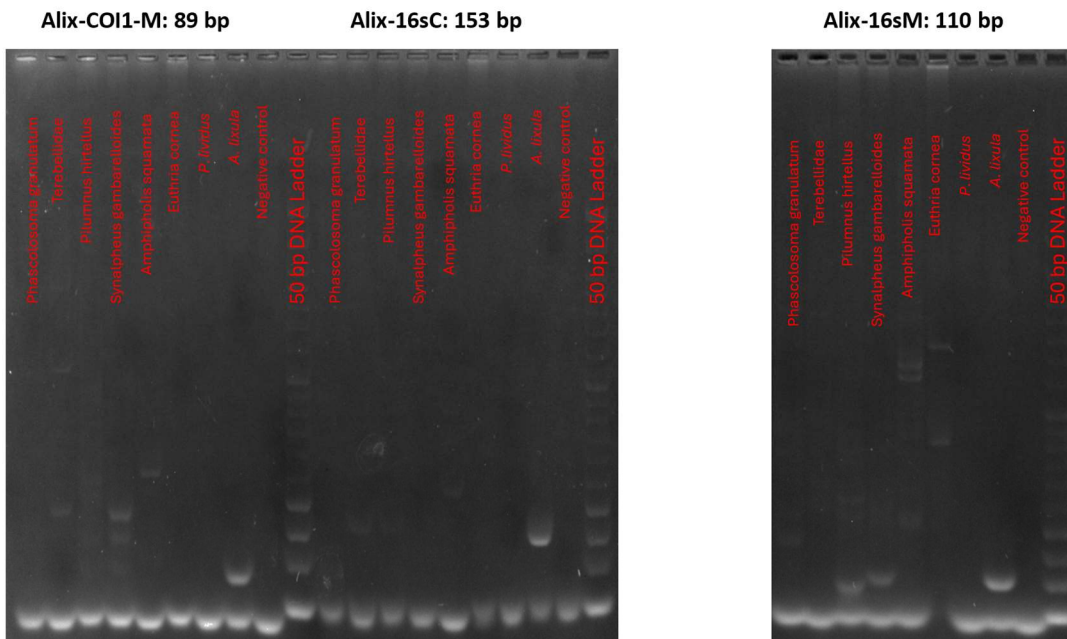


Fig. 4.3.5-Specificity test

Once we selected specific primers for *P. lividus* and *A. lixula*, we tested for their sensitivity, by diluting urchin DNA from 10 ng to 100 fg (100,000 fold). A strong band was visible for all primer pairs with as little as 100 pg DNA, and fainter bands, yet clearly distinguishable, up to 1 pg for primers Pliv-16S, Pliv-cytb-N and Alix-16sC, and up to 10 pg for Pl-COI-Nterm and Alix-COI1-N (Fig. 4.3.6).

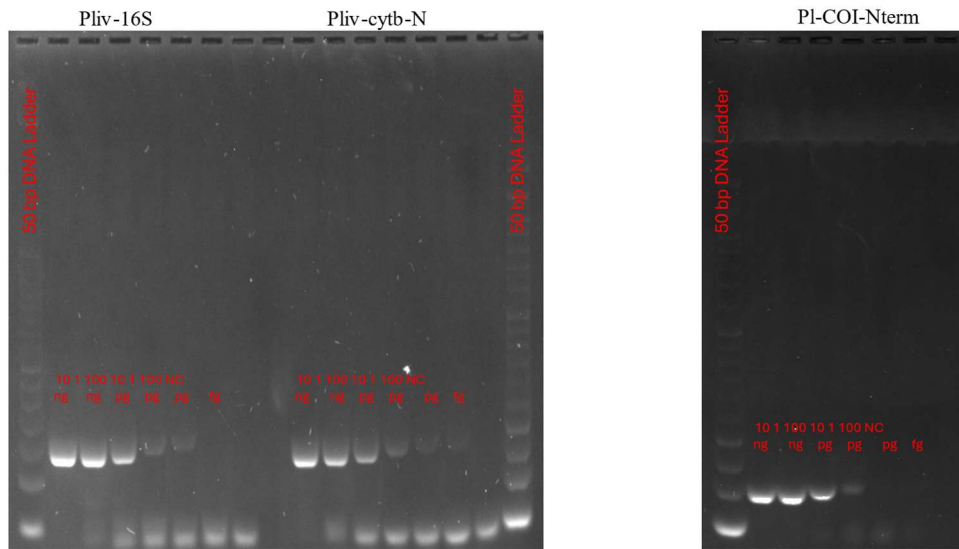


Fig. 4.3.6- Sensitivity test

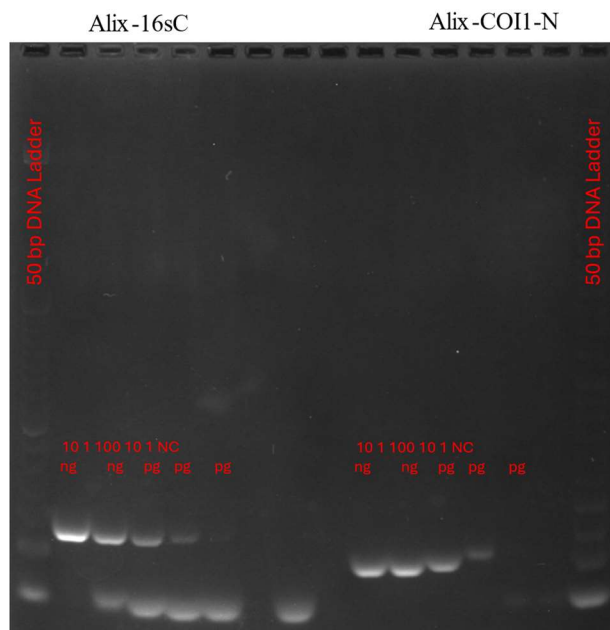


Fig. 4.3.6- Sensitivity test

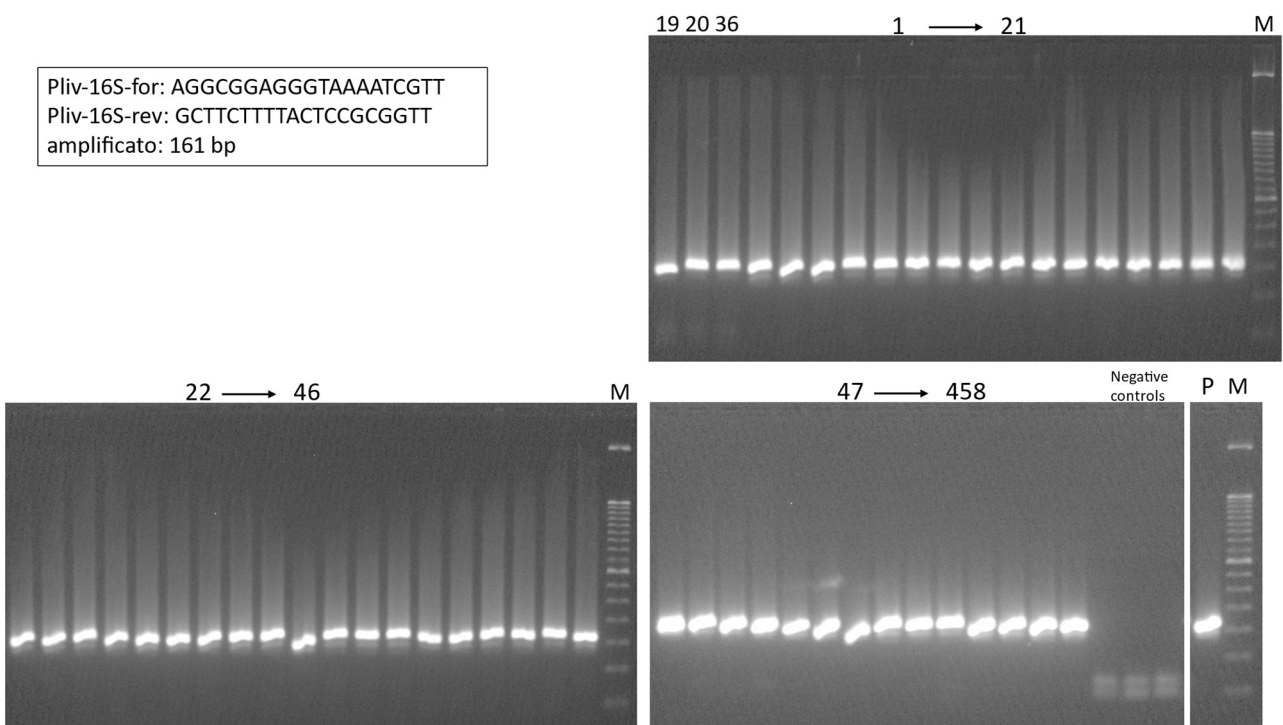
The selected primers therefore are sensitive enough to detect the small amount of urchin DNA present in the stomach of predators. Our tests were performed on purified DNA. However, in homogenates from whole predators and their gut content, the presence of excess amount of predator's DNA might interfere with prey's DNA amplification. To test this hypothesis, we diluted a small amount (100 pg) of urchin DNA with a thousand-fold excess of invertebrate DNA, selected from a representative of each major taxonomic group. All the primers amplified the corresponding urchin DNA with no interference from invertebrate DNA (Fig. 4.3.7), indicating that they are suitable for detecting the prey within the predator body.



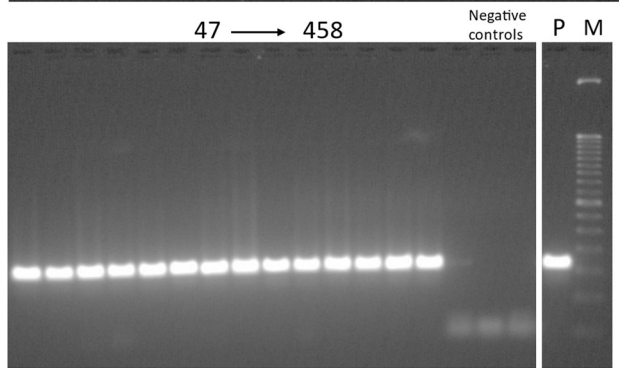
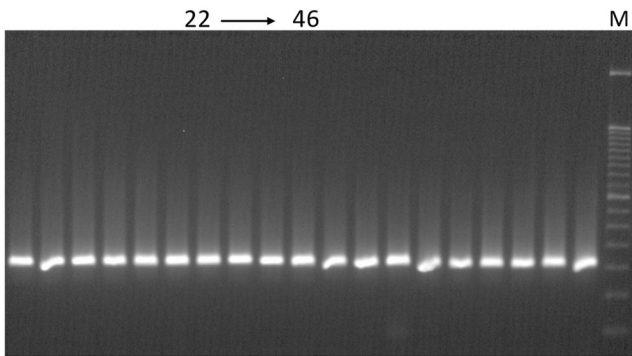
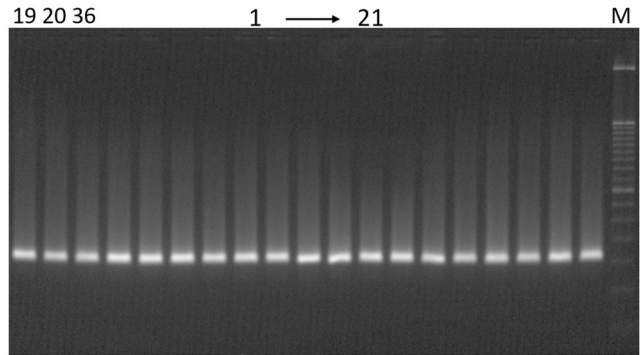
Fig. 4.3.7- Inhibition test

4.3.6 Detection of urchin DNA in invertebrate samples

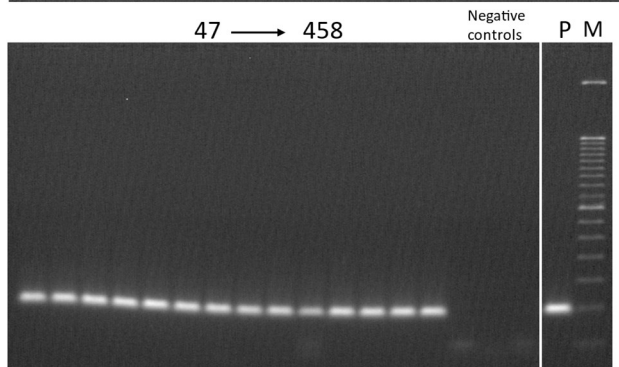
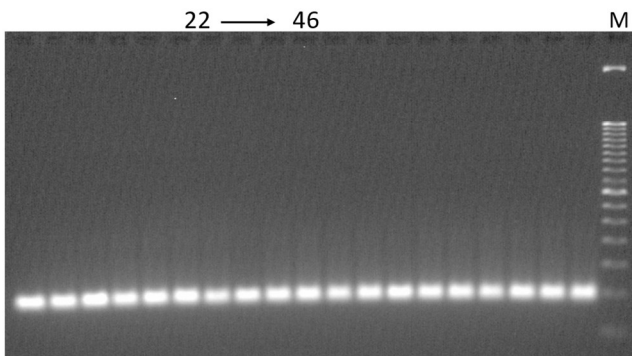
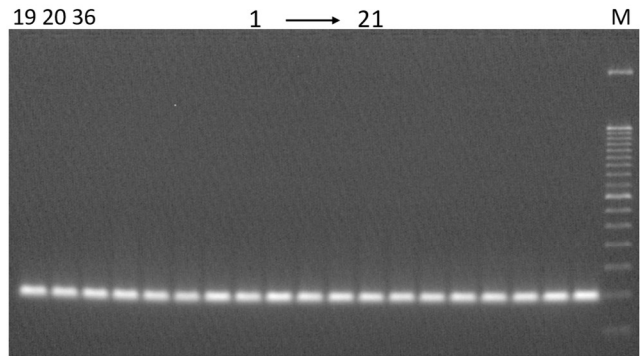
We analyzed all the samples by independent amplification with primer pairs Pliv-COI-Nterm, Pliv-16S and Pliv-cytb-N, specific for *P. lividus*. The 55 sea urchin juveniles all strongly amplified with *P. lividus* primers, as evidenced by the intense bands of the expected sizes. Conversely, the same samples did not produce any band when *A. lixula* specific primers Alix-16sC was used (Fig. 4.3.8). This result confirmed the barcoding results of a subset of urchins, indicating that all the juveniles belonged to the species *P. lividus*. Next, we then tested the invertebrates DNA with the three *P. lividus* specific primer pairs. The 29 invertebrate samples that had failed in the amplification with Geller's universal primers also did not amplify with *P. lividus* primers, confirming that they might contain PCR inhibitors or that their DNA quality was too low. Among the remaining 350 samples, 86 (26%) scored positive in at least one locus, 47 samples (13%) in at least two loci, and 23 (7%) scored positive for all the three loci, yielding intense bands (Table 4.2.1 and Fig.4.3.9. Conversely, 264 samples (75%) were negative, since they did not show any band for any primer set. 16S was the most sensitive locus, with 69 positive samples (20%), closely followed by CYTB (n=62, 18%). Conversely, COIN only detected 29 samples (8%).



Pliv-cytb-Nfor: TCTGGTGGAAATTCGGCTCT
Pliv-cytb-Nrev: TCGAAGCAGTCACCCGTAAT
amplificato: 155 bp



Pl-COI-Nterm-for: ttctcactccatcttgcggg
Pl-COI-Nterm-rev: aaaagacattcccggcggttc
amplificato 93 bp



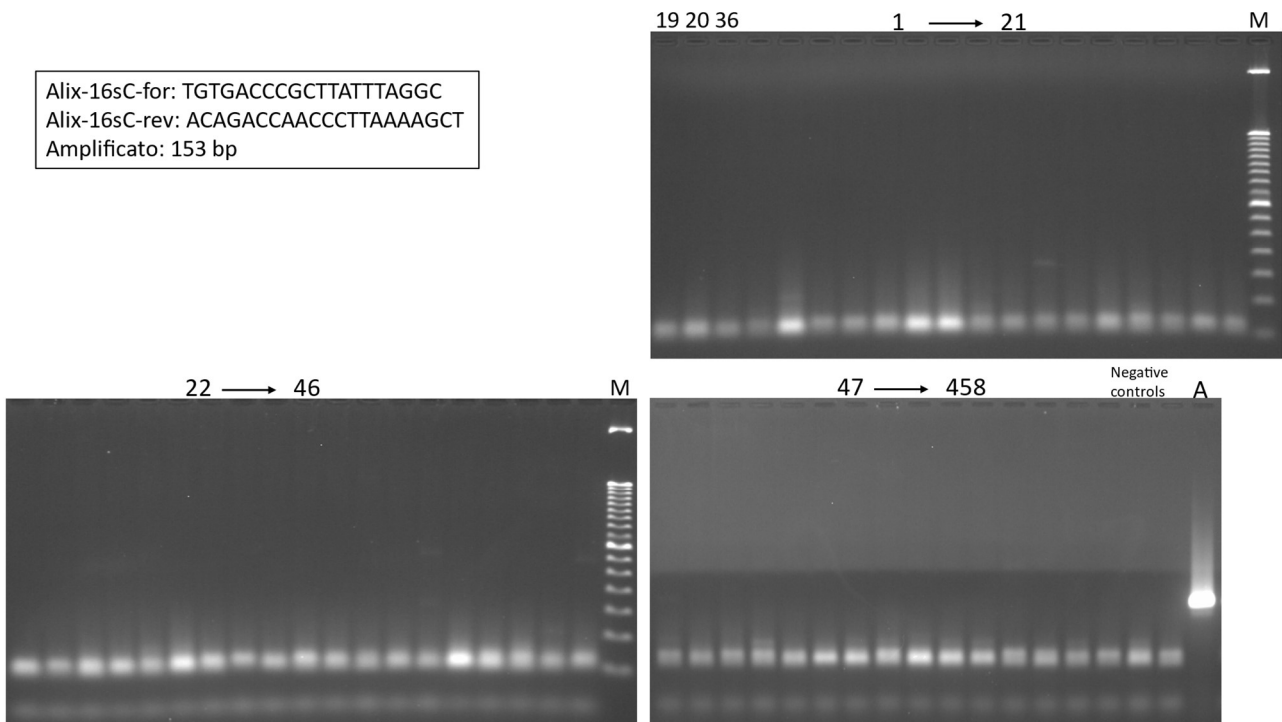
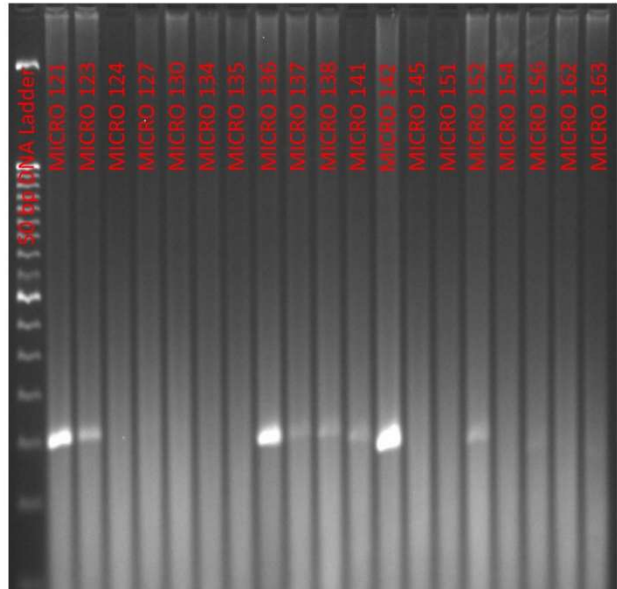
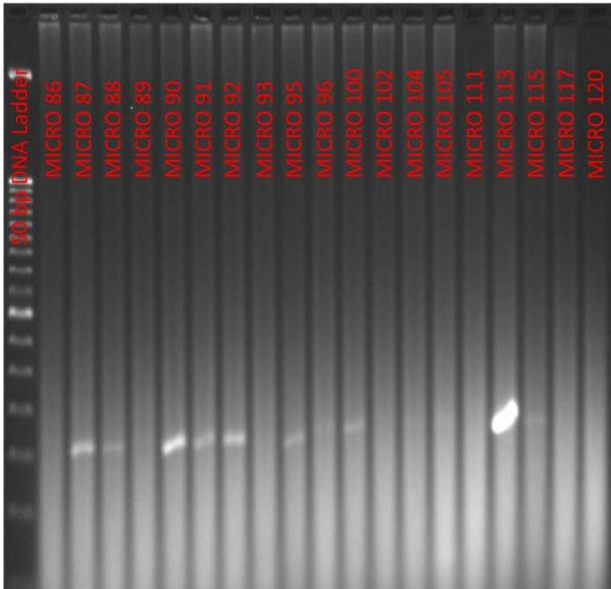


Fig. 4.3.8- Sea urchins settlers amplified with the *P. lividus* and *A. lixula* primers

Considering only the most conservative results from the 23 samples that strongly amplified all three *P. lividus* loci, positive invertebrates belonged to Alpheidae (n=3, 18% of all samples from the same family), Ampithoidae (n=2, 12%), Idoteidae (n=1, 100%) and Pilumnidae (n=1, 13%) among crustaceans, Amphiuroidae (n=5, 15%) and Ophiotrichidae (n=2, 3%) among serpentine stars, and Nereididae (n=3, 6%), Polynoidae (n=4, 20%) and Terebellidae (n=2, 12%) among Polychaetes. One Sipunculid specimen (8%) resulted positive to *P. lividus* DNA as well (Table 4.3.3). Excluding the locus COIN from the comparison due to its stringency, the 44 samples (13%) that scored positive to both 16S and CYTB included additional specimen of the afore mentioned families, plus whelks (Muricidae and Rissoidae), five more families of crustaceans (Diogenidae, Epiplatidae, Galatheidae, Inachidae, Paguridae) and one Ophiodermtidae specimen among the serpentine stars (Table 4.2.1; examples in Fig. 4.3.9).

Pliv-16S-for: AGGCGGAGGGTAAAATCGTT
Pliv-16S-rev: GCTTCTTTTACTCCGCGGT
amplicon: 161 bp



Pliv-16S-for: AGGCGGAGGGTAAAATCGTT
Pliv-16S-rev: GCTTCTTTACTCCGCGTT
amplicon: 161 bp

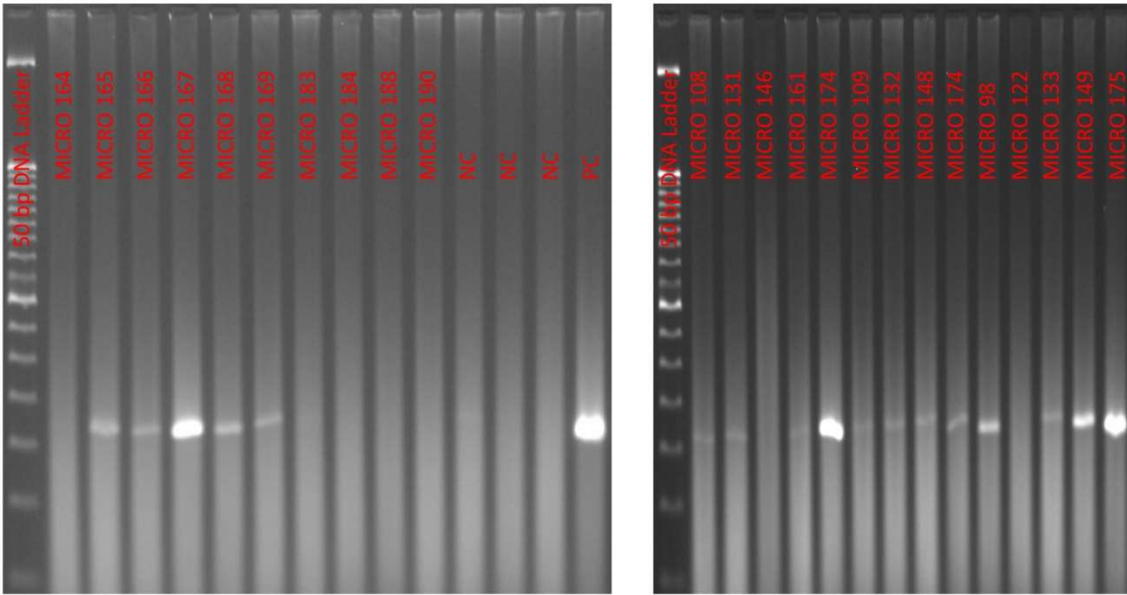
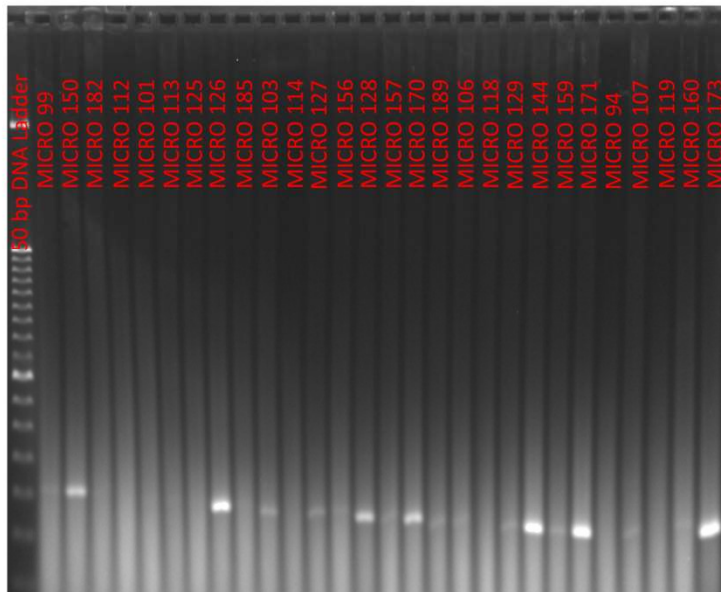


Fig. 4.3.9- Invertebrates samples amplified with the *P. lividus* specific primers

Pliv-16S-for: AGGCGGAGGGTAAAATCGTT
Pliv-16S-rev: GCTTCTTTACTCCGCGTT
amplicon: 161 bp



Pliv-cytb-Nfor: TCTGGTGAAATTCGGCTCT
 Pliv-cytb-Nrev: TCGAAGCAGTACCCGTAAT
 amplicon: 155 bp

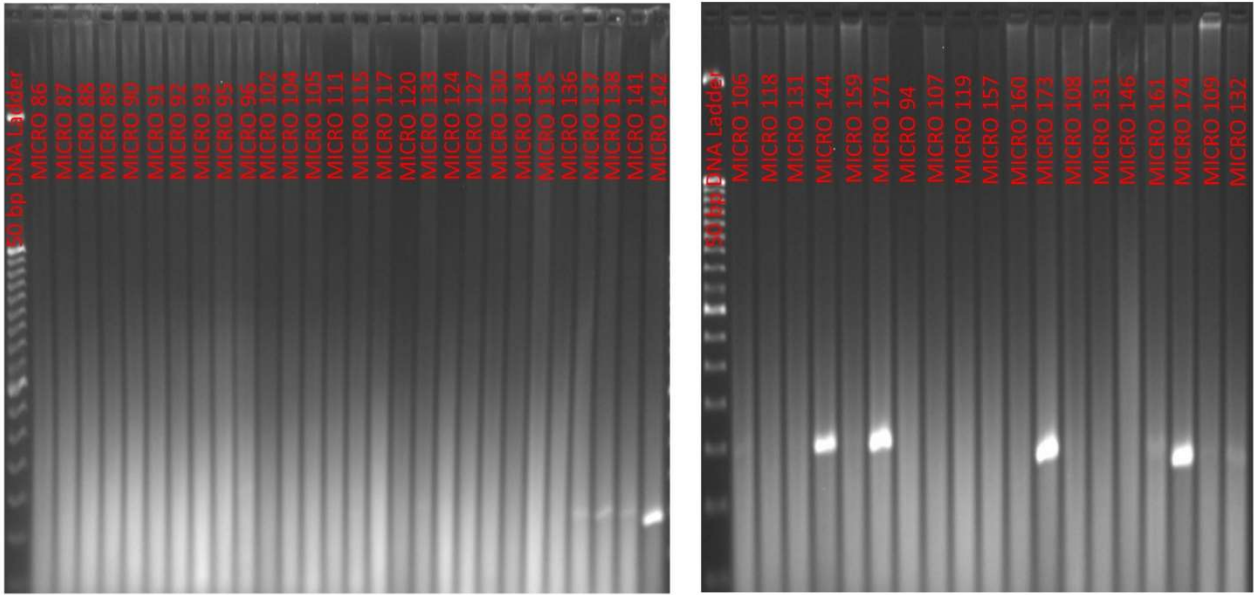
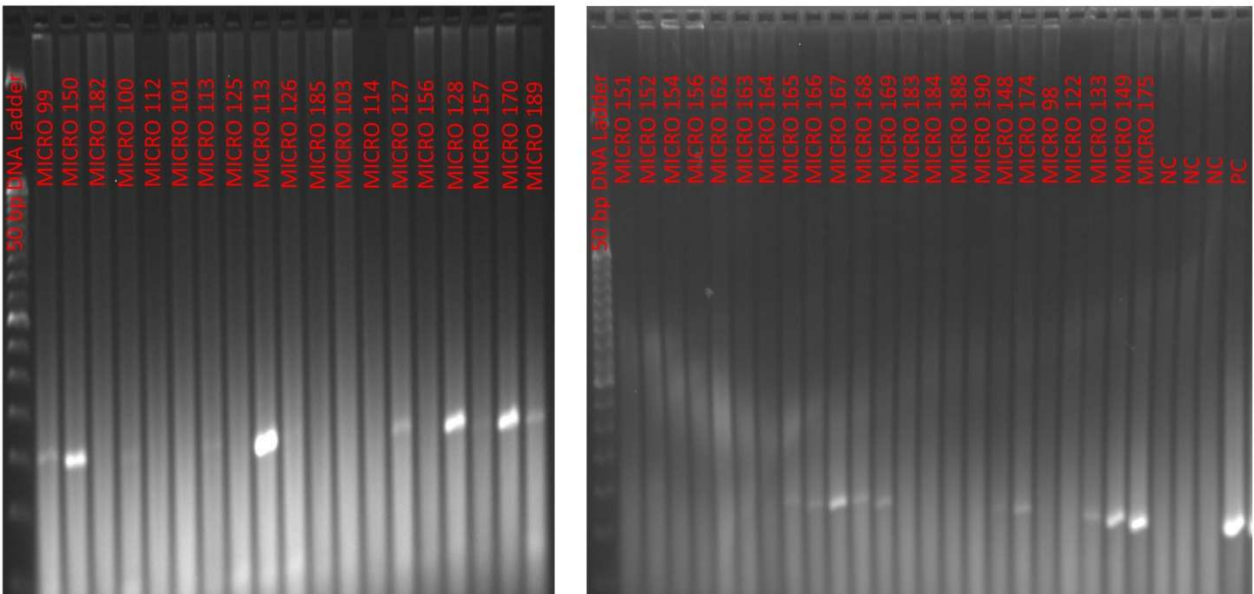


Fig. 4.3.9- Invertebrates samples amplified with the *P. lividus* specific primers

Pliv-cytb-Nfor: TCTGGTGAAATTCGGCTCT
 Pliv-cytb-Nrev: TCGAAGCAGTACCCGTAAT
 amplicon: 155 bp



PI-COI-Nterm-for: ttctcactccatcttgctggg
PI-COI-Nterm-rev: aaaagacattcccggcggttc
amplicon 93 bp

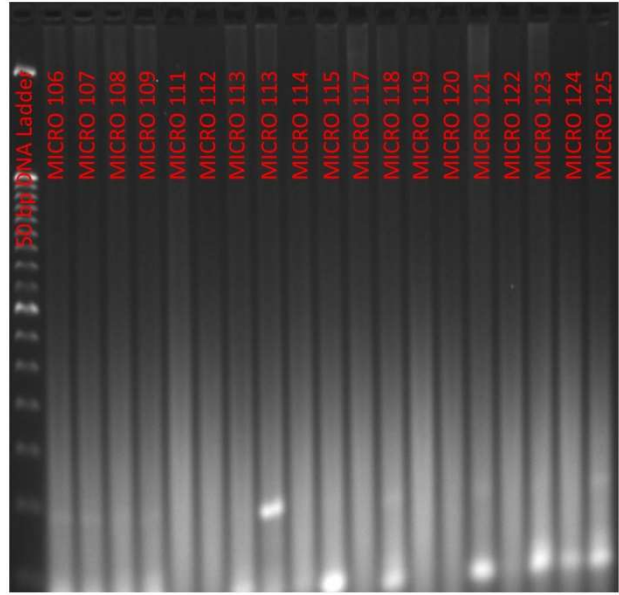
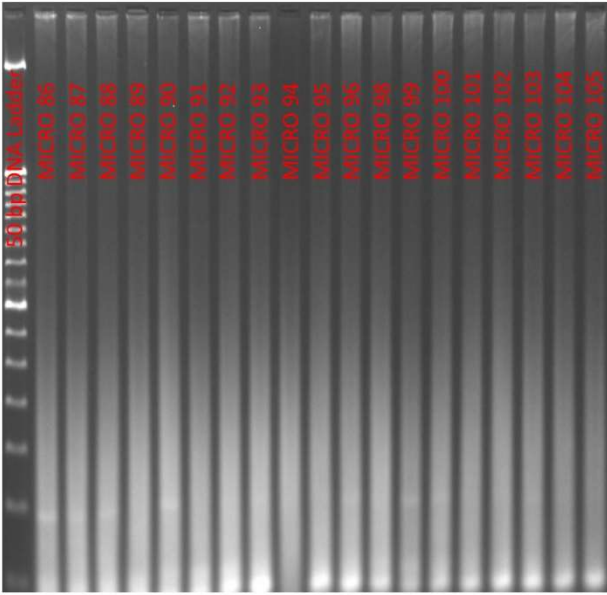
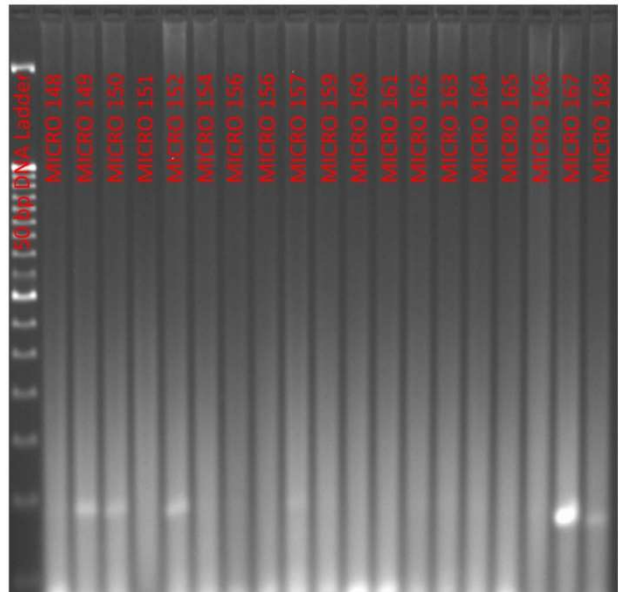
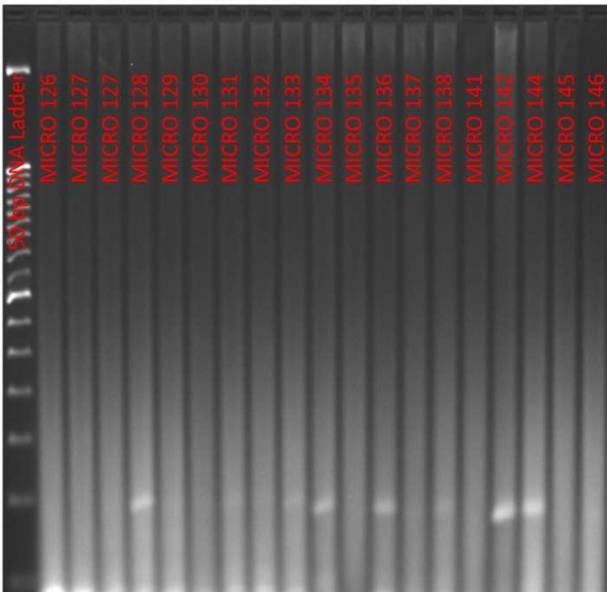


Fig. 4.3.9- Invertebrates samples amplified with the *P. lividus* specific primers

PI-COI-Nterm-for: ttctcactccatcttgctggg
PI-COI-Nterm-rev: aaaagacattcccggcggttc
amplicon 93 bp



PI-COI-Nterm-for: ttctcactccatcttgctggg
PI-COI-Nterm-rev: aaaagacattcccggcggttc
amplicon 93 bp

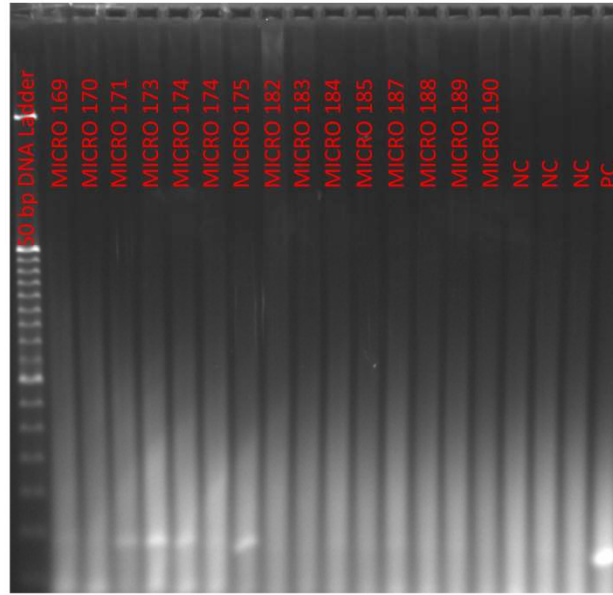
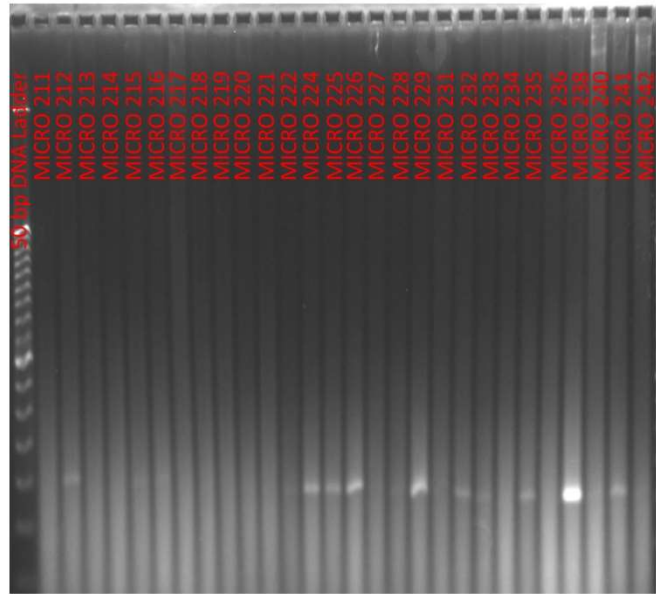
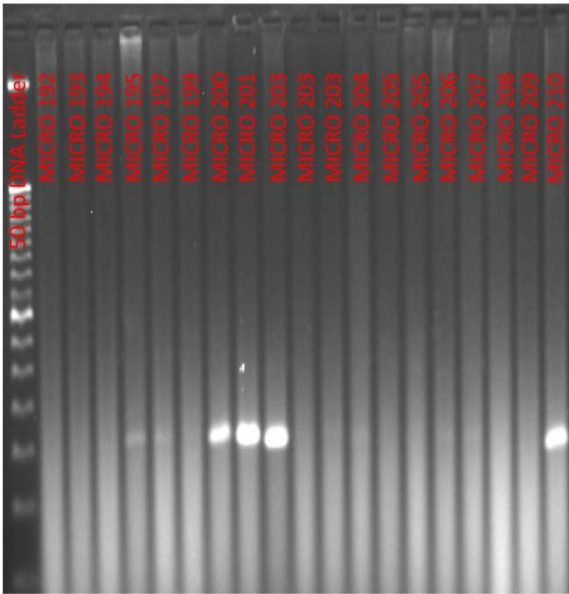


Fig. 4.3.9- Invertebrates samples amplified with the *P. lividus* specific primers

Pliv-16S-for: AGGCGGAGGGTAAAATCGTT
 Pliv-16S-rev: GCTTCTTTACTCCGCGTT
 amplicon: 161 bp



Pliv-16S-for: AGGCGGAGGGTAAAATCGTT
 Pliv-16S-rev: GCTTCTTTACTCCGCGTT
 amplicon: 161 bp

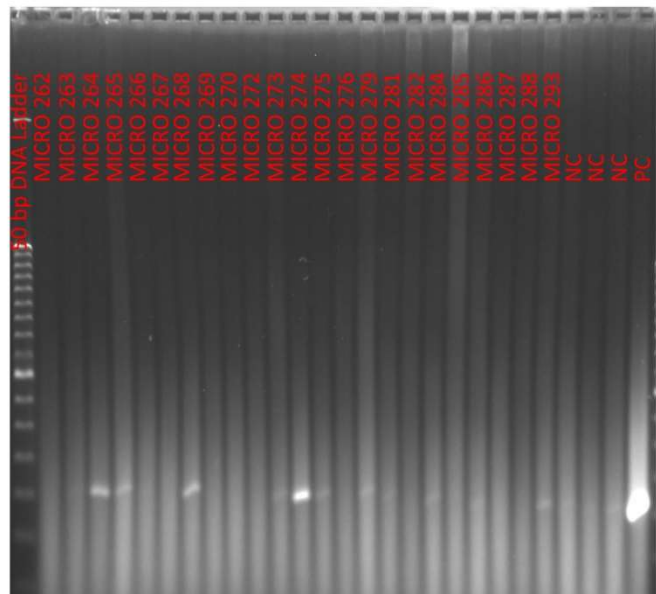
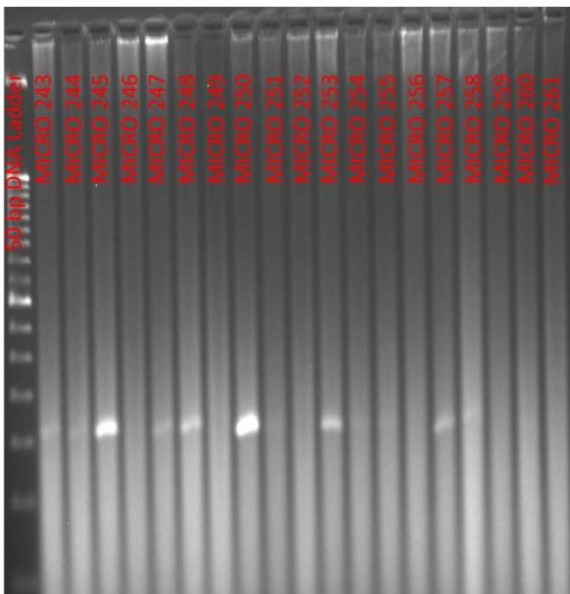


Fig. 4.3.9- Invertebrates samples amplified with the *P. lividus* specific primers

Pliv-cytb-Nfor: TCTGGTGGAAATTCGGCTCT
 Pliv-cytb-Nrev: TCGAAGCAGTCACCCGTAAT
 Amplicon : 155 bp

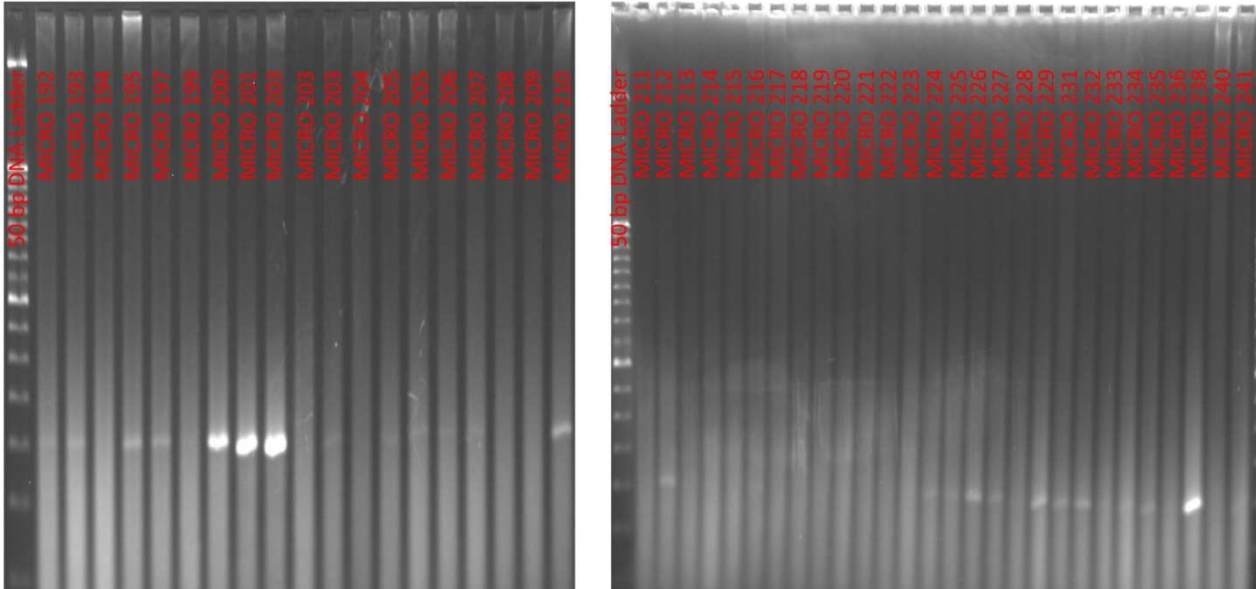
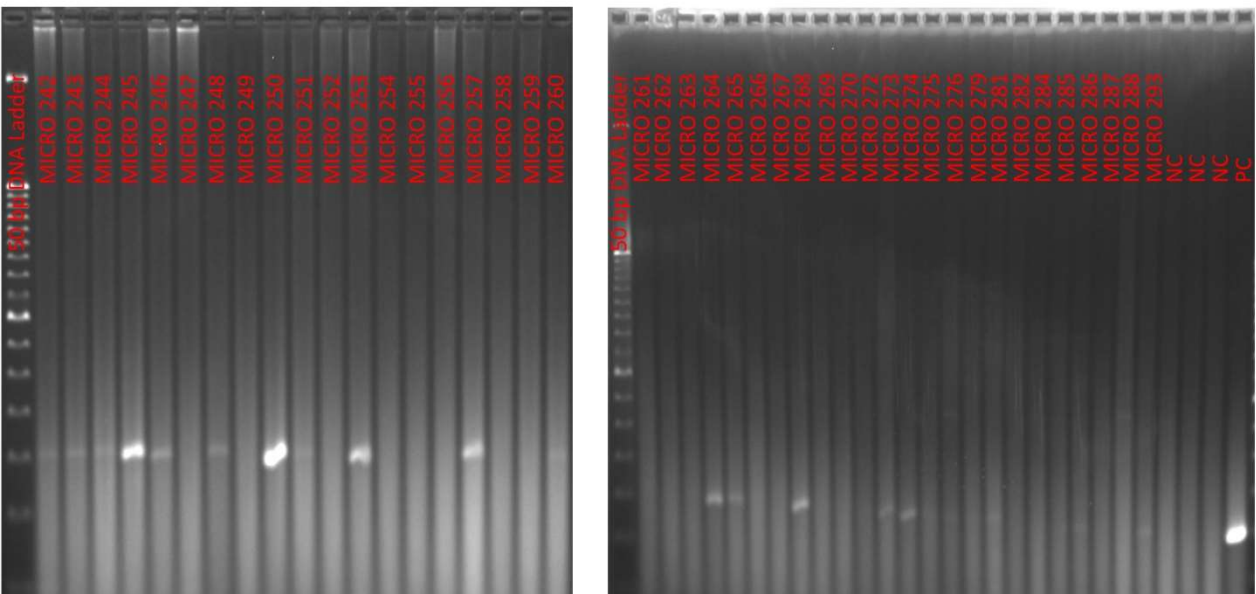


Fig. 4.3.9- Invertebrates samples amplified with the *P. lividus* specific primers

Pliv-cytb-Nfor: TCTGGTGGAAATTCGGCTCT
 Pliv-cytb-Nrev: TCGAAGCAGTCACCCGTAAT
 amplicon: 155 bp



PI-COI-Nterm-for: ttctcactccatcttgctggg
PI-COI-Nterm-rev: aaaagacattcccggcgcttc
amplicon 93 bp

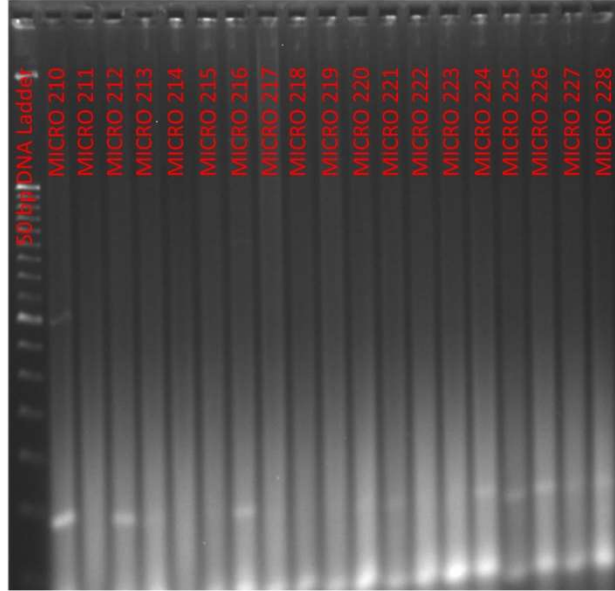
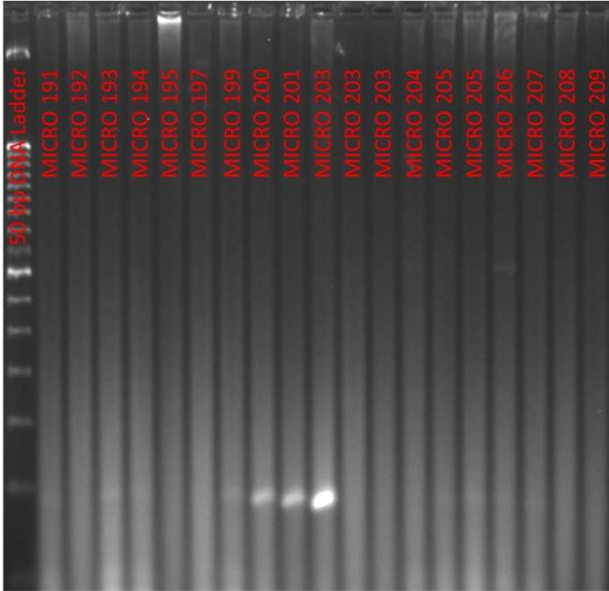
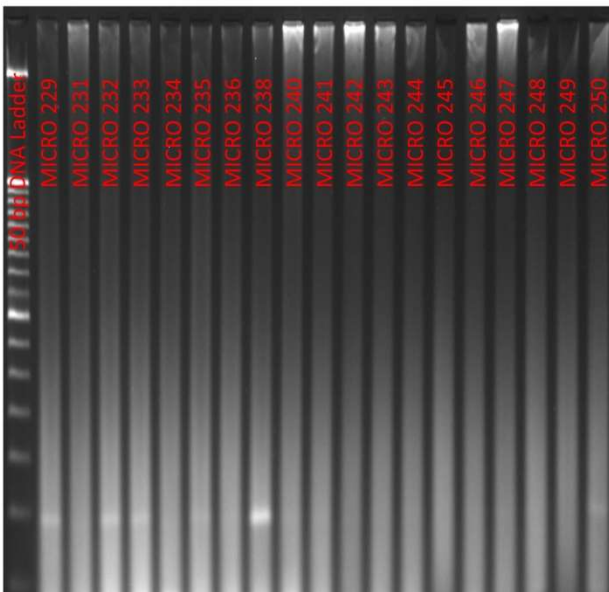


Fig. 4.3.9- Invertebrates samples amplified with the *P. lividus* specific primers

PI-COI-Nterm-for: ttctcactccatcttgctggg
PI-COI-Nterm-rev: aaaagacattcccggcgcttc
amplicon 93 bp



PI-COI-Nterm-for: ttctcactccatcttgctggg
 PI-COI-Nterm-rev: aaaagacattcccggcggtc
 amplicon 93 bp

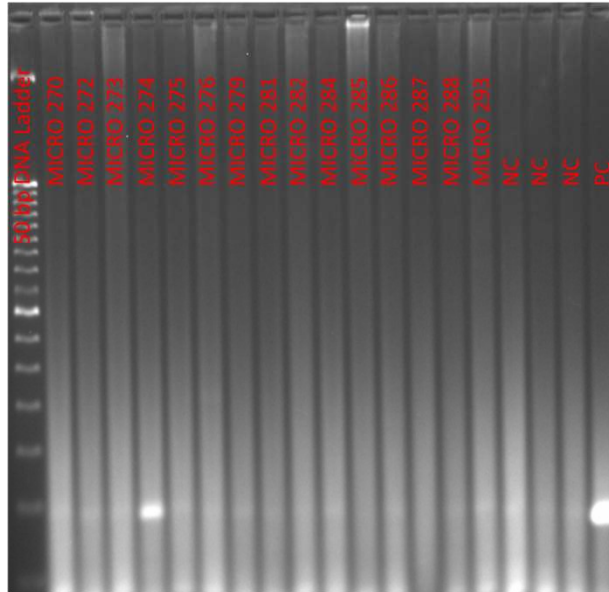
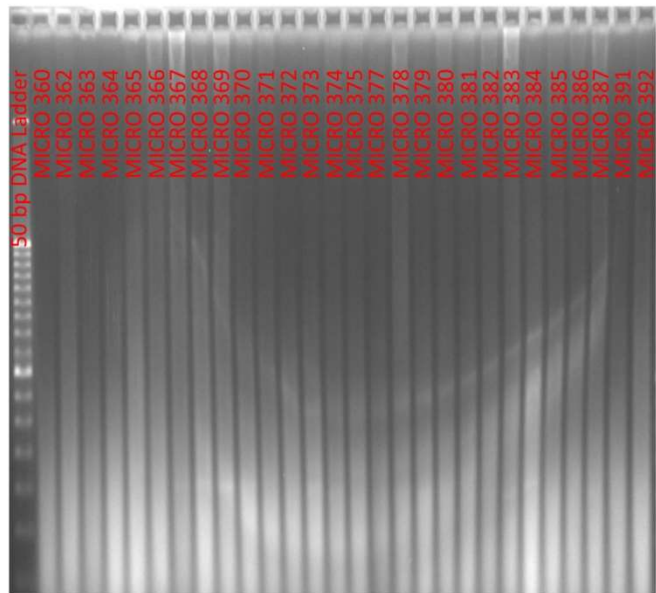
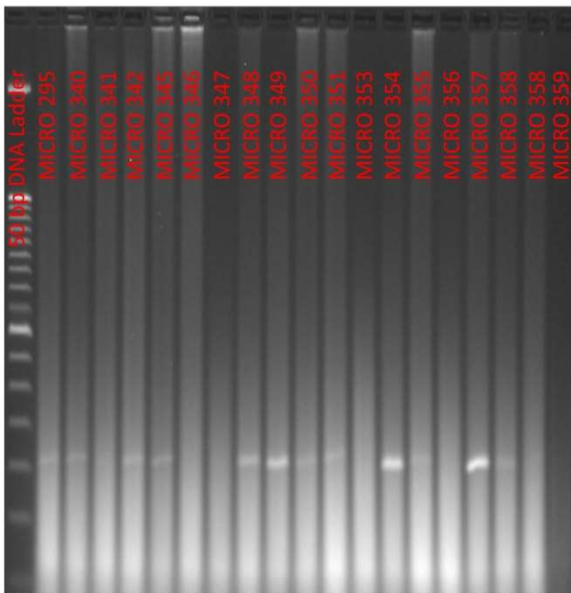


Fig. 4.3.9- Invertebrates samples amplified with the *P. lividus* specific primers

Pliv-16S-for: AGGCGGAGGGTAAAATCGTT
 Pliv-16S-rev: GCTTCTTTACTCCGCGTT
 amplicon: 161 bp



Pliv-16S-for: AGGCGGAGGGTAAAATCGTT
 Pliv-16S-rev: GCTTCTTTACTCCGCGTT
 amplicon: 161 bp

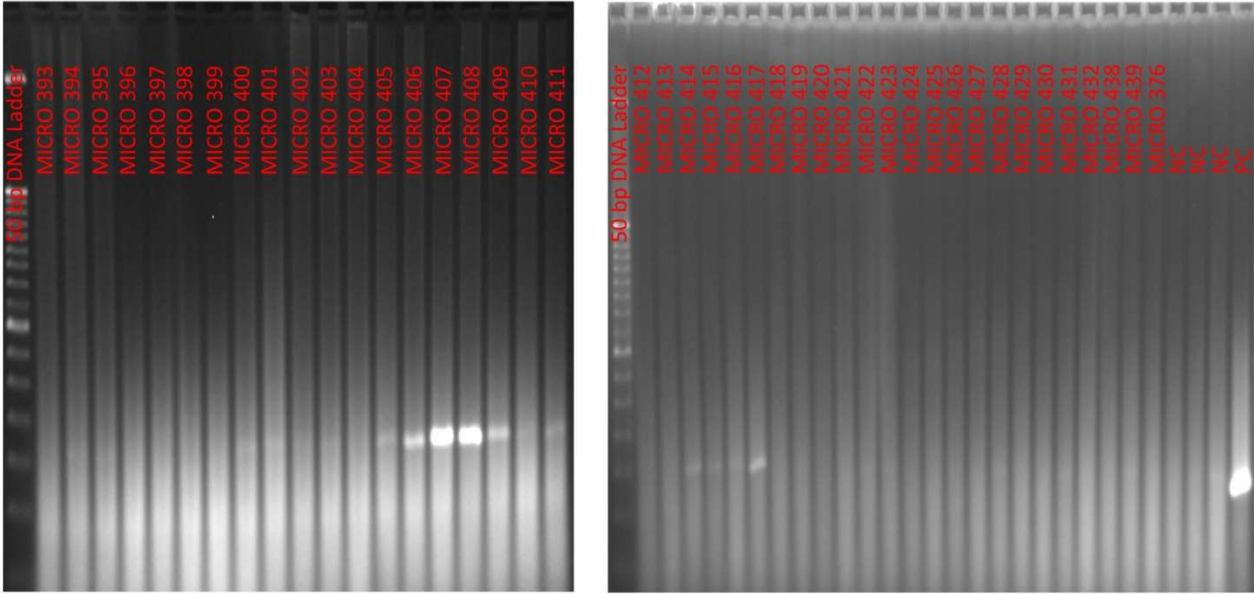
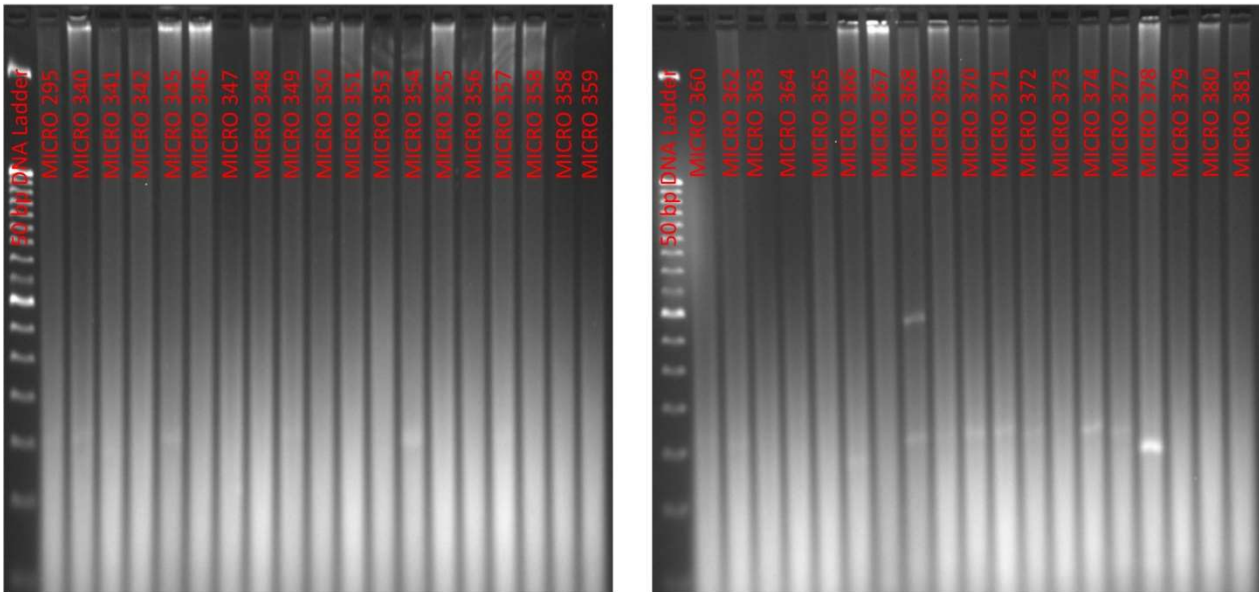


Fig. 4.3.9- Invertebrates samples amplified with the *P. lividus* specific primers

Pliv-cytb-Nfor: TCTGGTGAAATTCGGCTCT
 Pliv-cytb-Nrev: TCGAAGCAGTCACCCGTAAT
 amplicon: 155 bp



Pliv-cytb-Nfor: TCTGGTGGAAATTCGGCTCT
Pliv-cytb-Nrev: TCGAAGCAGTCACCCGTAAT
amplicon: 155 bp

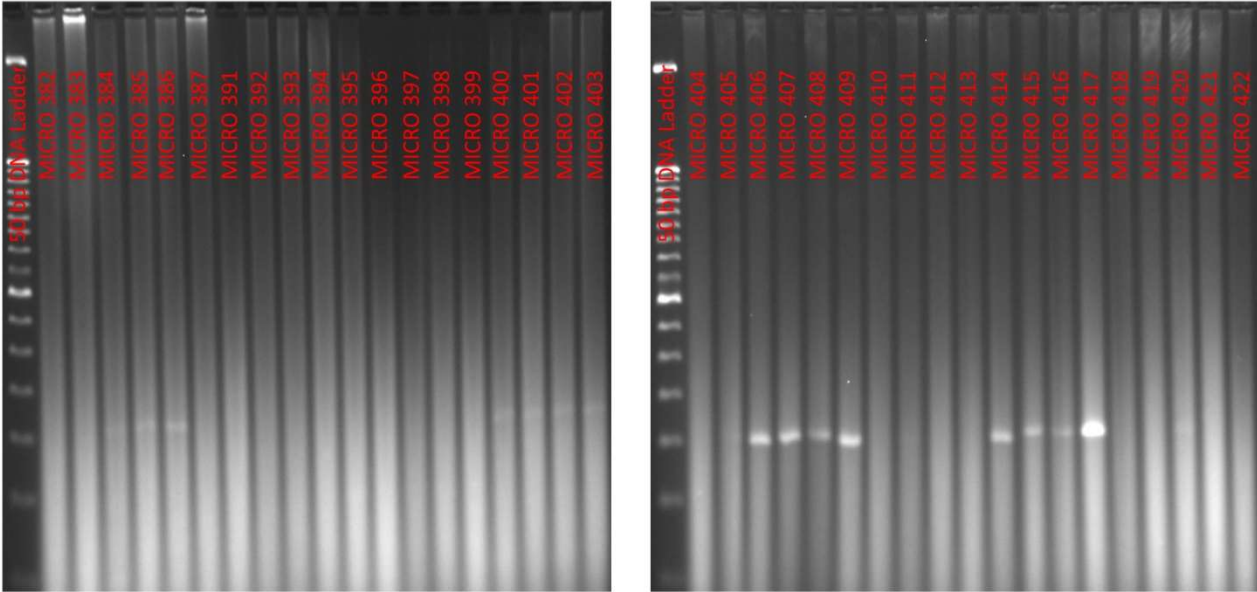
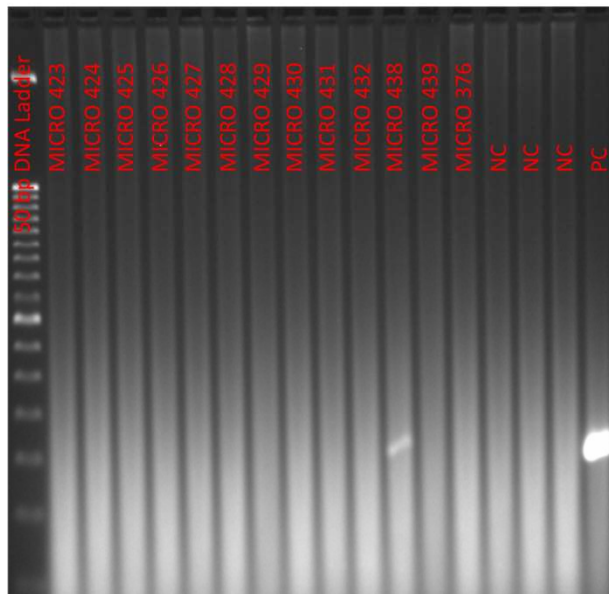


Fig. 4.3.9- Invertebrates samples amplified with the *P. lividus* specific primers

Pliv-cytb-Nfor: TCTGGTGGAAATTCGGCTCT
Pliv-cytb-Nrev: TCGAAGCAGTCACCCGTAAT
amplicon: 155 bp



PI-COI-Nterm-for: ttctcactccatcttgctggg
 PI-COI-Nterm-rev: aaaagacattcccgcgttc
 amplicon 93 bp

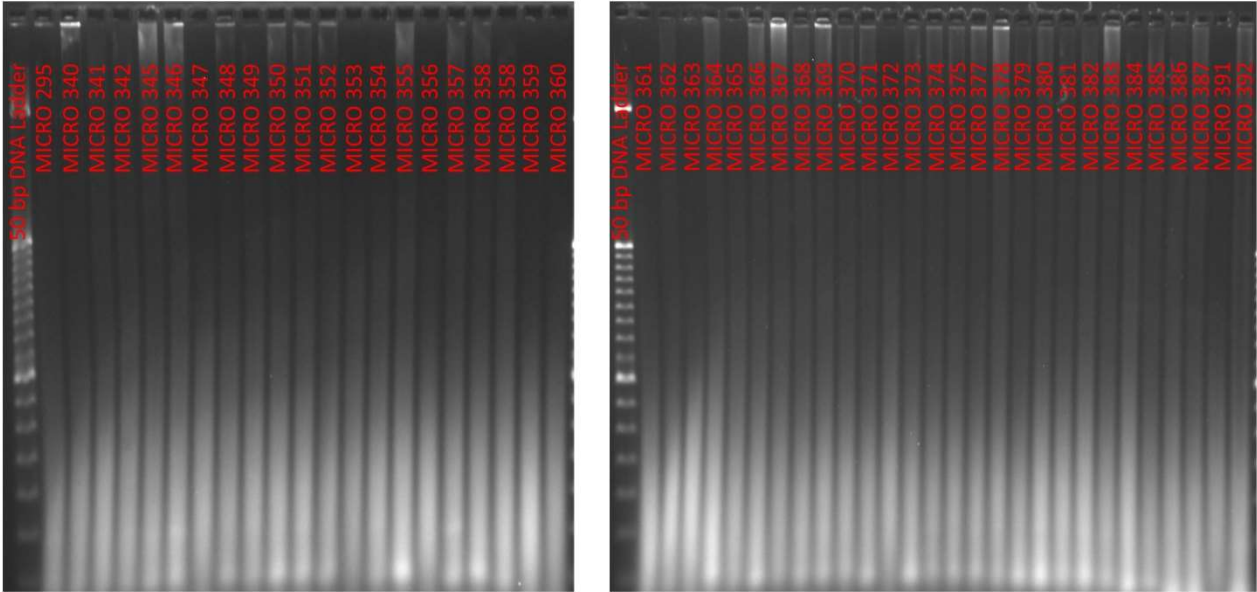
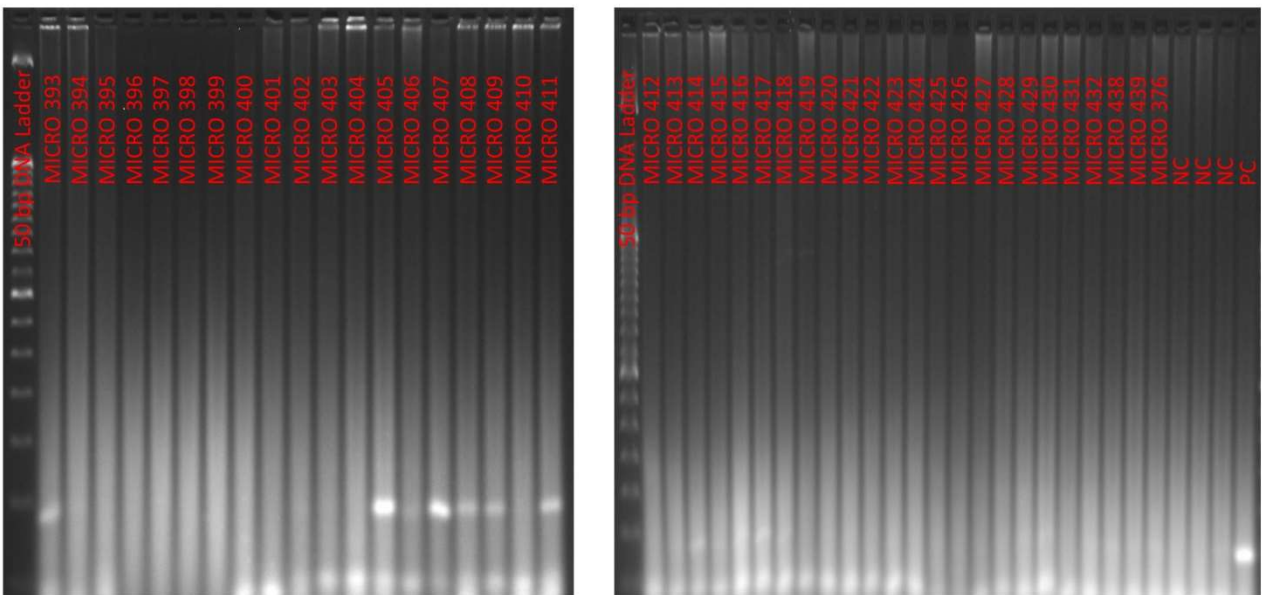


Fig. 4.3.9- Invertebrates samples amplified with the *P. lividus* specific primers

PI-COI-Nterm-for: ttctcactccatcttgctggg
 PI-COI-Nterm-rev: aaaagacattcccgcgttc
 amplicon 93 bp



Pliv-16S-for: AGGCGGAGGGTAAAATCGTT
Pliv-16S-rev: GCTTCTTTACTCCGCGTT
amplicon: 161 bp

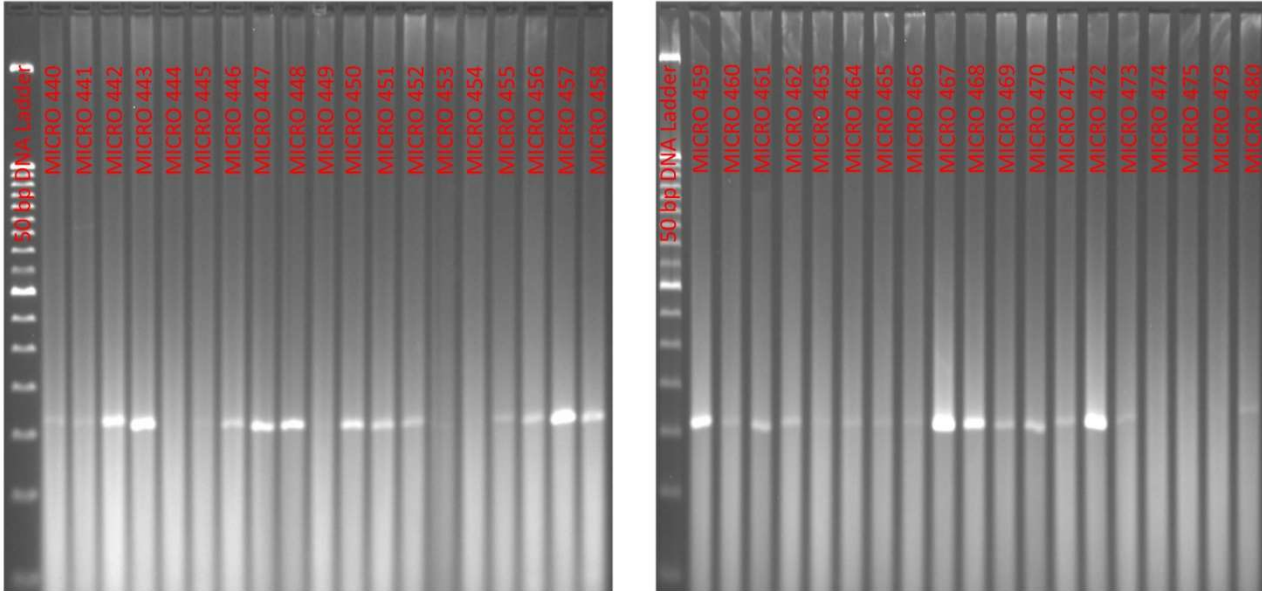
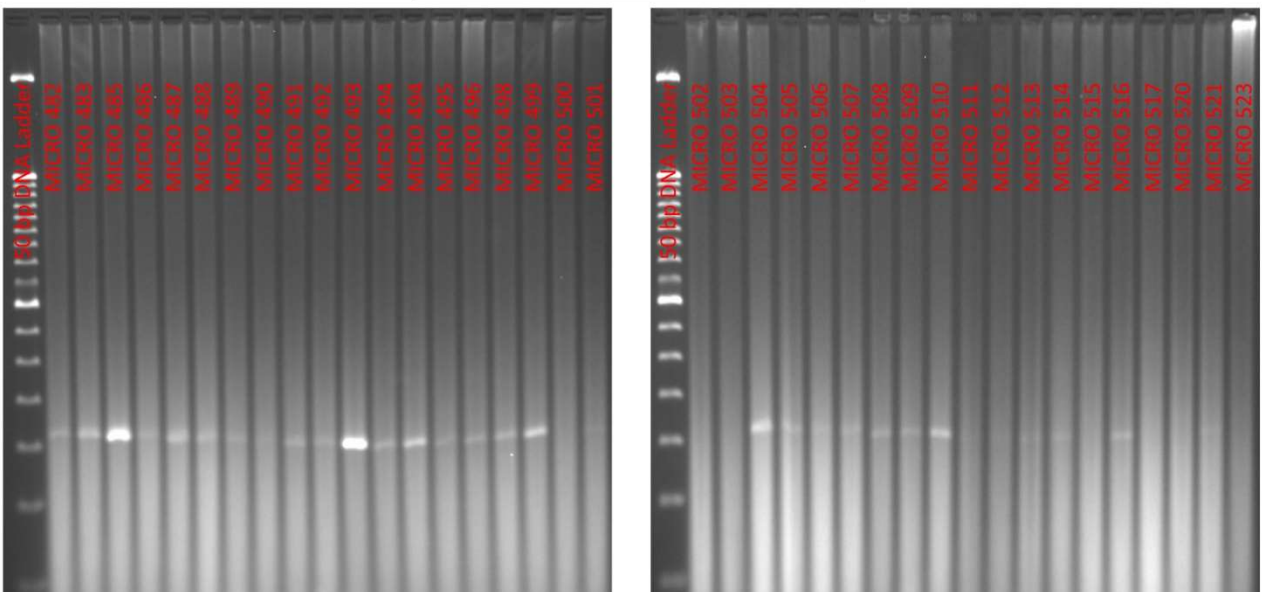


Fig. 4.3.9- Invertebrates samples amplified with the *P. lividus* specific primers

Pliv-16S-for: AGGCGGAGGGTAAAATCGTT
Pliv-16S-rev: GCTTCTTTACTCCGCGTT
amplicon: 161 bp



Pliv-16S-for: AGGCGGAGGGTAAAATCGTT
Pliv-16S-rev: GCTTCTTTACTCCGCGTT
amplicon: 161 bp

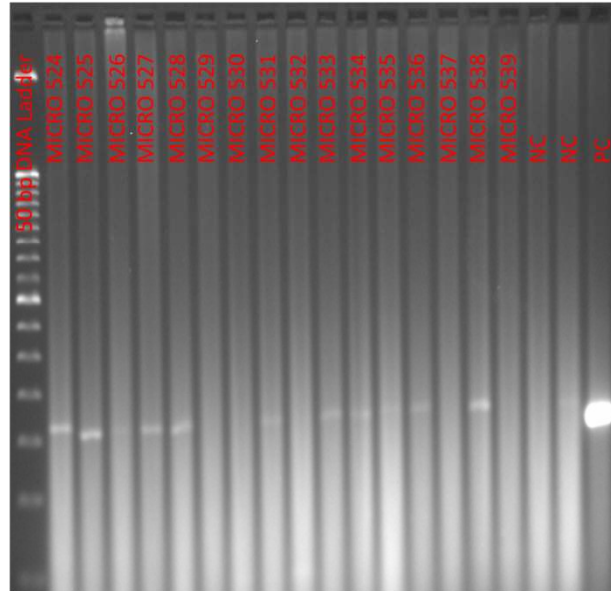
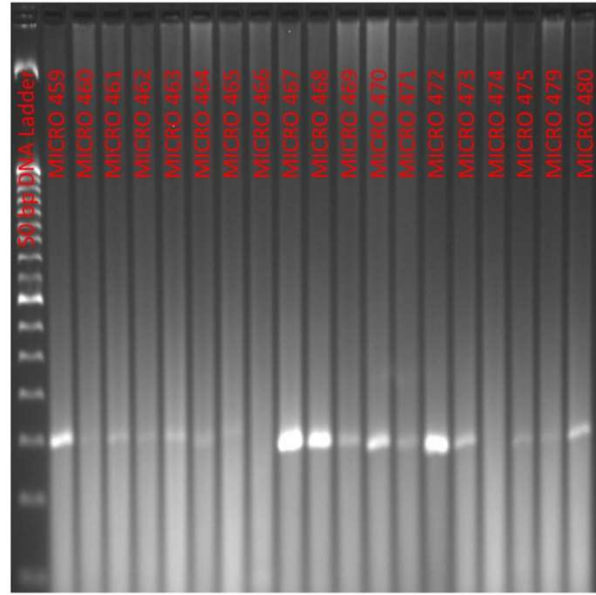
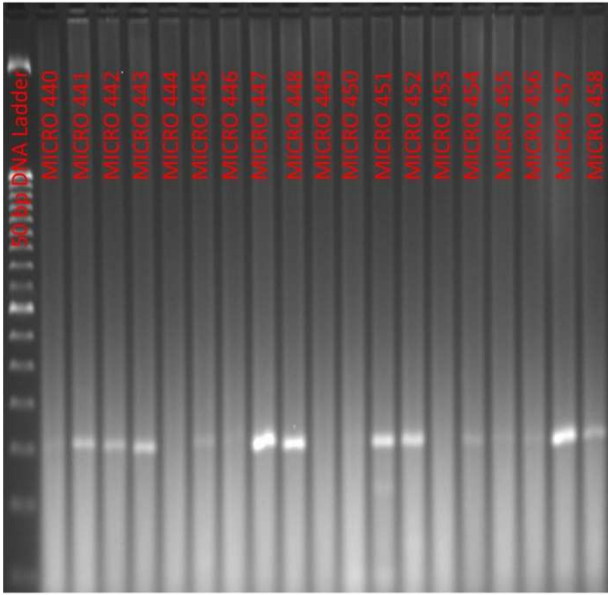


Fig. 4.3.9- Invertebrates samples amplified with the *P. lividus* specific primers

Pliv-cytb-Nfor: TCTGGTGAAATTCGGCTCT
Pliv-cytb-Nrev: TCGAAGCAGTACCCGTAAT
amplicon: 155 bp



Pliv-cytb-Nfor: TCTGGTGAAATTCGGCTCT
Pliv-cytb-Nrev: TCGAAGCAGTACCCGTAAT
amplicon: 155 bp

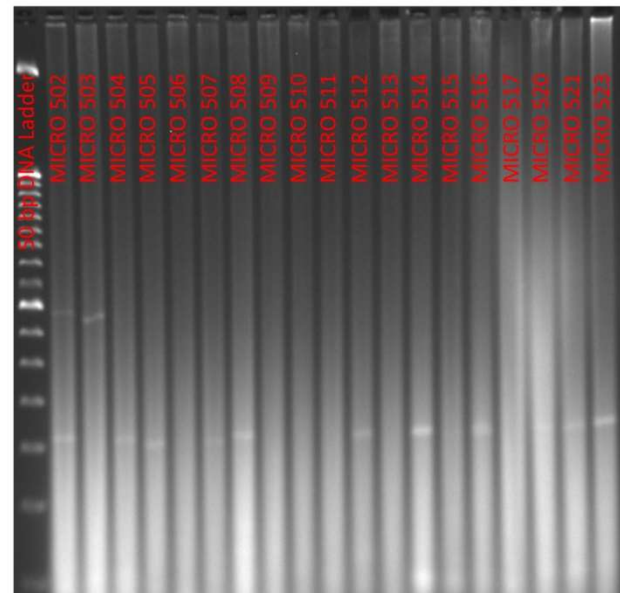
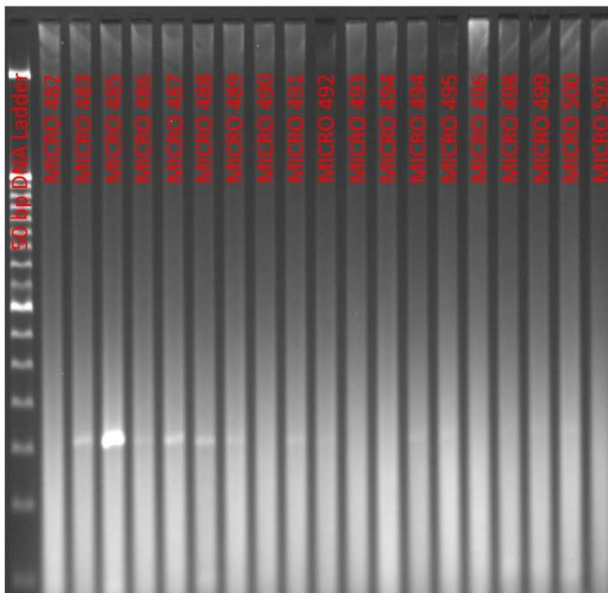
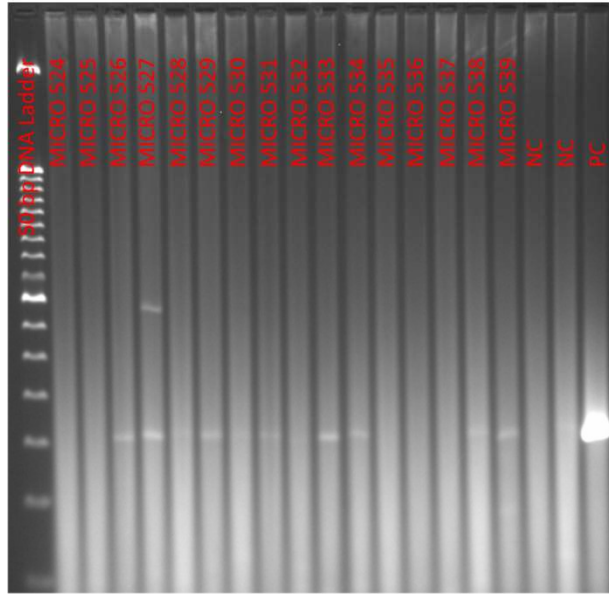


Fig. 4.3.9- Invertebrates samples amplified with the *P. lividus* specific primers

Pliv-cytb-Nfor: TCTGGTGGAAATTCCGGCTCT
 Pliv-cytb-Nrev: TCGAAGCAGTCAACCCGTAAT
 amplicon: 155 bp



Pl-COI-Nterm-for: ttctcactccatcttgcggg
 Pl-COI-Nterm-rev: aaaagacattcccggcggttc
 amplicon 93 bp

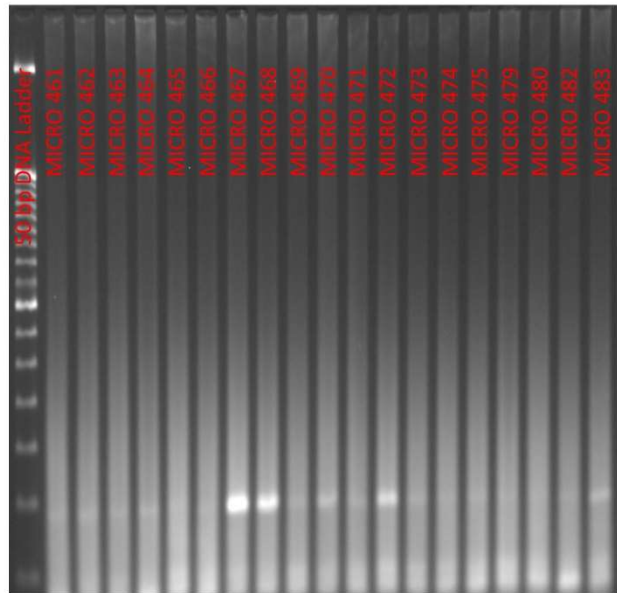
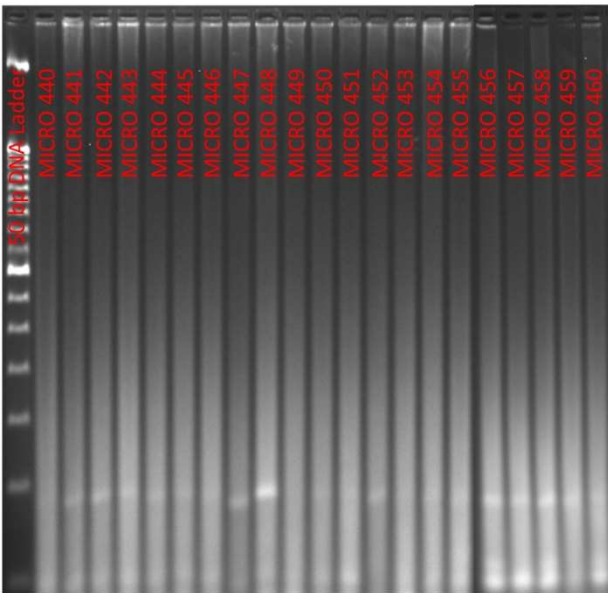
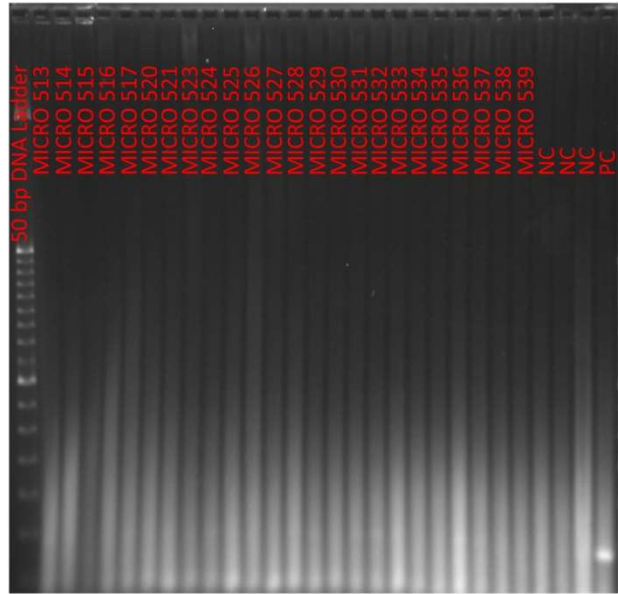
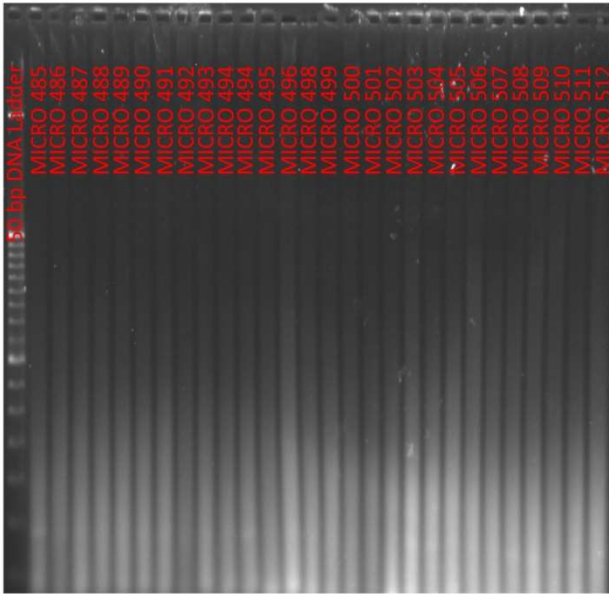


Fig. 4.3.9- Invertebrates samples amplified with the *P. lividus* specific primers

PI-COI-Nterm-for: ttctcactccatcttgctggg
 PI-COI-Nterm-rev: aaaagacattcccggcggtc
 amplicon 93 bp



Pliv-16S-for: AGGCGGAGGGTAAAATCGTT
 Pliv-16S-rev: GCTTCTTTTACTCCGCGGTT
 amplicon: 161 bp

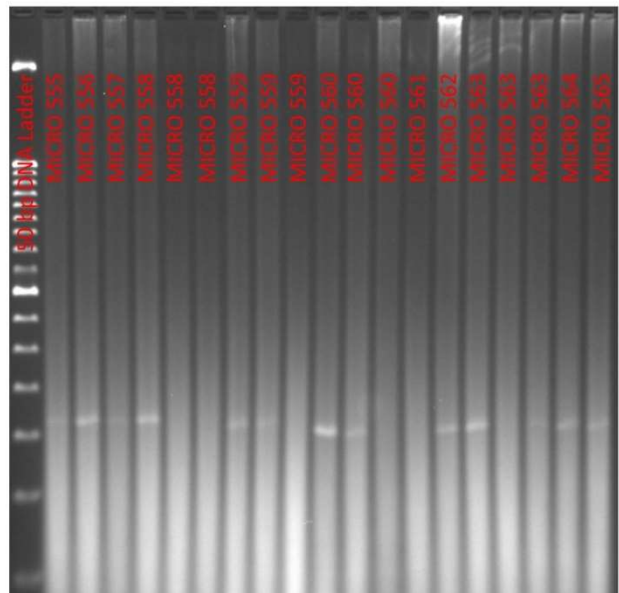
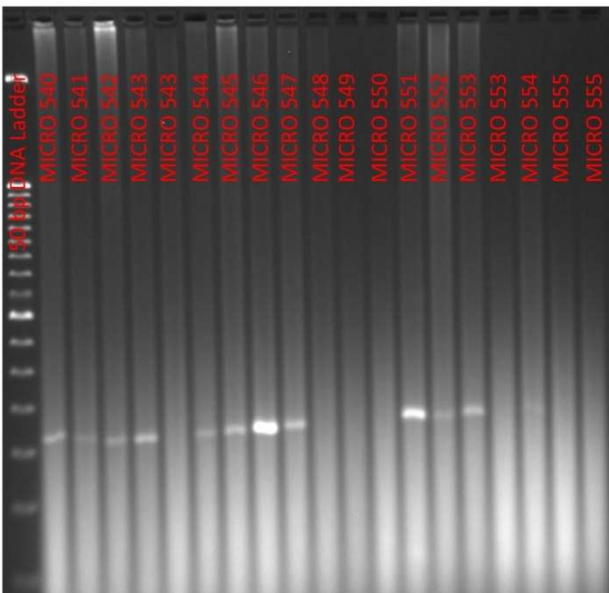
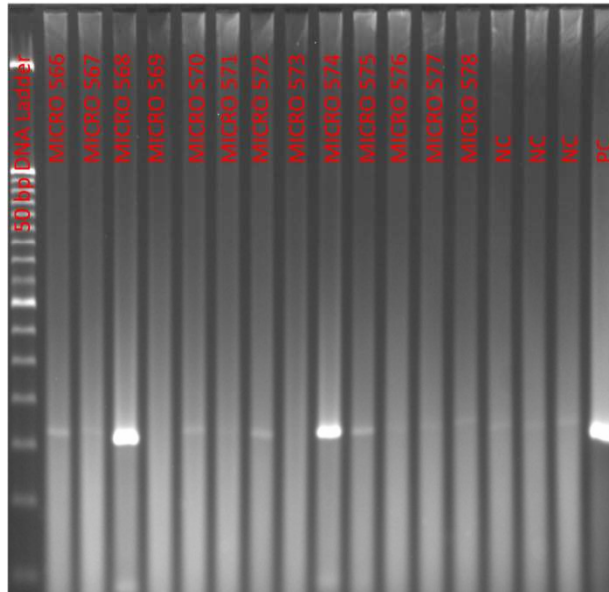


Fig. 4.3.9- Invertebrates samples amplified with the *P. lividus* specific primers

Pliv-16S-for: AGGCGGAGGGTAAAATCGTT
Pliv-16S-rev: GCTTCTTTACTCCGCGTT
amplicon: 161 bp



Pliv-cytb-Nfor: TCTGGTGAAATTCGGCTCT
Pliv-cytb-Nrev: TCGAAGCAGTACCCGTAAT
amplicon: 155 bp

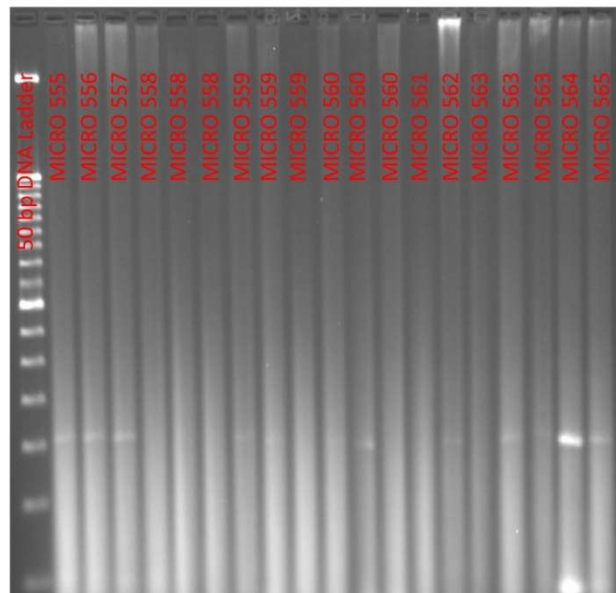
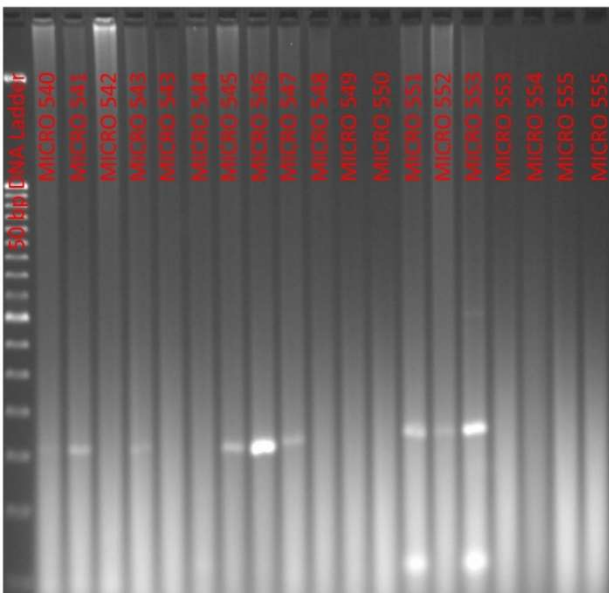
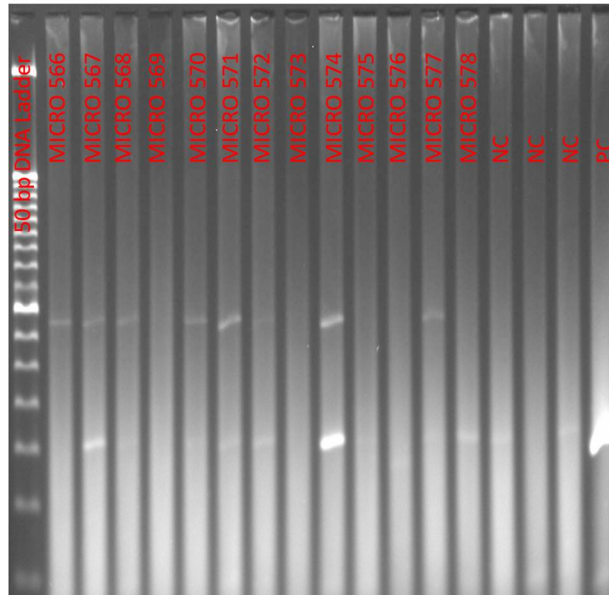


Fig. 4.3.9- Invertebrates samples amplified with the *P. lividus* specific primers

Pliv-cytb-Nfor: TCTGGTGAAATTCGGCTCT
Pliv-cytb-Nrev: TCGAAGCAGTCACCCGTAAT
amplicon: 155 bp



Pl-COI-Nterm-for: ttctcactccatcttgctggg
Pl-COI-Nterm-rev: aaaagacattcccggcggttc
amplicon 93 bp

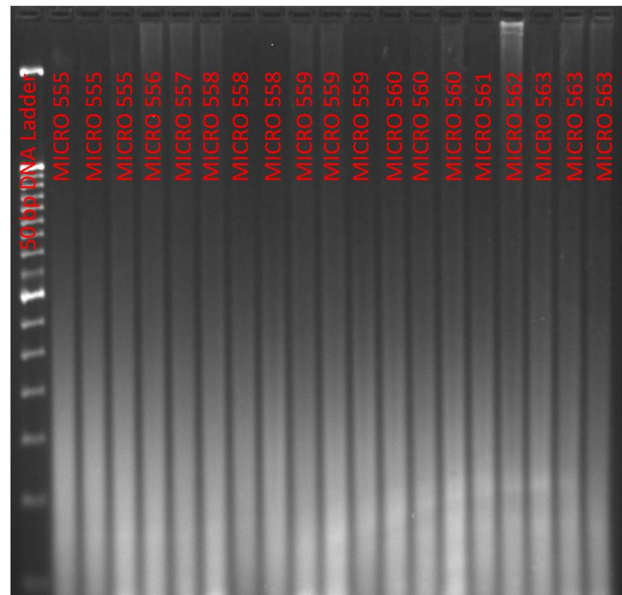
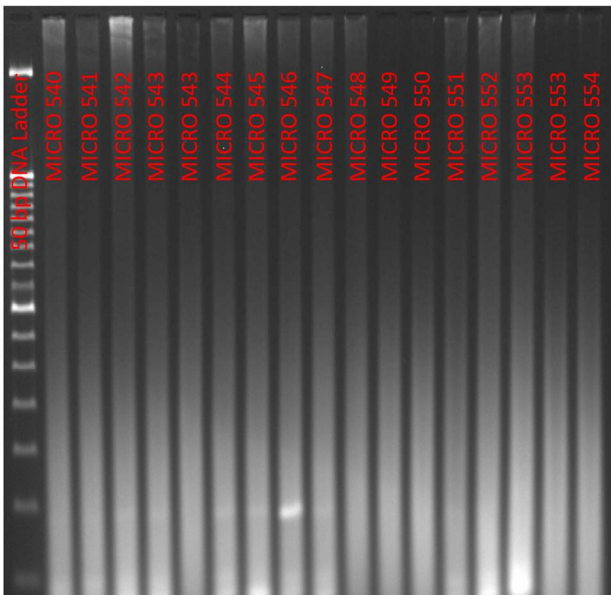


Fig. 4.3.9- Invertebrates samples amplified with the *P. lividus* specific primers

PI-COI-Nterm-for: ttctactccatcttgcggg
PI-COI-Nterm-rev: aaaagacattcccggcggtc
amplicon 93 bp

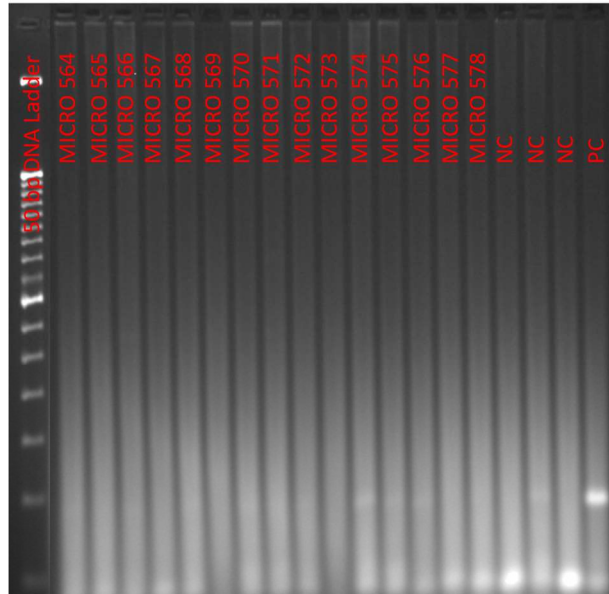


Fig. 4.3.9- Invertebrates samples amplified with the *P. lividus* specific primers

Class	Family	16S + CYTb + COI1	16S + CYTb	Negatives	tot
Gastropoda	Conidae	0	0	1	1
Gastropoda	Muricidae	0	1	2	3
Gastropoda	Nassariidae	0	0	1	1
Gastropoda	Rissoidae	0	2	7	9
Gastropoda	Tudiclidae	0	0	1	1
Malacostraca	Alpheidae	3	4	13	17
Malacostraca	Ampithoidae	2	2	15	17
Malacostraca	Bythograeidae	0	0	1	1
Malacostraca	Diogenidae	0	2	25	27
Malacostraca	Epialtidae	0	1	3	4
Malacostraca	Euryleptidae	0	0	1	1
Malacostraca	Galatheidae	0	3	4	7
Malacostraca	Idoteidae	1	1	0	1
Malacostraca	Inachidae	0	1	10	11
Malacostraca	Majoidea	0	0	1	1
Malacostraca	Paguridae	0	1	33	34
Malacostraca	Pilumnidae	1	2	6	8
Malacostraca	Polybiidae	0	0	1	1
Malacostraca	Xanthidae	0	0	1	1
Ophiuroidea	Amphiuridae	5	7	27	34
Ophiuroidea	Ophiodermatidae	0	1	4	5
Ophiuroidea	Ophiotrichidae	2	9	56	65
Polychaeta	Eunicidae	0	0	11	11
Polychaeta	Lumbrineridae	0	0	1	1
Polychaeta	Nereididae	2	2	29	31
Polychaeta	Oeonidae	0	0	2	2
Polychaeta	Phyllodocidae	0	0	1	1
Polychaeta	Polynoidae	4	4	16	20
Polychaeta	Terebellidae	2	4	13	17
Sipuncula	Phascolosomatidae	1	1	11	12
tot		23	48	297	345
Gastropoda		0	3	12	15

Malacostraca		7	17	114	131
Ophiuroidea		7	17	87	104
Polychaeta		8	10	73	83
Sipuncula		1	1	11	12
tot		23	48	297	345

Table 4.3.1- Samples positive to urchin DNA tests.

4.4 Discussion

Sea urchins play a pivotal role in driving infralittoral system dynamics, with high-density populations exerting a bulldozing effect on erect macroalgae, leading to the formation of barren grounds (Bonaviri et al., 2011, 2017; Sala et al., 1998). Estimations of predation pressure on sea urchins suggest a bimodal distribution related to urchin size, with small juveniles hiding efficiently in crevices, while adult urchins avoid predation due to their sheltering behavior, body size and defensive spines. According to this model, intermediate sized urchins would be more susceptible to predation (Fagerli et al., 2014 and reference therein; Redd et al., 2014; Tegner 1981; Sala and Zabala 1996). However, these estimates took into account mostly predation by fishes and large invertebrates such as lobsters. Smaller, crawling invertebrates might efficiently poke out of crevices and feed on urchin juveniles, exerting the most prominent control of urchin populations (Smith et al., 2023; Steneck 2013; Clemente 2013; Bonaviri et al., 2012; Sheibling 2008; Steneck et al., 2002; Rowley 1989;). Accordingly, for the Mediterranean urchin species *P. lividus*, over 75% of juveniles disappear within six months after settling in macroalgal forests (Sala and Zabala, 1996), while they persist in great numbers in barrens. In our surveys, we collected 379 invertebrates from Mediterranean fucal forests, belonging to Malacostraca, Ophiuroidea, Polychaeta, Gastropoda and Sipuncula. Species assignment requires a considerable level of taxonomic expertise, with scholars usually specializing onto one or few Classes and covering a limited geographical extent. Moreover, taxonomic knowledge is a realm suffering a severe decline in practitioners (Drew, 2011). Visual identification of a wide collection of invertebrates is, therefore, a daunting task requiring the involvement of multiple, uncommon experts. When samples are preserved for a long time, or they are not carefully handled, they may also lose structural details (such as color, appendices) that make taxonomic identification more challenging. Accordingly, several of our samples presented a fragmented body, due to processing of samples and their transport from the field to the dissecting and molecular laboratories, located in different countries. By microscope analysis, we were able to identify only 85 specimen (22%) at the species level, for the vast majority (86%) crustaceans. Our taxonomic confidence was lower for Ophiuroidea (14%), whereas we did not assign a specific

name to any of mollusks, Sipuncula or Polychaeta. For over 27% of samples, we even limited our identification to the Class level, especially for Polychaeta (68%) and Ophiuroidea (30%). Due to our lack of taxonomic expertise on many taxa, we relied on molecular barcoding as an assist for species identification. Over the years, cytochrome c oxidase 1 (COI1) has becoming the standard locus for barcoding of Metazoans, with thousands of annotated sequences deposited in public databases, such as BOLD (Barcode Of Life Data system). To sequence the COI1 locus, we first had to verify that the stored and processed samples were able to deliver DNA of sufficient quantity and quality for amplification. Despite most samples failed to show a high molecular weight band upon electrophoresis (indicative of abundant and intact genomic DNA) and many samples even presented a smear of degraded DNA, COI1 amplification and sequencing was successful for over 92% of samples (Table 4.2.1). Only 29 samples failed to produce a visible band (Fig. 4.3.3), probably because their DNA was too degraded to amplify, or because the extract contained PCR inhibitors. Consequently, although the same samples were also negative when tested with *P. lividus* specific primers, we cannot reach any conclusion regarding the presence of urchin DNA in those 29 samples without any visible band. For additional three samples, COI1 sequencing resulted in a *Photobacterium* spp. assignment rather than the related crabs. *Photobacterium* species are marine microorganisms, some known as pathogens for fishes and crabs, but they can also constitute the major component of crab microbiome (Jiang et al., 2023). It is therefore possible that these three specimens were infected by the bacterium, whose DNA abundance predominantly outraced the amplification reactions. Overall, barcoding strongly correlated with visual assignment. Minor disagreement at the Family level (4%) was most likely due to visual misidentification.

Sequencing of COI1 locus for a subset of the collected sea urchin settlers revealed that they all belonged to the species *P. lividus*. Yet, we designed and tested specific primers for both sea urchin species, in order to provide tools for molecular trophic studies in future spawning events in the Mediterranean and Atlantic. For primer design, we focused on mitochondrial DNA (mtDNA), since each diploid cell

contains only two copies of nuclear loci, but thousands of circular mtDNA molecules (Zhang 1993), less prone to degradation, making it easier to detect in digested samples. Additionally, sequences of mtDNA loci are widely available in public database for a large variety of species, facilitating the design of prey-specific primers. We selected three loci in the mtDNA: COI1; CYTB; and 16S). The COI1 locus, being the barcode standard, is highly polymorphic and sequences are available for many individuals within species, accounting for intraspecific variability. COI1 is also the most commonly used locus for assessing trophic relationships among species, reviewed in (Pompanon et al., 2012; King et al., 2008). CYTB locus has been used for Insects, Arachnida and fishes. Additionally, CYTB sequences have been used to discern the phylogeographic distribution of *P. lividus* populations in the Mediterranean (Maltagliati et al., 2010). 16S locus is also polymorphic, and among other species, it has been used to detect DNA of the sea urchins *Centrostephanus rodgersii* and *Heliocidaris erythrogramma* in lobster faecal samples in Tasmania (Redd et al., 2014; Smith et al., 2023).

Due to PCR sensitivity, caution is required when performing and interpreting molecular analyses, with multiple tests and controls needed (reviewed by King et al., 2008). The specific primers for *P. lividus* and *A. lixula* were designed by aligning hundreds of accessions of both urchin species from across the Mediterranean and Atlantic. Since these primers amplified DNA from urchins collected both in Catalonia and Sicily, located in distant areas of the Mediterranean, they proved not to be affected by intraspecific genetic variability. Primers were also tested for specificity, both in silico and by PCR, including invertebrates encompassing all the taxa collected in our surveys. We then selected three primer pairs specific for *P. lividus*, one for each mtDNA locus, and two primer pairs specific for *A. lixula*. Sensitivity tests showed that these primers were able to detect urchin DNA whereas present, even if quantities are as low as 1 to 10 pg. With a nuclear genome of 927.4 Mb (Marlé Taz et al., n.d.) and 2,000-20,000 copies of 15.697 Kb mtDNA per cell, 1 pg total DNA correspond to about 1 single individual and roughly correspond to a number of 1,400 to 20,000 mtDNA copies (Cantatore et al., 1989). However, estimates in samples with degraded DNA may be skewed. Primer efficiency was also

not affected by a thousand fold excess of exogenous DNA, from invertebrates belonging to different Classes, mimicking the scenario occurring in micropredators feeding on urchin settlers. Having passed all the control tests, the selected primer pairs can be confidently used as a molecular tool to study trophic interactions involving the sea urchins *P. lividus* and *A. lixula*.

Quantitative assessment of dietary intake in predator-prey interaction is a challenging task. Molecular techniques have been used to quantify the amount of prey consumed in captivity trials (Jarman et al., 2004), but evaluation in field samples is not straightforward (Redd et al., 2014.; Troedsson et al., 2007). The amount of prey DNA is dependent on the time of ingestion and, in the case of different predator species, on their rate of digestion. Therefore, it is usually not possible to discern between low levels of recent ingestion and high levels of past ingestion, when most of DNA has been degraded. For this reason, it is safer to adopt a qualitative approach with a binary outcome, positive or negative, regarding the presence of prey DNA. It must be stressed, however, that also qualitative assessments are subject to a certain degree of subjectiveness in the choice of threshold separating positive from negative samples. Threshold values can be based on the band intensity, as in this and other studies (Smith et al., 2023), or on Ct values in the case of qPCR analyses (Redd et al., 2014b). In the present work, we relied on the quantification of bands in the dilution series for each primer pair, to set the threshold of detection. To be more conservative in the result interpretation, the threshold was set high enough to discard the ambiguous bands, visible but with faint intensity. Though this is a common approach, it still maintains an arbitrary component that needs to be taken into account. Additionally, the choice of small amplicon sizes, instrumental in detecting degraded prey DNA in guts content, present the risk of spurious bands deriving from primer dimerization, which may affect interpretation. Longer electrophoresis separation and careful size interpolation may facilitate the discrimination between genuine and artifactual bands. In our analyses, the majority (75%) of samples were negative, showing no visible bands. Therefore, the issue of dimer bands probably does not apply to our amplification conditions, since it would affect samples regardless of the presence of template. As an additional measure of confidence in result

interpretation, we decided to analyze multiple loci. Both 16S and CYTB resulted in a similar number of positive samples (69 and 62, respectively) with 64-70% overlap. The locus COI1, on the contrary, was positive for only 29 samples, for the vast majority (79%) overlapping with both 16S and CYTB, and for additional 13% shared with either one of the other loci. The stringency of COI1 results most likely derives from its very small amplicon size (93 bp, as compared to 161 bp for 16S and 155 bp for CYTB), which makes band discrimination from primers more difficult. Moreover, COI1 locus, both in *P. lividus* and *A. lixula*, resulted less sensitive than 16S and CYTB, since diluted urchin DNA could be detected up to only 10 pg, compared to 1 pg of the other primer pairs (Fig. 4.3.6). For these reasons, though the 29 samples positive to all three loci represent the core of results with highest confidence, samples shared only by 16S and CYTB should be considered positive as well. It is very important to stress that direct predation is not the only event leading to the presence of urchin DNA in samples. Contamination is an obvious reason, though a careful handling procedure, use of separate machinery for samples and standard *P. lividus* DNA, and inclusion of several negative controls in each PCR run, let us believe that we prevented contamination to occur in our analyses. Accordingly, most of our samples (75%) did not amplify in any locus. Urchin DNA can be present within an invertebrate body as a result of secondary predation, i.e. when a predator eats another predator that had fed on *P. lividus*. Another level of trophic interaction that cannot be excluded by molecular analyses is scavenging on dead urchin material, rather than direct predation on settlers. Finally, urchin DNA can be present in the environment through their faeces or desegregation of their remains. This aspect is particularly concerning, since direct testing of unconsolidated sediments in Tasmanian reefs found urchin DNA in 20 to 100% of the samples (Redd et al., 2014) and sediments are known to be repositories for eDNA (Bowles et al. 2011). However, only a minority of lobsters fed with those sediment or directly with urchin faeces scored positive, probably because digestion eliminated the already degraded urchin DNA present in the sediment and urchin faeces, suggesting that environmental DNA might represent a minor issue (Redd et al., 2014a). Accordingly, most of our samples were negative. Yet, it is possible that the presence of *P. lividus* DNA in some of our positive samples derives from sediment or particulate

feeding. This is especially likely for the Terebellidae and Sipuncula specimens, known to feed by sediment filtration and accumulate organic material. All the other positive invertebrates are carnivorous, and events of direct predation on *P. lividus* settlers is the most likely scenario (Bonaviri et al., 2012). Members from the Alpheidae, Pilumnidae and Galatheidae families among crustaceans were particularly abundant as positive samples, especially relative to the total number of specimen of the same taxa collected (24%, 25% and 43%, respectively). Earlier works in aquaria showed that *Alpheus dentipes*, *Pilumnus villosissimus* and *Pilumnus hirtellus* are able to feed on *P. lividus* settlers (Bonaviri et al., 2012, Cano, 2024). Moreover, a field survey in the Canary islands observed a negative correlation between the abundance of sea urchin settlers and those of *Alpheus macrocheles* and two other crab species. In our study, we found four Alpheidae members (24% within Family) and two *P. villosissimus* (25%) positive to *P. lividus* DNA. Crabs from the Xanthidae Family were major predators in aquaria tests (Bonaviri et al., 2012). Unfortunately, we only found one specimen in our survey, which resulted negative. Conversely, we found only one positive out of 34 Paguridae members (3%), whereas *Calcinus tubularis* and *Pagurus anachoretus* fed on settlers in aquaria tests. Most likely then, hermit crabs are not effective predators of urchin settlers and the predation events measured in aquaria represent artifacts induced by the limited food choice and captivity conditions. In agreement with this hypothesis, though *Pagurus bernardus* fed on settlers of the urchin *Strongylocentrus droebachiensis* in aquaria, hermit crabs, though abundant, did not feed on tethered urchins along the Norwegian coast (Fagerli et al., 2014). It remains to be tested whether crabs from the Galatheidae Family, among the most common positive samples in our survey, are effective predators in aquaria trials. Among whelks, we found two positive specimens in the Families Muricidae and Rissoidae each (67% and 22%, respectively). Though never tested in captivity, the whelk *Buccinum undatum* was observed to predate on tethered urchins (Fagerli et al., 2014). Several positive invertebrates were found among the three Families of Ophiuridae collected in our survey, Amphiuroidae, Ophiodermatidae and Ophiotricidae (34%, 5% and 65%, respectively). Surprisingly, serpentine stars have been overlooked so far as potential predators of young sea urchins, although our findings suggest they might represent a major component of the predators

assemblage. Among Polychaeta, we found some Polynoidae (20%) and only few Nereididae (6%) positive to *P. lividus* DNA. In aquaria tests, *Nereis pelagica* did not feed on *S. droebachiensis* settlers, although the tested size of urchin was larger than the size of *P. lividus* settlers we commonly found in our surveys (3 mm vs. < 1 mm), which might act as a size exclusion threshold for this Class of predators.

In conclusion, in this study new specific primers were designed for *P. lividus* and *A. lixula* DNA in degraded samples, such as stomach contents; moreover, new potential micropredators of juvenile sea urchins were identified in the field, suggesting that micropredation may represent an important process in controlling sea urchin population density and maintaining the macroalgal forest state in temperate rocky reefs.

5. Conclusion

The formation of barren areas in temperate reefs brings a substantial concern due to its impact on the productivity and functioning of rocky reefs. The here presented evidence provide initial insight into the structure and functioning of Mediterranean mature barren grounds compared to macroalgal forested areas. Barren grounds are often perceived as stable states, but their structure and functioning evolve over time. The comparative analysis of benthic megafauna in coralline barren ground and macroalgal forest patches challenges previous assumptions about the biodiversity and functioning of these habitats. Contrary to the traditional view of barren grounds as lifeless zones, our investigation reveals significant species richness and abundance of benthic megafauna in coralline barrens, surpassing that of the faunal assemblages found in macroalgal forested patches. Encrusting coralline algae play a vital role in facilitating trophic interactions and supporting diverse benthic communities in barren patches, highlighting their importance in ecosystem resilience and functionality. These findings emphasize the critical roles of consumer-mediated coexistence and niche differentiation, where coralline barrens and their associated megafauna exploit resources differently than forested patches.

In the present thesis, two food-web models have been developed to depict a Mediterranean rocky reef using *in situ* data from both old barren grounds and macroalgae forest states of the Mediterranean rocky sublittoral ecosystem. The former is dominated by encrusting algae, while the latter is by erect macroalgae. The different algal assemblages significantly influenced total primary production, with the macroalgal forest state exhibiting twice the production of the barren ground state, consequently shaping the structure and functionality of the entire ecosystem. Both models revealed a prevalence of consumers with low trophic levels, likely influenced by the small size of the system and the relatively high standing crop of benthic macroalgae in each state. Analysis indicated a significant flow of energy into detritus from lower trophic levels, particularly in the forest state, suggesting a crucial role in energy recycling. Indicators highlighted the support of different functional groups in each food web model: Mega- and macro-fauna in the barren ground and macroalgal forest models, respectively. Sea urchins, particularly

omnivorous species, emerged as key players in the barren food web, contributing to matter recycling and acting as energy hubs. Conversely, certain benthic macrofauna groups exhibited higher importance in the macroalgal forest web, indicating their role in its functioning. The high productivity of the macroalgal forest state resulted in greater energy exportation, while the barren ground state effectively stored energy and hosted a diverse megafauna and supported a stable food web despite its relatively lower biomass and biodiversity. Overall, our findings shed light on the complex dynamics and functional roles of different organisms in the Mediterranean rocky reef ecosystem, emphasizing the resilience and adaptability of these systems to environmental changes and anthropogenic pressures. Moreover, this study provides molecular tools useful to study the trophic interactions involving the two major sea urchin species in the Mediterranean, *P. lividus* and *A. lixula*, whose populations outbreak are responsible for the onset and maintenance of the barren ground status in sublittoral rocky reefs. Our survey, conducted in two distant forest areas of the Mediterranean, confirmed the ability of some crustacean species to feed on *P. lividus* settlers and revealed many more potential micropredator candidates among different taxa, which altogether may act as the major factor controlling sea urchin population.

Understanding complex interactions is essential for effective conservation and management strategies. Recognizing the ecological importance of coralline barrens calls for a re-evaluation of current conservation approaches to ensure the protection of their unique biodiversity and ecosystem functions in the face of environmental change. Conducting time-series studies on both young and old barren grounds as well as macroalgal forest states of sublittoral rocky ecosystems would provide valuable information for informing management actions. By monitoring shifts in subtidal rocky ecosystems and their evolution over time, we can better understand the ecosystem dynamics and inform long-term strategies for a sustainable management of coastal subtidal rocky ecosystems.

Bibliography

- Adey, W. H., Halfar, J., & Williams, B. (2013). The coralline genus *Clathromorphum* Foslíe emend. Adey: Biological, physiological, and ecological factors controlling carbonate production in an arctic-subarctic climate archive. Smithsonian Contributions to the Marine Sciences No. 40. Smithsonian Institution Scholarly Press, Washington D.C.: 41 pp..
- Agnetta, D., Badalamenti, F., Ceccherelli, G., Di Trapani, F., Bonaviri, C., & Gianguzza, P. (2015). Role of two co-occurring Mediterranean Sea urchins in the formation of barren from *Cystoseira* canopy. *Estuarine, Coastal and Shelf Science*, 152, 73–77. <https://doi.org/10.1016/j.ecss.2014.11.023>
- Agnetta, D., Badalamenti, F., Colloca, F., Cossarini, G., Fiorentino, F., Garofalo, G., Patti, B., Pipitone, C., Russo, T., Solidoro, C., & Libralato, S. (2022). Interactive effects of fishing effort reduction and climate change in a central Mediterranean fishing area: Insights from bio-economic indices derived from a dynamic food-web model. *Frontiers in Marine Science*, 9. <https://doi.org/10.3389/fmars.2022.909164>
- Agnetta, D., Badalamenti, F., Colloca, F., D'Anna, G., Di Lorenzo, M., Fiorentino, F., Garofalo, G., Gristina, M., Labanchi, L., Patti, B., Pipitone, C., Solidoro, C., & Libralato, S. (2019). Benthic-pelagic coupling mediates interactions in Mediterranean mixed fisheries: An ecosystem modeling approach. *PLoS ONE*, 14(1). <https://doi.org/10.1371/journal.pone.0210659>
- Agnetta, D., Bonaviri, C., Badalamenti, F., Scianna, C., Vizzini, S., & Gianguzza, P. (2013). Functional traits of two co-occurring sea urchins across a barren/forest patch system. *Journal of Sea Research*, 76, 170–177. <https://doi.org/10.1016/j.seares.2012.08.009>
- Airoidi, L., & Beck, M. W. (2007). Loss, status and trends for coastal marine habitats of Europe. *Oceanography and Marine Biology*, 45, 345–405. <https://doi.org/10.1201/9781420050943.ch7>
- Andrew, N.L., Choat, J.H., 1985. Habitat related differences in the survivorship and growth of juvenile sea urchins. *Marine Ecology Progress Series* 27, 155–161.
- Antoniadou, C., & Chintiroglou, C. (2006). Trophic relationships of polychaetes associated with different algal growth forms. *Helgoland Marine Research*, 60(1), 39–49. <https://doi.org/10.1007/s10152-005-0015-2>
- Anderson, M. (2001). A new method for non-parametric multivariate analysis of variance. *Austral Ecology* 26(1): 32-46; <https://doi.org/10.1111/j.1442.9993.2001.01070.pp.x>
- Babcock, R. C., Shears, N. T., Alcalá, A. C., Barrett, N. S., Edgar, G. J., Lafferty, K. D., ... & Russ, G. R. (2010). Decadal trends in marine reserves reveal differential rates of change in direct and indirect effects. *Proceedings of the National Academy of Sciences*, 107(43), 18256-18261.

- Balch, T., Scheibling, R.E., 2000. Temporal and spatial variability in settlement and recruitment of echinoderms in kelp beds and barrens in Nova Scotia. *Marine Ecology Progress Series* 205, 139–154. Balch, T., Scheibling, R.E., 2001. Larval supply, settlement and recruitment in echinoderms. In: Jangoux, M., Lawrence, J.M. (Eds.), *Echinoderm Studies*, 6. AA Balkema, Rotterdam, pp. 1–83.
- Barbier, E. B., Hacker, S. D., Kennedy, C., Koch, E. W., Stier, A. C., & Silliman, B. R. (2011). The value of estuarine and coastal ecosystem services. In *Ecological Monographs* (Vol. 81, Issue 2, pp. 169–193). <https://doi.org/10.1890/10-1510.1>
- Baskett, M. L., & Salomon, A. K. (2010). Recruitment facilitation can drive alternative states on temperate reefs. *Ecology*, 91(6), 1763–1773. <https://doi.org/10.1890/09-0515.1>
- Bell, J. J. (2008). The functional roles of marine sponges. In *Estuarine, Coastal and Shelf Science* (Vol. 79, Issue 3, pp. 341–353). <https://doi.org/10.1016/j.ecss.2008.05.002>
- Bernal-Ibáñez, A., Gestoso, I., Wirtz, P., Kaufmann, M., Serrão, E. A., Canning-Clode, J., & Cacabelos, E. (n.d.). *The collapse of marine forests: drastic reduction in populations of the family Sargassaceae in Madeira Island (NE Atlantic)*. <https://doi.org/10.1007/s10113-021-01801-2/Published>
- Bernstein, B. B., B. E. Williams, and K. H. Mann. "The role of behavioral responses to predators in modifying urchins'(Strongylocentrotus droebachiensis) destructive grazing and seasonal foraging patterns." *Marine Biology* 63 (1981): 39-49.
- Bianchelli, S., Buschi, E., Danovaro, R., & Pusceddu, A. (2016). Biodiversity loss and turnover in alternative states in the Mediterranean Sea: A case study on meiofauna. *Scientific Reports*, 6. <https://doi.org/10.1038/srep34544>
- Bianchelli, S., & Danovaro, R. (2020). Impairment of microbial and meiofaunal ecosystem functions linked to algal forest loss. *Scientific Reports*, 10(1). <https://doi.org/10.1038/s41598-020-76817-5>
- Bonaviri, C., Fernández, T. V., Badalamenti, F., Gianguzza, P., Di Lorenzo, M., & Riggio, S. (2009). Fish versus starfish predation in controlling sea urchin populations in Mediterranean rocky shores. *Marine Ecology Progress Series*, 382, 129–138. <https://doi.org/10.3354/meps07976>
- Bonaviri, C., Fernández, T. V., Fanelli, G., Badalamenti, F., & Gianguzza, P. (2011). Leading role of the sea urchin *Arbacia lixula* in maintaining the barren state in southwestern Mediterranean. *Marine Biology*, 158(11), 2505–2513. <https://doi.org/10.1007/s00227-011-1751-2>
- Bonaviri, C., Gianguzza, P., Pipitone, C., & Hereu, B. (2012). Micropredation on sea urchins as a potential stabilizing process for rocky reefs. *Journal of Sea Research*, 73, 18–23. <https://doi.org/10.1016/j.seares.2012.06.003>
- Bonaviri, C., Graham, M., Gianguzza, P., & Shears, N. T. (2017). Warmer temperatures reduce the influence of an important keystone predator. *Journal of Animal Ecology*, 86(3), 490–500. <https://doi.org/10.1111/1365-2656.12634>

Branch, G. M. (n.d.). *THE RESPONSES OF SOUTH AFRICAN PATELLID LIMPETS TO INVERTEBRATE PREDATORS*.

Bulleri, F., Bertocci, I., & Micheli, F. (2002). Interplay of encrusting coralline algae and sea urchins in maintaining alternative habitats. *Marine Ecology Progress Series*, 243, 101–109.

Cameron, R.A., Schroeter, S.C., 1980. Sea urchin recruitment: effect of substrate selection on juvenile distribution. *Marine Ecology Progress Series* 2, 243–247.

Cano, I. (2024). *Assessing the influence of macroalgae and micropredation on the early life success of the echinoid *Diadema africanum**. <https://doi.org/10.21203/RS.3.RS-4164377/V1>

Cantatore, P., Roberti, M., Rainaldi, G., Gadaleta, M. N., & Saccone, C. (1989). *The Complete Nucleotide Sequence, Gene Organization, and Genetic Code of the Mitochondrial Genome of *Paracentrotus Ziuidus**". 264, 10965–10975. [https://doi.org/10.1016/S0021-9258\(18\)60413-2](https://doi.org/10.1016/S0021-9258(18)60413-2)

Caut, S., Angulo, E., & Courchamp, F. (2009). Variation in discrimination factors ($\Delta^{15}\text{N}$ and $\Delta^{13}\text{C}$): The effect of diet isotopic values and applications for diet reconstruction. *Journal of Applied Ecology*, 46(2), 443–453. <https://doi.org/10.1111/j.1365-2664.2009.01620.x>

Cheminée, A., Pastor, J., Bianchimani, O., Thiriet, P., Sala, E., Cottalorda, J. M., Dominici, J. M., Lejeune, P., & Francour, P. (2017). Juvenile fish assemblages in temperate rocky reefs are shaped by the presence of macro-Algae canopy and its three-dimensional structure. *Scientific Reports*, 7(1). <https://doi.org/10.1038/s41598-017-15291-y>

Chenelot, H., Jewett, S. C., & Hoberg, M. K. (2011a). Macrobenthos of the nearshore Aleutian Archipelago, with emphasis on invertebrates associated with *Clathromorphum nereostratum* (Rhodophyta, Corallinaceae). *Marine Biodiversity*, 41(3), 413–424. <https://doi.org/10.1007/s12526-010-0071-y>

Chenelot, H., Jewett, S. C., & Hoberg, M. K. (2011b). Macrobenthos of the nearshore Aleutian Archipelago, with emphasis on invertebrates associated with *Clathromorphum nereostratum* (Rhodophyta, Corallinaceae). *Marine Biodiversity*, 41(3), 413–424. <https://doi.org/10.1007/s12526-010-0071-y>

Christensen, V. (1995). E(OLOGI(IIL mODELLInG Ecosystem maturity-towards quantification. In *Ecological Modelling* (Vol. 77).

Christensen, V., & Walters, C. J. (2004). Ecopath with Ecosim: Methods, capabilities and limitations. *Ecological Modelling*, 172(2–4), 109–139. <https://doi.org/10.1016/j.ecolmodel.2003.09.003>

Clare, E. L. (2014). Molecular detection of trophic interactions: emerging trends, distinct advantages, significant considerations and conservation applications. *Evolutionary applications*, 7(9), 1144–1157.

Clemente, Sabrina, José Carlos Hernández, and Alberto Brito. "Evidence of the top–down role of predators in structuring sublittoral rocky-reef communities in a Marine Protected Area and nearby areas of the Canary Islands." *ICES Journal of Marine Science* 66.1 (2009): 64–71.

- Coll, M., & Libralato, S. (2012). Contributions of food web modelling to the ecosystem approach to marine resource management in the Mediterranean Sea. In *Fish and Fisheries* (Vol. 13, Issue 1, pp. 60–88). <https://doi.org/10.1111/j.1467-2979.2011.00420.x>
- Costa, G., Bertolino, M., Pinna, S., Bonaviri, C., Padiglia, A., Zinni, M., Pronzato, R., & Manconi, R. (2018). Mediterranean sponges from shallow subtidal rocky reefs: *Cystoseira* canopy vs barren grounds. *Estuarine, Coastal and Shelf Science*, 207, 293–302. <https://doi.org/10.1016/j.ecss.2018.04.002>
- Cucherousset, J., & Villéger, S. (2015). Quantifying the multiple facets of isotopic diversity: New metrics for stable isotope ecology. *Ecological Indicators*, 56, 152–160. <https://doi.org/10.1016/j.ecolind.2015.03.032>
- Cuff, J. P., Kitson, J. J., Hemprich-Bennett, D., Tercel, M. P., Browett, S. S., & Evans, D. M. (2023). The predator problem and PCR primers in molecular dietary analysis: swamped or silenced; depth or breadth? *Molecular Ecology Resources*, 23(1), 41-51.
- Dethier, M. N., Steneck, R. S. (2001). Growth and persistence of diverse intertidal crusts: survival of the slow in a fast-paced world. *Marine Ecology Progress Series*, 223, 89-100.
- Di Trapani, F., Agnetta, D., Bonaviri, C., Badalamenti, F., & Gianguzza, P. (2020). Unveiling the diet of the thermophilic starfish *Ophidiaster ophidianus* (Echinodermata: Asteroidea) combining visual observation and stable isotopes analysis. *Marine Biology*, 167(7). <https://doi.org/10.1007/s00227-020-03704-y>
- Drew, L. W. (2011). *Are We Losing the Science of Taxonomy?* 61(12). <https://doi.org/10.1525/bio.2011.61.12.4>
- Duarte, C. M., & BBVA Foundation - Cap Salines Lighthouse Coastal Research Station Colloquium (2007 : Madrid, S. (2009). *Global loss of coastal habitats : rates, causes and consequences*. Fundación BBVA.
- Duggins, D. O., Simenstad, C. A., & Estes, J. A. (1989). Magnification_of_Secondary_Production_by_Duggins. *Science*, 245(4914), 170–173.
- Fabbrizzi, E., Scardi, M., Ballesteros, E., Benedetti-Cecchi, L., Cebrian, E., Ceccherelli, G., De Leo, F., Deidun, A., Guarnieri, G., Falace, A., Fraissinet, S., Giommi, C., Mačić, V., Mangialajo, L., Mannino, A. M., Piazzini, L., Ramdani, M., Rilov, G., Rindi, L., ... Fraschetti, S. (2020). Modeling macroalgal forest distribution at mediterranean scale: Present status, drivers of changes and insights for conservation and management. *Frontiers in Marine Science*, 7. <https://doi.org/10.3389/fmars.2020.00020>
- Fagerli, C. W., Norderhaug, K. M., Christie, H., Pedersen, M. F., & Fredriksen, S. (2014). Predators of the destructive sea urchin *Strongylocentrotus droebachiensis* on the Norwegian coast. *Marine Ecology Progress Series*, 502, 207–218. <https://doi.org/10.3354/MEPS10701>
- Fanelli, G., & Piraino, S. (1998). *Opposite role of sea urchins and starfishes in marine benthic communities*. <https://www.researchgate.net/publication/236891739>

Fanellil, G., Piraino², S., Belmontel, G., Geraci³, S., & Boeroll, F. (1994). *Human predation along Apulian rocky coasts (SE Italy): desertification caused by Lithophaga lithophaga (Mollusca) fisheries* (Vol. 110).

Fey, P., Letourneur, Y., & Bonnabel, S. (2021). The α -minimum convex polygon as a relevant tool for isotopic niche statistics. *Ecological Indicators*, 130. <https://doi.org/10.1016/j.ecolind.2021.108048>

Filbee-Dexter, K., & Scheibling, R. E. (2014a). Sea urchin barrens as alternative stable states of collapsed kelp ecosystems. In *Marine Ecology Progress Series* (Vol. 495, pp. 1–25). <https://doi.org/10.3354/meps10573>

Filbee-Dexter, K., & Scheibling, R. E. (2014b). Sea urchin barrens as alternative stable states of collapsed kelp ecosystems. In *Marine Ecology Progress Series* (Vol. 495, pp. 1–25). <https://doi.org/10.3354/meps10573>

Filbee-Dexter, K., & Scheibling, R. E. (2016). Spatial Patterns and Predictors of Drift Algal Subsidy in Deep Subtidal Environments. *Estuaries and Coasts*, 39(6), 1724–1734. <https://doi.org/10.1007/s12237-016-0101-5>

Finn, J. T. (1976). Measures of Ecosystem Structure and Function Derived from Analysis of Flowst. In *J. theor. BioL* (Vol. 56).

Folke, C., Carpenter, S., Walker, B., Scheffer, M., Elmqvist, T., Gunderson, L., & Holling, C. S. (2004). Regime shifts, resilience, and biodiversity in ecosystem management. In *Annual Review of Ecology, Evolution, and Systematics* (Vol. 35, pp. 557–581). <https://doi.org/10.1146/annurev.ecolsys.35.021103.105711>

Gagnon, P., Himmelman, J. H., & Johnson, L. E. (2004). Temporal variation in community interfaces: Kelp-bed boundary dynamics adjacent to persistent urchin barrens. *Marine Biology*, 144(6), 1191–1203. <https://doi.org/10.1007/s00227-003-1270-x>

Galasso, N. M., Bonaviri, C., Trapani, F. Di, Picciotto, M., Gianguzza, P., Agnetta, D., & Badalamenti, F. (2015). Fish-seastar facilitation leads to algal forest restoration on protected rocky reefs. *Scientific Reports*, 5. <https://doi.org/10.1038/srep12409>

Garcia, A. M., Hoetinghaus, D. J., Vieira, J. P., & Winemiller, K. O. (2007). Isotopic variation of fishes in freshwater and estuarine zones of a large subtropical coastal lagoon. *Estuarine, Coastal and Shelf Science*, 73(3–4), 399–408. <https://doi.org/10.1016/j.ecss.2007.02.003>

Geller, J., Meyer, C., Parker, M., & Hawk, H. (2013). Redesign of PCR primers for mitochondrial cytochrome *c* oxidase subunit I for marine invertebrates and application in all-taxa biotic surveys. *Molecular Ecology Resources*, 13(5), 851–861. <https://doi.org/10.1111/1755-0998.12138>

Geraldi, N. R., Bertolini, C., Emmerson, M. C., Roberts, D., Sigwart, J. D., & O'Connor, N. E. (2017). Aggregations of brittle stars can perform similar ecological roles as mussel reefs. *Marine Ecology Progress Series*, 563, 157–167. <https://doi.org/10.3354/meps11993>

Gianguzza, P., Bonaviri, C., Milisenda, G., Barcellona, A., Agnetta, D., Vega Fernández, T., & Badalamenti, F. (2010). Macroalgal assemblage type affects predation pressure on sea urchins by

- altering adhesion strength. *Marine Environmental Research*, 70(1), 82–86. <https://doi.org/10.1016/j.marenvres.2010.03.006>
- Gianguzza, P., Di Trapani, F., Bonaviri, C., Agnetta, D., Vizzini, S., & Badalamenti, F. (2016). Size-dependent predation of the mesopredator *Marthasterias glacialis* (L.) (Asteroidea). *Marine Biology*, 163(3). <https://doi.org/10.1007/s00227-016-2835-9>
- Gizzi, F., Monteiro, J. G., Silva, R., Schäfer, S., Castro, N., Almeida, S., Chebaane, S., Bernal-Ibáñez, A., Henriques, F., Gestoso, I., & Canning-Clode, J. (2021). Disease Outbreak in a Keystone Grazer Population Brings Hope to the Recovery of Macroalgal Forests in a Barren Dominated Island. *Frontiers in Marine Science*, 8. <https://doi.org/10.3389/fmars.2021.645578>
- Gosselin, L.A., Qian, P.Y., 1997. Juvenile mortality in benthic marine invertebrates. *Marine Ecology Progress Series* 146, 265–282.
- Green R.H. (1979). Sampling design and statistical methods for environmental biologists. John Wiley & Sons, New York: 270 pp. [ISBN 0-471-03901-2]
- Griffith, A.M., Gosselin, L.A., (2008). Ontogenetic shift in susceptibility to predators in juvenile northern abalone, *Haliotis kamtschatkana*. *Journal of Experimental Marine Biology and Ecology* 360, 85–93.
- Graham, M. H. (2004). Effects of local deforestation on the diversity and structure of southern California giant kelp forest food webs. In *Ecosystems* (Vol. 7, Issue 4, pp. 341–357). Springer New York. <https://doi.org/10.1007/s10021-003-0245-6>
- Grime, J. P. (1998). Benefits of plant diversity to ecosystems: Immediate, filter and founder effects. In *Journal of Ecology* (Vol. 86, Issue 6, pp. 902–910). <https://doi.org/10.1046/j.1365-2745.1998.00306.x>
- Guidetti, P. (2006). Marine reserves reestablish lost predatory interactions and cause community changes in rocky reefs. *Ecological Applications*, 16(3), 963–976. [https://doi.org/10.1890/1051-0761\(2006\)016\[0963:MRRLPI\]2.0.CO;2](https://doi.org/10.1890/1051-0761(2006)016[0963:MRRLPI]2.0.CO;2)
- Hansen, M. D. (1978). Nahrung und Fret verhalten bei Sedimentfressern dargestellt am Beispiel von Sipunculiden und Holothurien*. In *Helgoliinder wiss. Meeresunters* (Vol. 31).
- Hays, G. C., Ferreira, L. C., Sequeira, A. M. M., Meekan, M. G., Duarte, C. M., Bailey, H., Bailleul, F., Bowen, W. D., Caley, M. J., Costa, D. P., Eguíluz, V. M., Fossette, S., Friedlaender, A. S., Gales, N., Gleiss, A. C., Gunn, J., Harcourt, R., Hazen, E. L., Heithaus, M. R., ... Thums, M. (2016). Key Questions in Marine Megafauna Movement Ecology. In *Trends in Ecology and Evolution* (Vol. 31, Issue 6, pp. 463–475). Elsevier Ltd. <https://doi.org/10.1016/j.tree.2016.02.015>
- Harrold, C., Lisin, S., Light, K.H., Tudor, S., 1991. Isolating settlement from recruitment of sea urchins. *Journal of Experimental Marine Biology and Ecology* 147, 81–94.
- Hereu, B., Zabala, M., Linares, C., Sala, E., 2004. Temporal and spatial variability in settlement of the sea urchin *Paracentrotus lividus* in the NW Mediterranean. *Marine Biology* 144, 1011–1018.

- Hernández, J. C., Clemente, S., Girard, D., Pérez-Ruzafa, Á., & Brito, A. (2010). Effect of temperature on settlement and postsettlement survival in a barrens-forming sea urchin. *Marine Ecology Progress Series*, 413, 69–80. <https://doi.org/10.3354/meps08684>
- Heymans, J. J., Coll, M., Libralato, S., Morissette, L., & Christensen, V. (2014). Global patterns in ecological indicators of marine food webs: A modelling approach. *PLoS ONE*, 9(4). <https://doi.org/10.1371/journal.pone.0095845>
- Heymans, J. J., Coll, M., Link, J. S., Mackinson, S., Steenbeek, J., Walters, C., & Christensen, V. (2016). Best practice in Ecopath with Ecosim food-web models for ecosystem-based management. *Ecological Modelling*, 331, 173–184. <https://doi.org/10.1016/j.ecolmodel.2015.12.007>
- Hind, K. R., Starko, S., Burt, J. M., Lemay, M. A., Salomon, A. K., & Martone, P. T. (2019). Trophic control of cryptic coralline algal diversity. *Proceedings of the National Academy of Sciences of the United States of America*, 116(30), 15080–15085. <https://doi.org/10.1073/pnas.1900506116>
- Hobson, K. A., Fisk, A., Karnovsky, N., Holst, M., Gagnon, J. M., & Fortier, M. (2002). A stable isotope ($\delta^{13}\text{C}$, $\delta^{15}\text{N}$) model for the North Water food web: Implications for evaluating trophodynamics and the flow of energy and contaminants. *Deep-Sea Research Part II: Topical Studies in Oceanography*, 49(22–23), 5131–5150. [https://doi.org/10.1016/S0967-0645\(02\)00182-0](https://doi.org/10.1016/S0967-0645(02)00182-0)
- Hooper, D. U., Chapin, F. S., Ewel, J. J., Hector, A., Inchausti, P., Lavorel, S., Lawton, J. H., Lodge, D. M., Loreau, M., Naeem, S., Schmid, B., Setälä, H., Symstad, A. J., Vandermeer, J., & Wardle, D. A. (2005). Effects of biodiversity on ecosystem functioning: A consensus of current knowledge. *Ecological Monographs*, 75(1), 3–35. <https://doi.org/10.1890/04-0922>
- Hopkins, J. B., & Ferguson, J. M. (2012). Estimating the diets of animals using stable isotopes and a comprehensive Bayesian mixing model. In *PLoS ONE* (Vol. 7, Issue 1). <https://doi.org/10.1371/journal.pone.0028478>
- Hunt, H.L., Scheibling, R.E., 1997. Role of early post-settlement mortality in recruitment of benthic marine invertebrates. *Marine Ecology Progress Series* 155, 269–301.
- Jackson, J. B. C., Kirby, M. X., Berger, W. H., Bjorndal, K. A., Botsford, L. W., Bourque, B. J., Bradbury, R. H., Cooke, R., Erlandson, J., Estes, J. A., Hughes, T. P., Kidwell, S., Lange, C. B., Lenihan, H. S., Pandolfi, J. M., Peterson, C. H., Steneck, R. S., Tegner, M. J., & Warner, R. R. (2001). Historical Overfishing and the Recent Collapse of Coastal Ecosystems. In *Source: Science, New Series* (Vol. 293, Issue 5530).
- Jarman, S. N., Deagle, B. E., & Gales, N. J. (2004). Group-specific polymerase chain reaction for DNA-based analysis of species diversity and identity in dietary samples. *Molecular Ecology*. <https://doi.org/10.1111/j.1365-294X.2004.02109.x>
- Jennings, L.B., Hunt, H., 2010. Settlement, recruitment and potential predators and competitors of juvenile echinoderms in the rocky subtidal zone. *Marine Biology* 157, 307–316.

- Jennings, L.B., Hunt, H., 2011. Small macrobenthic invertebrates affect the mortality and growth of early post-settlement sea urchins and sea stars in subtidal cobble habitat. *Marine Ecology Progress Series* 431, 173–182.
- Jepsen, D. B., & Winemiller, K. O. (2002). Structure of tropical river food webs revealed by stable isotope ratios. *Oikos*, 96(1), 46–55. <https://doi.org/10.1034/j.1600-0706.2002.960105.x>
- Jiang, X., Niu, M., Qin, K., Hu, Y., Li, Y., Che, C., Wang, C., Mu, C., & Wang, H. (2023). The shared microbiome in mud crab (*Scylla paramamosain*) of Sanmen Bay, China: core gut microbiome. *Frontiers in Microbiology*, 14, 1243334. <https://doi.org/10.3389/FMICB.2023.1243334/FULL>
- Kang, C. K., Choy, E. J., Son, Y., Lee, J. Y., Kim, J. K., Kim, Y., & Lee, K. S. (2008). Food web structure of a restored macroalgal bed in the eastern Korean peninsula determined by C and N stable isotope analyses. *Marine Biology*, 153(6), 1181–1198. <https://doi.org/10.1007/s00227-007-0890-y>
- Keramidas, I., Dimarchopoulou, D., Ofir, E., Scotti, M., Tsikliras, A. C., & Gal, G. (2023). Ecotrophic perspective in fisheries management: a review of Ecopath with Ecosim models in European marine ecosystems. In *Frontiers in Marine Science* (Vol. 10). Frontiers Media S.A. <https://doi.org/10.3389/fmars.2023.1182921>
- King, R. A., Read, D. S., Traugott, M., & Symondson, W. O. C. (2008). Molecular analysis of predation: A review of best practice for DNA-based approaches. In *Molecular Ecology*. <https://doi.org/10.1111/j.1365-294X.2007.03613.x>
- Kingsford, M. J., & Byrne, M. (2023). New South Wales rocky reefs are under threat. *Marine and Freshwater Research*, 74(2), 95–98. <https://doi.org/10.1071/mf22220>
- Knowlton, N. (2004). Multiple “stable” states and the conservation of marine ecosystems. In *Progress in Oceanography* (Vol. 60, Issues 2–4, pp. 387–396). <https://doi.org/10.1016/j.pocean.2004.02.011>
- Konar, B., & Estes, J. A. (2003). THE STABILITY OF BOUNDARY REGIONS BETWEEN KELP BEDS AND DEFORESTED AREAS. In *Ecology* (Vol. 84, Issue 1).
- Kremen, C. (2005). Managing ecosystem services: What do we need to know about their ecology? In *Ecology Letters* (Vol. 8, Issue 5, pp. 468–479). <https://doi.org/10.1111/j.1461-0248.2005.00751.x>
- Krumhansl, K. A., & Scheibling, R. E. (2012a). Production and fate of kelp detritus. In *Marine Ecology Progress Series* (Vol. 467, pp. 281–302). <https://doi.org/10.3354/meps09940>
- Krumhansl, K. A., & Scheibling, R. E. (2012b). Production and fate of kelp detritus. In *Marine Ecology Progress Series* (Vol. 467, pp. 281–302). <https://doi.org/10.3354/meps09940>
- Lawrence, J. M., & Larrain, A. (1994). The cost of arm autotomy in the starfish *Stichaster striatus*. *Marine Ecology Progress Series*, 109(2–3), 311. <https://doi.org/10.3354/meps109311>

- Layman, C. A., Araujo, M. S., Boucek, R., Hammerschlag-Peyer, C. M., Harrison, E., Jud, Z. R., Matich, P., Rosenblatt, A. E., Vaudo, J. J., Yeager, L. A., Post, D. M., & Bearhop, S. (2012). Applying stable isotopes to examine food-web structure: An overview of analytical tools. In *Biological Reviews* (Vol. 87, Issue 3, pp. 545–562). <https://doi.org/10.1111/j.1469-185X.2011.00208.x>
- Libralato, S., Christensen, V., & Pauly, D. (2006). A method for identifying keystone species in food web models. *Ecological Modelling*, 195(3–4), 153–171. <https://doi.org/10.1016/j.ecolmodel.2005.11.029>
- Ling, S. D., Johnson, C. R., Frusher, S. D., & Ridgway, K. R. (n.d.). *Overfishing reduces resilience of kelp beds to climate-driven catastrophic phase shift*. www.pnas.org/cgi/content/full/
- Ling, S. D., Scheibling, R. E., Rassweiler, A., Johnson, C. R., Shears, N., Connell, S. D., Salomon, A. K., Norderhaug, K. M., Pérez-Matus, A., Hernández, J. C., Clemente, S., Blamey, L. K., Hereu, B., Ballesteros, E., Sala, E., Garrabou, J., Cebrian, E., Zabala, M., Fujita, D., & Johnson, L. E. (2015a). Global regime shift dynamics of catastrophic sea urchin overgrazing. *Philosophical Transactions of the Royal Society B: Biological Sciences*, 370(1659), 1–10. <https://doi.org/10.1098/rstb.2013.0269>
- Ling, S. D., Scheibling, R. E., Rassweiler, A., Johnson, C. R., Shears, N., Connell, S. D., Salomon, A. K., Norderhaug, K. M., Pérez-Matus, A., Hernández, J. C., Clemente, S., Blamey, L. K., Hereu, B., Ballesteros, E., Sala, E., Garrabou, J., Cebrian, E., Zabala, M., Fujita, D., & Johnson, L. E. (2015b). Global regime shift dynamics of catastrophic sea urchin overgrazing. *Philosophical Transactions of the Royal Society B: Biological Sciences*, 370(1659), 1–10. <https://doi.org/10.1098/rstb.2013.0269>
- Maltagliati, F., Giuseppe, G. Di, Barbieri, M., Castelli, A., & Dini, F. (2010). Phylogeography and genetic structure of the edible sea urchin *Paracentrotus lividus* (Echinodermata: Echinoidea) inferred from the mitochondrial cytochrome b gene. *Biological Journal of the Linnean Society*, 100, 910–923.
- Mamelona, J., & Pelletier, É. (2005). Green urchin as a significant source of fecal particulate organic matter within nearshore benthic ecosystems. *Journal of Experimental Marine Biology and Ecology*, 314(2), 163–174. <https://doi.org/10.1016/j.jembe.2004.08.026>
- Maneveldt, G. W., Van der Merwe, E., & Keats, D. W. (2016). Updated keys to the non-geniculate coralline red algae (Corallinophycidae, Rhodophyta) of South Africa. *South African Journal of Botany*, 106, 158–164. <https://doi.org/10.1016/j.sajb.2016.07.002>
- Marlé Taz, F., Couloux, A., Poulain, J., Labadie, K., Da Silva, C., Mangenot, S., Noel, B., Poustka, A. J., Dru, P., Pegueroles, C., Borra, M., Lowe, E. K., Lhomond, G., Besnardeau, L., Phanie, S., Gras, L., Ye, T., Gavriouchkina, D., Russo, R., ... Lepage, T. (n.d.). *Analysis of the *P. lividus* sea urchin genome highlights contrasting trends of genomic and regulatory evolution in deuterostomes*. <https://doi.org/10.1016/j.xgen.2023.100295>
- McClanahan, T. R., & Sala, E. (1997). A Mediterranean rocky-bottom ecosystem fisheries model PII S 0 3 0 4-3 8 0 0 (9 7) 0 0 1 2 1-X. In *Ecological Modelling* (Vol. 104).

- McCoy, S. J., & Kamenos, N. A. (2015). Coralline algae (Rhodophyta) in a changing world: Integrating ecological, physiological, and geochemical responses to global change. *Journal of Phycology*, 51(1), 6–24. <https://doi.org/10.1111/jpy.12262>
- Moleón, M., Sánchez-Zapata, J. A., Donázar, J. A., Revilla, E., Martín-López, B., Gutiérrez-Cánovas, C., Getz, W. M., Morales-Reyes, Z., Campos-Arceiz, A., Crowder, L. B., Galetti, M., González-Suárez, M., He, F., Jordano, P., Lewison, R., Naidoo, R., Owen-Smith, N., Selva, N., Svenning, J. C., ... Tockner, K. (2020). Rethinking megafauna. In *Proceedings of the Royal Society B: Biological Sciences* (Vol. 287, Issue 1922). Royal Society Publishing. <https://doi.org/10.1098/rspb.2019.2643>
- Norderhaug, K. M., Christie, H., Fosså, J. H., & Fredriksen, S. (2005). Fish-macrofauna interactions in a kelp (*Laminaria hyperborea*) forest. *Journal of the Marine Biological Association of the United Kingdom*, 85(5), 1279–1286. <https://doi.org/10.1017/S0025315405012439>
- Novoa, E. A. M. (2020). *Reinstatement of the genera Gongolaria Boehmer and Ericaria Stackhouse (Sargassaceae, Phaeophyceae)*. 172.
- Ojeda, F. P., & Dearborn, J. H. (1989). Community structure of macroinvertebrates inhabiting the rocky subtidal zone in the Gulf of Maine: seasonal and bathymetric distribution *. *MARINE ECOLOGY PROGRESS SERIES Mar. Ecol. Prog. Ser.*, 57, 147–161. <https://doi.org/10.0>
- O'Reilly, C. M., Hecky, R. E., Cohen, A. S., & Plisnier, P. D. (2002). Interpreting stable isotopes in food webs: Recognizing the role of time averaging at different trophic levels. *Limnology and Oceanography*, 47(1), 306–309. <https://doi.org/10.4319/lo.2002.47.1.0306>
- Orfanidis, S., Rindi, F., Cebrian, E., Frascchetti, S., Nasto, I., Taskin, E., Bianchelli, S., Papathanasiou, V., Kosmidou, M., Caragnano, A., Tsioli, S., Ratti, S., Fabbri, E., Verdura, J., Tamburello, L., Beqiraj, S., Kashta, L., Sota, D., Papadimitriou, A., ... Danovaro, R. (2021). Effects of Natural and Anthropogenic Stressors on Fuclean Brown Seaweeds Across Different Spatial Scales in the Mediterranean Sea. *Frontiers in Marine Science*, 8. <https://doi.org/10.3389/fmars.2021.658417>
- Ortiz-Zayas, J. R., Lewis, W. M., Saunders, J. F., McCutchan, J. H., & Scatena, F. N. (2005). Metabolism of a tropical rainforest stream. *Journal of the North American Benthological Society*, 24(4), 769–783. <https://doi.org/10.1899/03-094.1>
- Osman, R.W., Whitlatch, R.B., 1995. Predation on early ontogenetic life stages and its effect on recruitment into a marine epifaunal community. *Marine Ecology Progress Series* 117, 111–126.
- Osman, R.W., Whitlatch, R.B., 2004. The control of the development of a marine benthic community by predation on recruits. *Journal of Experimental Marine Biology and Ecology* 311, 117–145.
- Osman, R.W., Whitlatch, R.B., Malatesta, R.J., 1992. Potential role of micro-predators in determining recruitment into a marine community. *Marine Ecology Progress Series* 83, 35–43.
- Parmesan, C., Yohe, G., & Andrus, J. E. (2003). *A globally coherent fingerprint of climate change impacts across natural systems*. www.nature.com/nature

- Parnell, A. C., Inger, R., Bearhop, S., & Jackson, A. L. (2010). Source partitioning using stable isotopes: Coping with too much variation. *PLoS ONE*, 5(3). <https://doi.org/10.1371/journal.pone.0009672>
- Pearse, J.S., Hines, A.H., 1987. Long-term population dynamics of sea urchins in a central California kelp forest: rare recruitment and rapid decline. *Marine Ecology Progress Series* 39, 275–283.
- Pearce, C. M., & Scheibling, R. E. (1990). Induction of metamorphosis of larvae of the green sea urchin, *Strongylocentrotus droebachiensis*, by coralline red algae. *Biological Bulletin*, 179(3), 304–311. <https://doi.org/10.2307/1542322>
- Peterson, B. J., & Fry, B. (1987a). STABLE ISOTOPES IN ECOSYSTEM STUDIES. In *Attn. Rev. Ecol. Syst* (Vol. 18). www.annualreviews.org/aronline
- Peterson, B. J., & Fry, B. (1987b). STABLE ISOTOPES IN ECOSYSTEM STUDIES. In *Attn. Rev. Ecol. Syst* (Vol. 18). www.annualreviews.org/aronline
- Petraitis, P. S., & Dudgeon, S. R. (2004). Detection of alternative stable states in marine communities. *Journal of Experimental Marine Biology and Ecology*, 300(1–2), 343–371. <https://doi.org/10.1016/j.jembe.2003.12.026>
- Phillips, D. L., & Gregg, J. W. (2003). Source partitioning using stable isotopes: Coping with too many sources. *Oecologia*, 136(2), 261–269. <https://doi.org/10.1007/s00442-003-1218-3>
- Piazzzi, L., Bonaviri, C., Castelli, A., Ceccherelli, G., Costa, G., Curini-Galletti, M., Langeneck, J., Manconi, R., Montefalcone, M., Pipitone, C., Rosso, A., & Pinna, S. (2018). Biodiversity in canopy-forming algae: Structure and spatial variability of the Mediterranean *Cystoseira* assemblages. *Estuarine, Coastal and Shelf Science*, 207, 132–141. <https://doi.org/10.1016/j.ecss.2018.04.001>
- Piazzzi, L., Bulleri, F., & Ceccherelli, G. (2016). Limpets compensate sea urchin decline and enhance the stability of rocky subtidal barrens. *Marine Environmental Research*, 115, 49–55. <https://doi.org/10.1016/j.marenvres.2016.01.009>
- Pinna, S., Piazzzi, L., Ceccherelli, G., Castelli, A., Costa, G., Curini-Galletti, M., Gianguzza, P., Langeneck, J., Manconi, R., Montefalcone, M., Pipitone, C., Rosso, A., & Bonaviri, C. (2020). Macroalgal forest vs sea urchin barren: Patterns of macro-zoobenthic diversity in a large-scale Mediterranean study: Macro-zoobenthos of barren and macroalgal forests. *Marine Environmental Research*, 159. <https://doi.org/10.1016/j.marenvres.2020.104955>
- Pinnegar, J. K., Polunin, N. V. C., Francour, P., Badalamenti, F., Chemello, R., Harmelin-Vivien, M. L., ... & Pipitone, C. (2000). Trophic cascades in benthic marine ecosystems: lessons for fisheries and protected-area management. *Environmental conservation*, 27(2), 179-200.
- Piroddi, C., Coll, M., Steenbeek, J., Moy, D. M., & Christensen, V. (2015). Modelling the Mediterranean marine ecosystem as a whole: Addressing the challenge of complexity. *Marine Ecology Progress Series*, 533, 47–65. <https://doi.org/10.3354/meps11387>
- POMPANON_et_al-2012-Molecular_Ecology*. (n.d.).

- Post, D. M. (2002). Using stable isotopes to estimate trophic position: Models, methods, and assumptions. *Ecology*, 83(3), 703–718. [https://doi.org/10.1890/0012-9658\(2002\)083\[0703:USITET\]2.0.CO;2](https://doi.org/10.1890/0012-9658(2002)083[0703:USITET]2.0.CO;2)
- Prado, P., Romero, J., Alcoverro, T., 2009. Welcome mats? The role of seagrass meadow structure in controlling post-settlement survival in a keystone sea-urchin species. *Estuarine and Coastal Marine Science* 85, 472–478.
- Privitera, D., Noli, M., Falugi, C., Chiantore, M., 2011. Benthic assemblages and temperature effects on *Paracentrotus lividus* and *Arbacia lixula* larvae and settlement. *Journal of Experimental Marine Biology and Ecology* 407, 6–11.
- Prado, P., Romero, J., Alcoverro, T., 2009. Welcome mats? The role of seagrass meadow structure in controlling post-settlement survival in a keystone sea-urchin species. *Estuarine and Coastal Marine Science* 85, 472–478.
- Rassweiler, A., Schmitt, R. J., & Holbrook, S. J. (2010). Triggers and maintenance of multiple shifts in the state of a natural community. *Oecologia*, 164(2), 489–498. <https://doi.org/10.1007/s00442-010-1666-5>
- Redd, K. S., Jarman, S. N., Frusher, S. D., & Johnson, C. R. (n.d.). *A molecular approach to identify prey of the southern rock lobster*. <https://doi.org/10.1017/S0007485308005981>
- Redd, K. S., Ling, S. D., Frusher, S. D., Jarman, S., & Johnson, C. R. (2014a). Using molecular prey detection to quantify rock lobster predation on barrens-forming sea urchins. *Molecular Ecology*. <https://doi.org/10.1111/mec.12795>
- Redd, K. S., Ling, S. D., Frusher, S. D., Jarman, S., & Johnson, C. R. (2014b). Using molecular prey detection to quantify rock lobster predation on barrens-forming sea urchins. *Molecular Ecology*, 23(15), 3849–3869. <https://doi.org/10.1111/mec.12795>
- Righi, S., Prevedelli, D., & Simonini, R. (2020). Ecology, distribution and expansion of a Mediterranean native invader, the fireworm *Hermodice carunculata* (Annelida). *Mediterranean Marine Science*, 21(3), 575–591. <https://doi.org/10.12681/MMS.23117>
- Rowley, R.J., 1989. Settlement and recruitment of sea urchins (*Strongylocentrotus* spp.) in a sea-urchin barren ground and a kelp bed: are populations regulated by settlement or post-settlement processes? *Marine Biology* 100, 485–494.
- Sala, E., Boudouresque, C. F., & Harmelin-Vivien, M. (1998). Fishing, Trophic Cascades, and the Structure of Algal Assemblages: Evaluation of an Old but Untested Paradigm. *Oikos*, 82(3), 425. <https://doi.org/10.2307/3546364>
- Sala, E., Kizilkaya, Z., Yildirim, D., & Ballesteros, E. (2011). Alien marine fishes deplete algal biomass in the Eastern Mediterranean. *PLoS ONE*, 6(2). <https://doi.org/10.1371/journal.pone.0017356>
- Sala, E., Graham, M.H., 2002. Community-wide distribution of predator–prey interaction strength in kelp forests. *Proceedings of the National Academy of Sciences of the United States of America* 99 (6), 3678–368

Sala, E., Zabala, M., 1996. Fish predation and the structure of the sea urchin *Paracentrotus lividus* populations in the NW Mediterranean. *Marine Ecology Progress Series* 140, 71–81.

Scheibling, R.E., Robinson, M.C., 2008. Settlement behaviour and early post-settlement predation of the sea urchin *Strongylocentrotus droebachiensis*. *Journal of Experimental Marine Biology and Ecology* 365, 59–66

Salomon, A. K., Shears, N. T., Langlois, T. J., & Babcock, R. C. (2008). CASCADING EFFECTS OF FISHING CAN ALTER CARBON FLOW THROUGH A TEMPERATE COASTAL ECOSYSTEM. In *Ecological Applications* (Vol. 18, Issue 8).

Schaal, G., Riera, P., & Leroux, C. (2010). Trophic ecology in a Northern Brittany (Batz Island, France) kelp (*Laminaria digitata*) forest, as investigated through stable isotopes and chemical assays. *Journal of Sea Research*, 63(1), 24–35. <https://doi.org/10.1016/j.seares.2009.09.002>

Scheffer, M., & Carpenter, S. R. (2003). Catastrophic regime shifts in ecosystems: Linking theory to observation. In *Trends in Ecology and Evolution* (Vol. 18, Issue 12, pp. 648–656). Elsevier Ltd. <https://doi.org/10.1016/j.tree.2003.09.002>

Seitz, R. D., Wennhage, H., Bergström, U., Lipcius, R. N., & Ysebaert, T. (2014). Ecological value of coastal habitats for commercially and ecologically important species. In *ICES Journal of Marine Science* (Vol. 71, Issue 3, pp. 648–665). Oxford University Press. <https://doi.org/10.1093/icesjms/fst152>

Shears, N. T., & Babcock, R. C. (2003). Continuing trophic cascade effects after 25 years of no-take marine reserve protection. *Marine Ecology Progress Series*, 246, 1–16. <https://doi.org/10.3354/meps246001>

Smith, J. E., Keane, J., Oellermann, M., Mundy, C., Gardner, C., Ying, M., & Chiu, J. (2023). *Lobster predation on barren-forming sea urchins is more prevalent in habitats where small urchins are common: a multi-method diet analysis*. 74(18), 1493–1505. <https://doi.org/10.1071/MF23140>

Steneck, R. S., Graham, M. H., Bourque, B. J., Corbett, D., Erlandson, J. M., Estes, J. A., & Tegner, M. J. (2002). Kelp forest ecosystems: Biodiversity, stability, resilience and future. In *Environmental Conservation* (Vol. 29, Issue 4, pp. 436–459). <https://doi.org/10.1017/S0376892902000322>

Steneck, R. S., Leland, A., McNaught, D. C., & Vavrinec, J. (2013). Ecosystem flips, locks, and feedbacks: the lasting effects of fisheries on Maine's kelp forest ecosystem. *Bulletin of Marine Science*, 89(1), 31-55.

Suding, K. N., Gross, K. L., & Houseman, G. R. (2004). Alternative states and positive feedbacks in restoration ecology. In *Trends in Ecology and Evolution* (Vol. 19, Issue 1, pp. 46–53). Elsevier Ltd. <https://doi.org/10.1016/j.tree.2003.10.005>

Tamburello, L., Chiarore, A., Fabbrizzi, E., Colletti, A., Franzitta, G., Grech, D., Rindi, F., Rizzo, L., Savinelli, B., & Frascetti, S. (2022). Can we preserve and restore overlooked macroalgal forests? In *Science of the Total Environment* (Vol. 806). Elsevier B.V. <https://doi.org/10.1016/j.scitotenv.2021.150855>

- Tavares, D. C., Moura, J. F., Acevedo-Trejos, E., & Merico, A. (2019). Traits shared by marine megafauna and their relationships with ecosystem functions and services. In *Frontiers in Marine Science* (Vol. 6, Issue May). Frontiers Media SA. <https://doi.org/10.3389/fmars.2019.00262>
- Taylor, R. B. (1998). Density, biomass and productivity of animals in four subtidal rocky reef habitats: the importance of small mobile invertebrates *Marine Ecology Progress Series* 172:37-51
- Teagle, H., Hawkins, S. J., Moore, P. J., & Smale, D. A. (2017). The role of kelp species as biogenic habitat formers in coastal marine ecosystems. In *Journal of Experimental Marine Biology and Ecology* (Vol. 492, pp. 81–98). Elsevier B.V. <https://doi.org/10.1016/j.jembe.2017.01.017>
- Tegner, M. J., & Dayton, P. K. (1981). Population structure, recruitment and mortality of two sea urchins (*Strongylocentrotus franciscanus* and *S. purpuratus*) in a kelp forest. *Mar Ecol Prog Ser*, 5(255), 68.
- Troedsson, C., Frischer, M. E., Nejstgaard, J. C., & Thompson, E. M. (2007). Molecular quantification of differential ingestion and particle trapping rates by the appendicularian *Oikopleura dioica* as a function of prey size and shape. *Limnology and Oceanography*, 52(1), 416–427. <https://doi.org/10.4319/lo.2007.52.1.0416>
- Tuya, F., Hernández, J. C., & Clemente, S. (2006). Is there a link between the type of habitat and the patterns of abundance of holothurians in shallow rocky reefs? *Hydrobiologia*, 571(1), 191–199. <https://doi.org/10.1007/s10750-006-0240-y>
- Ulanowicz, R.E. (1986). A phenomenological perspective of ecological development. Special Technical Publication 921. *American Society for Testing and Materials*: 9 pp.
- Ulanowicz, R.E. (1997). *Ecology, the ascendant perspective*. Columbia University Press, New York: 201 pp.
- Valiela I. (2006). *Global coastal change*. Blackwell, Malden: 368 pp. [ISBN 978-1-4051-3685-3].
- Vasconcellos, M., Mackinson, S., Sloman, K., & Paulya, D. (1997). The stability of trophic mass-balance models of marine ecosystems: a comparative analysis. In *Ecological Modelling* (Vol. 100).
- Vergés, A., & Campbell, A. H. (2020). Kelp forests. In *Current Biology* (Vol. 30, Issue 16, pp. R919–R920). Cell Press. <https://doi.org/10.1016/j.cub.2020.06.053>
- Vizzini, S., & Mazzola, A. (2008). The fate of organic matter sources in coastal environments: A comparison of three Mediterranean lagoons. *Hydrobiologia*, 611(1), 67–79. <https://doi.org/10.1007/s10750-008-9458-1>
- Vizzini, S., Sarà, G., Mateo, M. A., & Mazzola, A. (2003). $\delta^{13}\text{C}$ and $\delta^{15}\text{N}$ variability in *Posidonia oceanica* associated with seasonality and plant fraction. *Aquatic Botany*, 76(3), 195–202. [https://doi.org/10.1016/S0304-3770\(03\)00052-4](https://doi.org/10.1016/S0304-3770(03)00052-4)
- Wai, T. C., & Williams, G. A. (2005). The relative importance of herbivore-induced effects on productivity of crustose coralline algae: Sea urchin grazing and nitrogen excretion. *Journal of Experimental Marine Biology and Ecology*, 324(2), 141–156. <https://doi.org/10.1016/j.jembe.2005.04.010>

- Wernberg, T., Krumhansl, K., Filbee-Dexter, K., & Pedersen, M. F. (2018). Status and trends for the world's kelp forests. In *World Seas: An Environmental Evaluation Volume III: Ecological Issues and Environmental Impacts* (pp. 57–78). Elsevier. <https://doi.org/10.1016/B978-0-12-805052-1.00003-6>
- Włodarska-Kowalczyk, M., Kukliński, P., Ronowicz, M., Legeżyńska, J., & Gromisz, S. (2009). Assessing species richness of macrofauna associated with macroalgae in Arctic kelp forests (hornsund, svalbard). *Polar Biology*, 32(6), 897–905. <https://doi.org/10.1007/s00300-009-0590-9>
- Wu, Z., Zhang, X., Lozano-Montes, H. M., & Loneragan, N. R. (2016). Trophic flows, kelp culture and fisheries in the marine ecosystem of an artificial reef zone in the Yellow Sea. *Estuarine, Coastal and Shelf Science*, 182, 86–97. <https://doi.org/10.1016/j.ecss.2016.08.021>
- Wulff, J. (n.d.). *Assessing and monitoring coral reef sponges: Why and how?* <https://www.researchgate.net/publication/233669506>
- Yorke, C. E., Page, H. M., & Miller, R. J. (2019a). Sea urchins mediate the availability of kelp detritus to benthic consumers. *Proceedings of the Royal Society B: Biological Sciences*, 286(1906). <https://doi.org/10.1098/rspb.2019.0846>
- Yorke, C. E., Page, H. M., & Miller, R. J. (2019b). Sea urchins mediate the availability of kelp detritus to benthic consumers. *Proceedings of the Royal Society B: Biological Sciences*, 286(1906). <https://doi.org/10.1098/rspb.2019.0846>
- Zang, Z., Campbell, A., Leus, D. & Bureau, D. (2011). Recruitment patterns and juvenile-adult associations of red sea urchins in three areas of British Columbia. *Fisheries Research* 109(1-2), 276-284.
- Zaidi, R. H., Jaal, Z., Hawkes, N. J., Hemingway, J., & Symondson, W. O. C. (1999). Can multiple-copy sequences of prey DNA be detected amongst the gut contents of invertebrate predators? *Molecular Ecology*. <https://doi.org/10.1046/j.1365-294X.1999.00823.x>